

A thesis submitted of the requirements for the degree of Doctorate (Dr. rer. nat) from  
the Faculty of Biology at the Ludwig-Maximilians–University, Munich, Germany

**Dissecting the molecular mechanism of glutathione-  
dependent regulation of cell proliferation and cell death**

**Alexander Seiler**

GSF-National Research Center for Environment and Health, Institute for Clinical  
Molecular Biology and Tumor Genetics, Munich, Germany

Munich, August 2007

First Examiner:

Prof. Dr. Dirk Eick

Second Examiner:

PD Dr. Angelika Böttger

Third Examiner:

Prof. Dr. Michael Boshart

Fourth Examiner:

Prof. Dr. Stefan Jentsch

Fifth Examiner:

Prof. Dr. Dirk Schüler

Sixth Examiner:

Prof. Dr. Jürgen Soll

Date of oral examination:

29. November 2007

<b>Contents</b>	<b>page</b>
<b>Contents.....</b>	<b>I</b>
<b>List of abbreviations.....</b>	<b>IV</b>
<b>1 Introduction .....</b>	<b>1</b>
1.1 The mammalian selenoproteome .....	1
1.1.1 Deiodinases (DI) .....	3
1.1.2 Thioredoxin reductases (TrxR) .....	4
1.1.3 Glutathione peroxidases (GPxs).....	4
1.1.3.1 Glutathione peroxidase 1 (GPx1).....	6
1.1.3.2 Glutathione peroxidase 2 (GPx2).....	7
1.1.3.3 Glutathione peroxidase 3 (GPx3).....	7
1.1.3.4 Phospholipid hydroperoxide glutathione peroxidase (PHGPx).....	8
1.1.3.4 Other glutathione peroxidases.....	8
1.1.4 Other selenoproteins.....	8
1.2 The biosynthesis of selenoproteins .....	9
1.2.1 Sec-tRNA biosynthesis (SelA, SelC, SPS) .....	9
1.2.2 Co-translational Sec incorporation (SECIS, EFsec, SBP2, SelB).....	10
1.3 GSH biosynthesis and the Cys/(Cys) <sub>2</sub> -cycle .....	12
1.3.1 Cellular functions of GSH.....	12
1.3.2 The $\gamma$ -glutamyl and the Cys/(Cys) <sub>2</sub> cycle of GSH biosynthesis.....	13
1.4 Phospholipid hydroperoxide glutathione peroxidase (PHGPx,GPx4) .....	15
1.4.1 The genetic and molecular structure of PHGPx.....	15
1.4.2 The catalytic mechanism of PHGPx .....	16
1.4.3 The cellular functions of PHGPx .....	17
1.4.3.1 PHGPx as an anti-apoptotic factor.....	17
1.4.3.2 PHGPx and spermatogenesis .....	18
1.4.3.3 A regulatory role for glutathione peroxidases in arachidonic acid metabolism.....	19
1.5 Objectives.....	21
<b>2 Materials.....</b>	<b>22</b>
<b>3 Methods .....</b>	<b>29</b>
3.1 Cell culture and related techniques .....	29
3.1.1 Murine embryonic fibroblasts (MEFs).....	29
3.1.2 ES cell like $\gamma$ -GCS knockout cells .....	29
3.1.3 Determination of cell number .....	30
3.1.4 Cryo conservation and thawing of cells .....	30
3.1.5 Microscopy pictures and time-lapse videos .....	30
3.1.6 Genetic transfer methods.....	31
3.1.6.1 Transfection of siRNA .....	31
3.1.6.2 Electroporation.....	31
3.1.6.3 Lentiviral infection.....	31
3.2 Genotyping .....	33

<b>Contents</b>	<b>page</b>
3.3 Cloning techniques .....	33
3.3.1 Preparation of plasmid DNA .....	33
3.3.2 Restriction digestion .....	34
3.3.3 Phenol-chloroform extraction and ethanol precipitation of DNA .....	34
3.3.4 DNA ligation .....	35
3.3.5 Klenow fragment fill-in reaction .....	35
3.3.6 Dephosphorylation of linearized plasmid DNA .....	35
3.3.7 Preparation of competent cells .....	36
3.3.8 Heat shock transformation .....	36
3.4 Cloning of expression vectors .....	36
3.4.1 pCAG-3SIP-based vectors (MCM, eGFP, xCT) .....	36
3.4.2 p442-PL1-based PHGPx expression vectors .....	37
3.4.3 Cloning of tagged PHGPx .....	37
3.4.4 PHGPx Mutagenesis .....	39
3.4.5 Bcl-2 expression vectors .....	39
3.5 Immunoblotting and Immunocytochemistry .....	40
3.5.1 Western blot .....	40
3.5.2 The production of antibodies for murine PHGPx .....	41
3.5.3 Immunocytochemistry and confocal microscopy .....	41
3.6 Determination of mRNA levels .....	42
3.6.1 RNA isolation and cDNA synthesis .....	42
3.6.2 Quantitative RT-PCR .....	43
3.7 Northern blot .....	43
3.8 Flow cytometry (FACS analysis) .....	44
3.8.1 Intracellular peroxide detection .....	44
3.8.2 Detection of lipid peroxidation .....	45
3.8.3 Cell viability detection by flow cytometry .....	45
3.9 Detection of HETE/HPETE and LTB <sub>4</sub> detection by HPLC .....	46
3.10 Detection of Cys/(Cys) <sub>2</sub> and GSH .....	46
3.10.1 Cys and GSH detection by HPLC .....	46
3.10.2 Determination of cellular L-cystine uptake capacity .....	47
3.10.3 Determination of extracellular mercaptans .....	48
<b>4 Results .....</b>	<b>49</b>
4.1 Inducible inactivation of PHGPx in primary MEFs .....	49
4.2 PHGPx depletion causes rapid cell death .....	52
4.3 The reconstitution of PHGPx expression with a lentiviral add-back system rescues PHGPx knockout cells .....	54
4.4 Vitamin E, but not water-soluble antioxidants rescue PHGPx-deficient cells from cell death .....	58
4.5 Deletion of PHGPx causes cell death, resulting from massive lipid peroxidation ..	60
4.6 The crosstalk between PHGPx and arachidonic acid metabolism .....	62
4.7 Cell death is mediated by AIF translocation in PHGPx knockout cells .....	70
4.8 The physiological role of catalytically important amino acids of PHGPx .....	72
4.9 xCT overexpression rescues $\gamma$ -GCS-deficient cells from GSH depletion .....	77

<b>Contents</b>	<b>page</b>
<b>5 Discussion .....</b>	<b>87</b>
5.1 PHGPx regulates cell death via a cascade of events, including 15-LOX activation, lipid peroxidation, and AIF translocation. ....	87
5.2 Mutational analysis of PHGPx revealed functional interchangeability of Sec with Cys: a model to study a putative redox sensor function of PHGPx .....	96
5.3 The Cys/(Cys) <sub>2</sub> -cycle rescues GSH deficiency in $\gamma$ -GCS knockout cells.....	100
<b>6 References .....</b>	<b>108</b>
<b>7 Summary .....</b>	<b>122</b>
<i>Curriculum vitae</i> .....	124
<b>Acknowledgement .....</b>	<b>127</b>
<b>Supplementary data on CD .....</b>	<b>129</b>

**List of abbreviations**

2-ME	$\beta$ -mercaptoethanol
AIF	apoptosis inducing factor
Ala	alanine
Amp	ampicillin
APAF-1	apoptotic protease activating factor-1
ATP	adenosine triphosphate
Ba	butyric acid
BOOH	butylhydroperoxide
BSO	L-buthionine sulfoximine
CMV	cytomegalovirus
COX	cyclooxygenase
Cre	Cre recombinase
Cys	cysteine (reduced)
(Cys) <sub>2</sub>	cystine (oxidised Cys dimer)
DCF	dichlorofluorescein
DI	deiodinase
DMSO	dimethylsulfoxide
DTNB	5,5'-dithio-bis(2-nitrobenzoic acid)
DTT	dithiothreitol
DUOX	dual oxidase
Ea	alternative exon (of the PHGPx gene)
EDTA	ethylenediamine-N,N,N',N'-tetra-acetic acid
EFsec	Sec-specific elongation factor
eGFP	enhanced green fluorescence protein
ETYA	5,8,11,14-eicosatetraenoic acid
FACS	fluorescence associated cell sorting
FAD	flavin adenine dinucleotide
FSH-tag	Flag-Strep-HA-tag
$\gamma$ -GCS	$\gamma$ -glutamyl cysteine synthetase
GGT	$\gamma$ -glutamyl transpeptidase
$\gamma$ -Glu-AA	$\gamma$ -glutamyl amino acid transporter
Gln	glutamine
Glu	glutamate
Gly	glycine
GPx	glutathione peroxidase
GSH	glutathione (reduced)
GSH-EE	glutathione ethyl ester
GSH-S	glutathione synthase
GSSG	glutathione dimer (oxidised)
GTP	guanosine triphosphate
HETE	hydroxyeicosatetraenoic acid
HPETE	hydroperoxyeicosatetraenoic acids
HPLC	high pressure liquid chromatography
HSP90	heat shock protein 90
IL-1	interleukin-1
LOX	lipoygenase
IRES	internal ribosomal entry site
KLH	keyhole limpet hemocyanin

LMP agarose	low melting point agarose
LTB <sub>4</sub>	leukotriene B <sub>4</sub>
Lys	lysine
MEFs	murine embryonic fibroblasts
MER	mutated oestrogen receptor
MOMP	mitochondrial outer membrane permeabilization
MOPS	3-(N-morpholino) propansulfonic acid
NAC	N-acetylcysteine
NADPH	nicotinamide adenine dinucleotide phosphate (reduced form)
NDGA	nordihydroguaiaretic acid
NF- $\kappa$ B	nuclear factor $\kappa$ B
NOX	NADPH oxidase
nucmem	nuclear membrane anchor
OVA	ovalbumin
PAGE	polyacrylamide gel electrophoresis
PARP-1	poly(ADP-ribose) polymerase-1
PBS	phosphate buffered saline
PFA	paraformaldehyde
PGB <sub>2</sub>	prostaglandine B <sub>2</sub>
PGG <sub>2</sub>	prostaglandine G <sub>2</sub>
PHGPx	phospholipid hydroperoxide glutathione peroxidase
PI	propidium iodide
PLA <sub>2</sub>	phospholipase A <sub>2</sub>
PPAR	peroxisome proliferator-activated receptor
PRPP	5-phosphoribosyl-1-pyrophosphate
ROS	reactive oxygen species
Se	selenium
SBP2	SECIS binding protein 2
SDS	sodium dodecyl sulfate
Sec	selenocysteine
SECIS	selenocysteine insertion sequence
SelA/B/C/P/R	selenoprotein A/B/C/P/R
Ser	serine
SFFV	spleen focus forming virus
SLA	soluble liver antigen
SMCP	sperm mitochondrion-associated cysteine-rich protein
SPS2	selenophosphate synthetase 2
Tam	4-hydroxytamoxifen
TAPe	enhanced tandem affinity purification
TNF	tumour necrosis factor
Toc	$\alpha$ -tocopherol
Trp	tryptophan
Trx	thioredoxin
TrxR	thioredoxin reductase
VitE	vitamin E
WT	wild type

## **1 Introduction**

### **1.1 The mammalian selenoproteome**

Selenium (Se) is an important trace element for some eubacteria, archaea and eukaryotes that exerts its biological functions mainly through its direct incorporation into selenoproteins as a component of the 21<sup>st</sup> amino acid selenocysteine (Sec). Sec is part of the reactive centre in most selenoproteins and comprises a higher reactivity compared with its sulphur containing analogue cysteine (Cys). This has been shown by targeted mutagenesis of Sec to Cys and other amino acids in various selenoproteins, such as glutathione peroxidases (Maiorino et al., 1995) and thioredoxin reductases (Lee et al., 2000; Zhong et al., 2000), which leads to a dramatic decrease in enzyme activity. Yet, the reasons for the incorporation of Sec instead of Cys are not fully understood. Unlike the 20 amino acids of the universal genetic code, Sec is encoded by the opal codon UGA in a process that requires translational recoding, as UGA is normally translated as a stop codon (Chambers et al., 1986; Zinoni et al., 1986). Consequently, many selenoproteins have been originally misannotated due to wrong interpretations of the UGA codon as translational terminator. As a result of the rapid progression of genome sequencing and improved bioinformatic tools, the number of identified selenoproteins has increased dramatically over the last few years. Recent computational approaches revealed 310 prokaryotic selenoproteins in the largest microbial sequence dataset, the Sargasso Sea environmental genome project (Zhang et al., 2005). The functional analysis of the recently discovered selenoproteins, however, could not keep pace with the velocity of newly designated selenoproteins.

The first mammalian selenoenzyme, glutathione peroxidase 1 (GPx1), has been discovered by two independent groups in 1973 (Flohe et al., 1973; Rotruck et al., 1973). Initial *in vivo* labelling experiments with <sup>75</sup>Se-selenite in rat suggested 30-50 different mammalian Se-containing proteins (Behne et al., 1996a). Recent computational approaches, however, revealed not more than 25 mammalian selenoenzymes (table 1). This discrepancy may arise from splice variants or the use of alternative start codons on a single gene. In 2003, Kryukov et al. characterized the mammalian selenoproteome *in silico* by an algorithm, based on the identification of



predicted secondary structures of the selenocysteine insertion sequence (SECIS) and the presence of catalytically conserved Cys-containing homologues. This approach revealed 24 selenoproteins in mouse and rat, and a 25<sup>th</sup> human selenoprotein, designated GPx6 (Kryukov et al., 2003). Interestingly, GPx6 is a Cys-containing orthologue in mouse and rat. The mammalian selenoproteins investigated so far share little sequence homology and exert quite diverse enzymatic functions. Yet, some of the characterized selenoproteins can be subdivided into the families of glutathione peroxidases (GPxs), thioredoxin reductases (TrxRs) and deiodinases. All known human selenoproteins are summarized in table 1 (Kryukov et al., 2003).

**Table 1:** The human selenoproteome consists of 25 enzymes (GPx6 is a Cys-containing homologue in rodents). All known human selenoproteins are listed in alphabetical order. Deiodinases (DIs), glutathione peroxidases (GPxs), and thioredoxin reductases (TrxRs) are classified into protein families. Due to its relevance for this work GPx4 (PHGPx) is highlighted in grey (Kryukov et al., 2003).

<b>Selenoprotein</b>	<b>Chromosomal location (number of exons)</b>	<b>Sec location in protein (length of protein)</b>
15kDa	1p22.3 (5)	93 (162)
DI1	1p32.3 (4)	126 (249)
DI2	14q31.1 (2)	133 (265)
DI3	14q32	144 (278)
GPx1	3p21.31 (2)	47 (201)
GPx2	14q23.3 (2)	40 (190)
GPx3	5q33.1 (5)	73 (226)
GPx4 (PHGPx)	19p13.3 (7)	73 (197)
GPx6	6p22.1 (5)	73 (221)
H	11q12.1 (4)	44 (122)
I	2p23.3 (10)	387 (397)
K	3p21.31 (5)	92 (94)
M	22q12.2 (5)	48 (145)
N	1p36.11 (12)	428 (556)
O	22q13.33 (9)	667 (669)
P	5p12 (4)	59, 300, 318, 330, 345, 352, 367, 369, 376, 378 (381)
R	16p13.3 (4)	95 (116)
S	15q26.3 (6)	188 (189)
SPS2		60 (448)
T	3q24 (6)	36 (182)
TrxR1	12q23.3 (15)	498 (499)
TrxR2	3q21.2 (16)	655 (656)
TrxR3	22q11.21 (18)	522 (523)
V	19q13.13 (6)	273 (346)
W	19q13.32 (6)	13 (87)

Care must be taken by the interpretation of experimental results involving the overexpression of individual selenoproteins and in particular by Se depletion/repletion and supplementation studies. Alterations in cellular Se availability have significant influence on the expression of selenoproteins, which may cause a profound effect on the redox metabolism of the cell. Individual selenoproteins respond in a different manner to selenium deprivation/repletion, which has been described as the “hierarchy” of selenoprotein expression. This phenomenon has especially been investigated for members of the GPx family, revealing a specific kinetic in the loss of expression during selenium depletion as well as differences in the rate of the *de novo* synthesis of GPxs during selenium repletion (Bermano et al., 1995; Fujieda et al., 2007; Lei et al., 1995; Wingler et al., 1999). GPx1 and GPx3 expression decreased rapidly even under moderate Se-deficiency, whereas GPx2 and GPx4 expression is maintained. The relative position within the deduced hierarchy (GPx2>GPx4>GPx3=GPx1) was considered to reflect the biological significance of the respective GPx (Brigelius-Flohe, 1999). Yet, findings from knockout mice indicate that GPx4 is of major importance within the family of GPxs, GPx4 deficiency in mice causes early embryonic lethality, whereas all other GPx knockout mice are fully viable. The complexity of selenoprotein expression and especially the partial redundancy of family members demand a profound knowledge of the molecular functions of all selenoproteins, when investigated in cellular or animal model systems.

### **1.1.1 Deiodinases (DI)**

Three mammalian deiodinase enzymes have been cloned so far, which differ mainly in their biochemical activity, tissue distribution and developmental expression pattern. Deiodinases cleave specific iodine carbon bonds in thyroid hormones, thereby regulating hormonal activity. Thyroid hormones are involved in proliferation, development, differentiation and regulate most metabolic functions in vertebrates. The synthesis of thyroid hormones occurs exclusively in the thyroid gland, whose main secretory product is L-thyroxine (T<sub>4</sub>). T<sub>4</sub> is activated in the extrathyroidal tissue by type I 5'-deiodinase (5'-DI1) and type II 5'-deiodinase (5'-DI2), which catalyze the deiodination to T<sub>3</sub> (3,5,3'-triiodo-L-thyronine). Type III 5'-deiodinase (5'-DI3) inactivates the thyroid hormones T<sub>4</sub> and T<sub>3</sub> by removing iodine atoms from the inner tyrosyl ring (Kohrle, 2000).

### 1.1.2 Thioredoxin reductases (TrxR)

Thioredoxins (Trx) are small redox-active enzymes that regulate a variety of cellular processes, including cell-cell communication, redox metabolism, proliferation and apoptosis (Arner and Holmgren, 2000). Trx activity is regulated by TrxRs and NADPH as a cofactor. Three distinct genes for mammalian TrxR are known, including the cytosolic (TrxR1), the mitochondrial (TrxR2), and the testis-specific TrxR (TrxR3). TrxRs are homodimeric flavoproteins with two interacting N- and C-terminal catalytic centers. Electrons from NADPH are transferred via the FAD prosthetic group to the N-terminal Cys-containing catalytic site from where they are passed on to the Sec- and Cys-containing C-terminal catalytic site of the second TrxR molecule. The major function of TrxRs is the NADPH-dependent reduction of thioredoxin, but several other substrates have been reported (Arner and Holmgren, 2000). Due to the flexible structure of the C-terminal tail, the reduced Sec at the penultimate position of the C-terminus provides electrons to a wide range of low molecular weight compounds as well as large substrates. Targeted inactivation of either TrxR1 or TrxR2 in genetically modified mice leads to embryonic death at gestational days 10.5 and 13.5, respectively (Conrad et al., 2004; Jakupoglu et al., 2005).

### 1.1.3 Glutathione peroxidases (GPxs)

The family of mammalian GPxs includes seven isoenzymes (GPx1-7). Mammalian GPx1, GPx2, GPx3 and PHGPx (GPx4) are selenoproteins, whereas GPx6 is a selenoprotein in humans but a Cys-containing homologue in rodents. GPxs reduce  $\text{H}_2\text{O}_2$  and alkyl hydroperoxides to  $\text{H}_2\text{O}$  and their corresponding alcohols, respectively. GSH serves as electron donor, which in turn is recycled by GSH reductase and NADPH/ $\text{H}^+$  (figure 1). Yet, GSH should not be considered as the sole physiological reducing substrate for all GPxs, since GPx3 has been shown to use also thioredoxin or glutaredoxin as reductant (Bjornstedt et al., 1994).

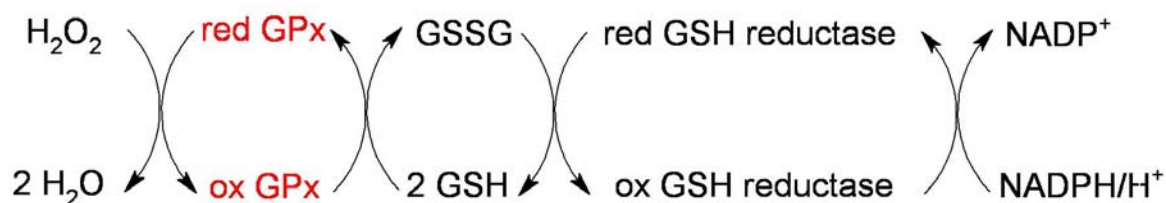


**Figure 1:** Reaction mechanism of glutathione peroxidases (GPxs). GPxs reduce hydrogen peroxide and alkyl hydroperoxides to  $\text{H}_2\text{O}$  and alcohols, respectively. Two moles of GSH are required to fully reduce one mole of GPx. Oxidized GSH (GSSG) is recycled by GSH reductase at the expense of NADPH/ $\text{H}^+$ .

The specificity for various hydroperoxide substrates differs markedly among the GPx isoforms. Whereas GPx1 reduces only soluble hydroperoxides, such as H<sub>2</sub>O<sub>2</sub> and some organic hydroperoxides, PHGPx and to some extent GPx3 also reduce phospholipid-associated hydroperoxides like phosphatidylcholine hydroperoxide. However, PHGPx is the only GPx that efficiently acts on hydroperoxides integrated in cellular membranes. GPx1, GPx2 and GPx3 are homotetramers in contrast to the smaller monomeric structure of PHGPx.

All Sec containing GPxs share the same enzymatic mechanism involving a conserved catalytic triad, consisting of Sec, Gln and Trp (figure 2). The substitution of Sec by Cys severely impairs peroxidase activity as shown for GPx1 (Rocher et al., 1992) and PHGPx (Maiorino et al., 1995) *in vitro*. Thus the relevance of Cys-containing GPx isoforms for the detoxification of peroxides is still unclear. The reduced enzyme activity of Cys-containing isoforms may account for an involvement in the regulation of enzymes with redox-sensitive motifs, such as Cys and metal co-factors.

Gene :	Sequence :	
GPx1	-----MCAARLSAAAQST-----	VYAFSARPLTGGEVPSLGLSR 034
GPx2	-----MAYIAKS-----	FYDLSAIGLDG-EKIDFNTFR 027
GPx3	MARILRASCLLSLLLAGFVPPGRGQEKSKTDCHGGMSGTIYIYEGALTDIGEEYIPFKQYA	060
GPx4	-----MCASRDDWRCARS-----	MHEFSAKDIDG-HMVCLDKYR 033
		.: .* : * . : :
GPx1	GKVLLEIENVASLUGTTIRDYTEMNDLQKRLGPRGLVVLGFPCNQFGHENGKNEEILNSL	094
GPx2	GRAVLEIENVASLUGTTTRDYNQLNELQCRF-PRRLVVLGFPCNQFGHENCQNEEILNSL	086
GPx3	GKYILFVNVASYUGLTD-QYLELNALQEELGPFGLVILGFPSNQFGKQEPGENSEILPSL	119
GPx4	GFVCIVTNVASQUGKTDVNYTQLVDLHARYAECGLRILAFPCNQFGRQEPGSNQEIK---	090
	* : . **** ** * : * :: * : . * : * . ** . **** : * . * . **	
GPx1	KYVRPGGGFEPNFTLFEKCEVNGEKAHPLFTFLRNALPTPSDDPTALMTDPKYIIWSPVC	154
GPx2	KYVRPGGGYQPTFSLTQKCDVNGQNEHPVFAYLKDCLPYPYDDPFSLMTDPKLIWSPVR	146
GPx3	KYVRPGGGFVPNFQLFEKGDVNGEKEQKQFYTFKNSCPP----TAELLGSPGRLFWPEPMK	175
GPx4	---EFAAGYNVKFDMYSKICVNGDDAHLWKWMK-----VQPK---GRGML	130
	. . . * : . * : . * **** . : . : : : . * :	
GPx1	RNDIANKNFEKFLVGPDPVRRYSRRFRFTIDIEPDIETLLSQSGNS----	201
GPx2	RSDVSNFEKFLIGPEGEPFRYSRSFQTINIEPDIKRLKVAI-----	190
GPx3	IHDRSNFEKFLVGPDPGVMRWYHRTTVSNVKMDILSYMRRQAALSARGK	226
GPx4	GNAIKSNFTKFLIDKNGCVVKRYGPMEEPQVIEKDLPCYL-----	170
	: *** *** . : * . * : : : * : :	

**Figure 2:** Amino acid sequence alignment of *murine* Sec-containing GPxs, using ClustalW V1.82 (“\*” = identical amino acid; “:” = conserved substitution; “.” = semi-conserved substitution). The conserved catalytic triad of Sec (U), Gln (Q), and Trp (W) is highlighted in red. The sequence homology of the 4 GPxs ranges between 33-60 %. PHGPx shares the least sequence homology to the other glutathione peroxidases (33–39 %).

Hydroperoxides have long been considered as mere toxic compounds, generated by electron leakage from the respiratory chain or exogenous sources like ultraviolet light, ionizing radiation, chemotherapeutic drugs, and environmental toxins (Finkel and Holbrook, 2000). Over the last couple of years, it has become apparent that hydroperoxides are not only detrimental but are also involved in the regulation of various cellular processes by changing the redox state of the cell. The cellular redox state has been reported to affect cell signalling, cell-cycle progression (Menon and Goswami, 2007), proliferation, apoptosis, and differentiation (Steinbeck et al., 1998). A well established model for redox-mediated signalling is the reversible inactivation of protein tyrosine phosphatases by oxidation, which in turn causes an activation of protein tyrosine kinase signalling (Chiarugi and Buricchi, 2007). Hydroperoxides have been implicated in the activation of NF- $\kappa$ B by TNF (Kretz-Remy et al., 1996) and IL-1 (Brigelius-Flohe et al., 1997). While apoptosis can be easily triggered by excess hydroperoxides (Hampton and Orrenius, 1998; Sandstrom et al., 1994), hydroperoxides have also been reported to enhance the rate of proliferation (Dypbukt et al., 1994). These findings have drastically changed the perspective of hydroperoxides from mere toxic metabolic by-products to important molecules which have a substantial and physiological impact on various cellular processes. GPxs have distinct roles in the defense against oxidative stress, yet redox sensing and redox regulation are interesting paradigms, which may highlight still enigmatic functions of GPxs.

#### **1.1.3.1 Glutathione peroxidase 1 (GPx1)**

GPx1 was originally discovered in 1957 (Mills, 1957) and was the first mammalian selenoenzyme described independently by two groups in 1973 (Flohe et al., 1973; Rotruck et al., 1973). It is a ubiquitously expressed, homotetrameric cytosolic enzyme (therefore also referred as cGPx), reducing H<sub>2</sub>O<sub>2</sub> and a range of organic peroxides, including cholesterol and long chain fatty acid hydroperoxides to their respective alcohols. GPx1 can only reduce free fatty acid peroxides released from phospholipids by phospholipase A2 (PLA<sub>2</sub>). GPx1 knockout mice do not show any overt phenotype under normal conditions (Ho et al., 1997), unless when challenged with electrophilic agents such as the herbicides paraquat and diquat (Cheng et al., 1998; Fu et al., 1999). GPx1-deficient mice are also more susceptible to myocardial ischemia reperfusion injury (Yoshida et al., 1997) and stroke (Crack et al., 2001). Noteworthy,

the loss of GPx1 does not influence the expression levels of GPx2 (Chu et al., 1997), GPx3 and PHGPx (Cheng et al., 1997), candidates which were considered to substitute GPx1 deficiency, at least to some extent. Hence, GPx1 appears to be dispensable under physiological conditions in mice, but essential for the protection from oxidative stress induced detriment.

Interestingly, GPx1 knockout mice infected with a benign coxsackie virus develop myocarditis. The transfer of viruses isolated from cardiomyopathic GPx1 knockout mice to normal littermates caused an identical pathology, indicating a rapid genetic mutation from an avirulent to a virulent pathogen. This may be caused by increased oxidative mutations of viral DNA in the absence of GPx1 (Beck et al., 1998; Beck et al., 1995; Diamond et al., 2001).

#### **1.1.3.2 Glutathione peroxidase 2 (GPx2)**

Only limited information is available regarding the physiological function of GPx2. GPx1 and GPx2 comprise similar substrate specificity in that they efficiently reduce H<sub>2</sub>O<sub>2</sub> or fatty acid hydroperoxides, but do not reduce phospholipid hydroperoxides. GPx2 is a homotetrameric enzyme found in liver and the epithelium of the gastrointestinal tract (therefore also referred as giGPx), suggesting an important function in the defense against ingested hydroperoxides in food. GPx2 is one of the few enzymes whose expression is well preserved under Se-deficiency, however, targeted inactivation of GPx2 in the mouse did not cause any pathological phenotype (Esworthy et al., 2000).

#### **1.1.3.3 Glutathione peroxidase 3 (GPx3)**

The extracellular GPx3 is mainly present in plasma (therefore also referred as pGPx) and intestine. GPx3 shows enzymatic activity towards phospholipid hydroperoxides, and thus may be implicated in protecting outer cell membranes from lipid peroxidation (Yamamoto et al., 1993). In humans, GPx3 is mainly expressed in kidney, and to a minor extent in heart, lung and other tissues (Ursini et al., 1985). High expression and secretion of GPx3 into renal tissue led to the hypothesis that the kidney is the main site of GPx3 function (Avisar et al., 1994), albeit its physiological function has not yet been resolved. Whether GPx3 is a mere antioxidant enzyme is not clear, since no efficient reductant for GPx3 in the plasma has been identified

(Bjornstedt et al., 1994). GPx3 has been considered as a regulator of the host's defense reaction by counteracting the oxidative burst of stimulated phagocytes, which in turn may activate lipoxygenases (LOXs) and cyclooxygenases (COXs) that produce inflammatory mediators (Brigelius-Flohe, 1999).

#### **1.1.3.4 Phospholipid hydroperoxide glutathione peroxidase (PHGPx)**

Due to its relevance for this work, PHGPx will be discussed in detail below (see chapter 1.4).

#### **1.1.3.5 Other glutathione peroxidases**

GPx5 is a non-Sec containing isoform which is exclusively found in the epididymis (Schwaab et al., 1998; Vernet et al., 1996). In general, Cys-containing isoforms generally comprise a relatively low peroxidase activity compared to their Sec-containing counterparts, thus its function as a putative GPx is still debated. GPx6 has been discovered only recently as a human selenoprotein with Cys homologues in rodents. GPx6 transcripts were only detected in embryos and in the olfactory epithelium (Kryukov et al., 2003). GPx7 is an additional non-Sec-containing cytoplasmic isoform with barely detectable GPx activity *in vitro* (Utomo et al., 2004).

#### **1.1.4 Other selenoproteins**

The plasma glycoprotein selenoprotein P (SeIP) contains up to 10 Sec residues per polypeptide chain, depending on intracellular Sec availability (Hill et al., 1991). It is the only known selenoprotein containing more than one Sec residue. Efficient Sec incorporation (figure 3) in SeIP is achieved by two different types of SECIS elements in the 3'-untranslated region of SeIP mRNA. The vast majority of SeIP is secreted by the liver, providing more than 50 % of total plasma selenium. This rendered SeIP a transport and storage protein for selenium in mammals; but antioxidant and heavy metal chelating functions are discussed as well. Interestingly, SeIP gene disruption in transgenic mice leads to 80-90% decrease in Se-plasma levels and the activities of various selenoproteins drop significantly in brain, kidney and testis (Hill et al., 2003; Schweizer et al., 2004a). While Se-deficiency does not impair embryonic development, approximately three weeks post partum, knockout mice showed reduced weight gain, sporadic fatalities, and symptoms like ataxia (Schomburg et al., 2003). Yet, most symptoms could be overcome by feeding mice with a Se-enriched

diet (Hill et al., 2003). These findings render SelP dispensable for survival under conditions when sufficient inorganic Se is provided by food, e.g. breast feeding from mother to offspring (Schweizer et al., 2004b).

The Selenoprotein R (SelR) is a methionine-R-sulfoxide reductase that exists only in vertebrates, but Cys-containing homologues in other eukaryotes and prokaryotes exist (Kryukov et al., 2002). Thioredoxin provides reducing equivalents for SelR.

Selenophosphate synthetase 2 (SPS2) catalyzes the formation of mono-selenophosphate from inorganic selenium sources, required for tRNA<sup>[Ser]Sec</sup> synthesis. The tRNA<sup>[Ser]Sec</sup> is essential for co-translational Sec incorporation into nascent polypeptide chains (refer to chapter 1.2).

Functional and structural data is still very limited for many selenoproteins, including selenoprotein 15 kDa, GPx6, H, I, K, M, N, O, S, T, V and W. Reasons are either their very recent discovery and also general technical difficulties in the analysis of selenoprotein function due to their relatively low abundance in cells and tissues.

## **1.2 The biosynthesis of selenoproteins**

Sec incorporation into the nascent polypeptide chain occurs during ribosomal translation; however, it is far more complex as compared to the classical incorporation of the other 20 amino acids. Sec is encoded by the UGA codon in a process that requires translational recoding, since UGA is usually translated as a Stop codon. Sec incorporation requires a specific *cis*-acting mRNA secondary structure, the SECIS element, and at least 5 different gene products (SelC, SelA, SPS, SBP2, EFsec) in eukaryotes.

### **1.2.1 Sec-tRNA biosynthesis (SelA, SelC, SPS)**

The biosynthesis of the Sec-specific tRNA is distinctive from the other 20 amino acids, in that its synthesis always occurs on its tRNA. The Sec biosynthesis pathway and its incorporation into the nascent polypeptide chain have been elucidated in great detail in *E. coli* in the early nineties mainly by Böck's group (LMU Munich), but



the exact mechanism in mammals still awaits final completeness. The SelC gene (Trsp in mammals) encodes a unique tRNA<sup>[Ser]Sec</sup> that becomes initially aminoacylated with Ser by serine synthetase in both prokaryotes and eukaryotes (Park et al., 1997). Disruption of SelC in transgenic mice causes early embryonic death (E6.5), highlighting the importance of at least one selenoprotein during early mammalian development (Bosl et al., 1997). The Ser-loaded tRNA<sup>[Ser]Sec</sup> serves as scaffold for Sec synthesis. In *E. coli*, the SelA gene product, selenocysteine synthase, converts Ser-tRNA<sup>[Ser]Sec</sup> to Sec-tRNA<sup>[Ser]Sec</sup> in a two-step reaction, involving removal of the hydroxyl-group from Ser and the addition of mono-selenophosphate. Bacterial selenocysteine synthase has been identified several years ago but its eukaryotic counterpart is still unknown. Mono-selenophosphate, the activated form of selenium, is synthesized from selenide and ATP by selenophosphate synthetase (SPS) (Glass et al., 1993). Two mammalian SPS isoforms, designated as SPS1 and SPS2, have been cloned (see also chapter 1.1.4). Interestingly, SPS2 is a selenoprotein which may auto-regulate selenoprotein synthesis in a negative feedback mechanism (Guimaraes et al., 1996).

### **1.2.2 Co-translational Sec incorporation (SECIS, EFsec, SBP2, SelB)**

Since the UGA codon comprises a dual role in cell biology, several *cis*- and *trans*-acting factors are required to discriminate between Stop and Sec codon. Those factors include (i) the *cis*-acting stem-loop structure in the mRNA sequence of selenoproteins, designated the SECIS element and two *trans*-acting factors, (ii) the SECIS Binding Protein (SBP2) (Copeland et al., 2000), and (iii) the Sec-specific elongation factor (EFsec or SelB) (Fletcher et al., 2001). The efficiency of Sec insertion has been determined for the bacterial formiat dehydrogenase and is rather low, ranging around 4 % compared to the incorporation of other amino acids. This has been nicely shown by mutating the Sec codon to a Ser codon, which increased the amino acid insertion efficiency to 95 % (Suppmann et al., 1999).

Eukaryotic and archaeal SECIS elements are located in the 3' untranslated region of the selenoprotein mRNA (figure 3). The distance of the UGA codon and the SECIS element can be as far as 4000 bp (Buettner et al., 1998), whereas in prokaryotic mRNAs the SECIS element is located just downstream of the UGA codon as part of the coding region of the selenoprotein. Eukaryotic SECIS elements are composed of

two helices, an internal and apical loop, and a conserved non-Watson-Crick interacting nucleotide quartet, located at the base of helix 2. Some large apical loops contain an additional ministem that presumably stabilizes the SECIS element.

SBP2 is recruited in eukaryotic cells by the SECIS element to form a stable SECIS-SBP2 complex (Copeland et al., 2000; Low et al., 2000). SBP2 binds the elongation factor EFsec, which in turn recruits Sec-loaded  $\text{tRNA}^{\text{Ser}^{\text{Sec}}}$  (Fagegaltier et al., 2000; Tujebajeva et al., 2000). This complex translocates to the ribosome, where  $\text{tRNA}^{\text{Ser}^{\text{Sec}}}$  is released to the ribosomal A-site by GTP hydrolysis. Recently, the eukaryotic ribosomal protein L30 has been implicated in Sec incorporation (Chavatte et al., 2005). L30 is considered to replace SBP2 upon binding of the complex to the ribosome, triggering the release of  $\text{tRNA}^{\text{Ser}^{\text{Sec}}}$ . Eventually, the polypeptide chain at the P-site is transferred to the  $\text{tRNA}^{\text{Ser}^{\text{Sec}}}$ , forming a peptide bond with Sec. The elongation factor EFsec is specific for Sec incorporation and differs from EF-Tu, which is involved in the aminoacyl-tRNA delivery of the other 20 amino acids. SBP2 along with EFsec constitute the functional equivalent of a single elongation factor in prokaryotic selenoprotein synthesis, designated SelB (Forchhammer et al., 1989).

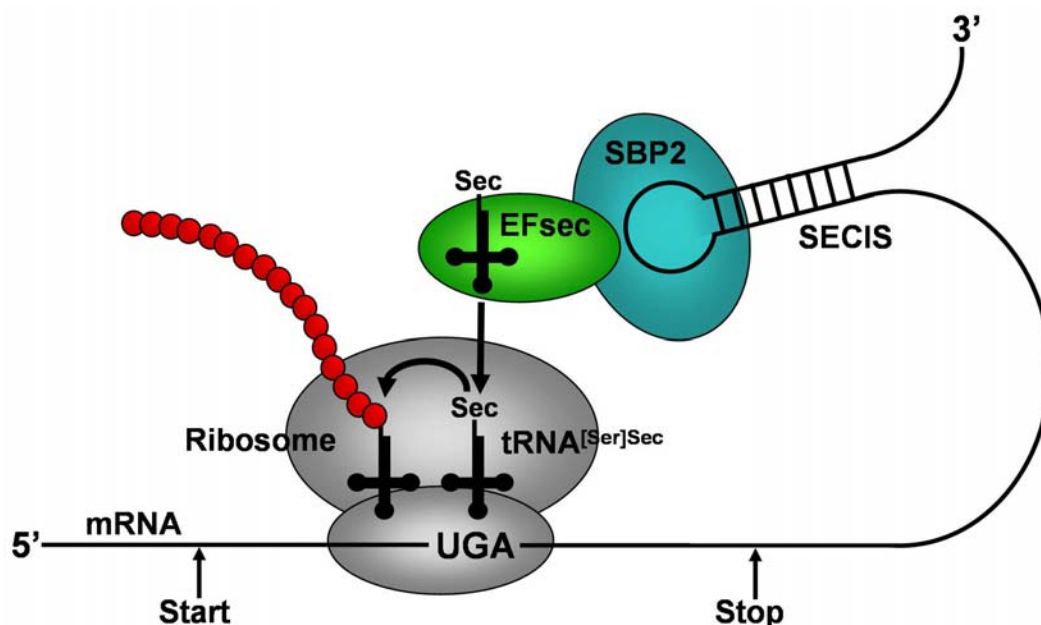


**Figure 3:** Mechanism of mammalian Sec incorporation. The  $\text{tRNA}^{\text{Ser}^{\text{Sec}}}$  (black shamrock shape), carrying Sec, is depicted in a complex with EFsec (green), SBP2 (blue) and the SECIS element (black hairpin loop). This complex translocates  $\text{tRNA}^{\text{Ser}^{\text{Sec}}}$  to the ribosomal A-site, encoded by an in-frame UGA codon in the mRNA sequence. Released  $\text{tRNA}^{\text{Ser}^{\text{Sec}}}$  provides Sec for the ribosomal elongation reaction in which Sec is incorporated into the nascent polypeptide chain (red) by peptide bond formation. Translational start and stop codons of the translated mRNA are indicated by black arrows.

Recently two additional eukaryotic proteins, SECp43 and soluble liver antigen (SLA), have been implicated in selenoprotein biosynthesis. SECp43 and SLA form a complex with tRNA<sup>[Ser]Sec</sup>. Targeted knockdown of both factors reduced overall selenoprotein biosynthesis (Xu et al., 2005), but detailed characterization of both factors requires further studies.

### **1.3 GSH biosynthesis and the Cys/(Cys)<sub>2</sub>-cycle**

#### **1.3.1 Cellular functions of GSH**

GPxs belong to a class of GSH-dependent redox enzymes, mainly using electrons from the reducing equivalent GSH. The tripeptide GSH (L-gammaglutamyl-L-cysteinylglycine) is the predominant non-protein sulfhydryl compound in the cell. It is present in millimolar concentrations (up to 10 mM) and exists predominantly in its reduced form. The oxidised form of GSH consists of two GSH molecules (GSSG), connected by a disulfide bond and represents about 1 % of the overall GSH pool under normal conditions. GSH is the major endogenous scavenger of reactive oxygen species (ROS) in the cell, by acting as a reducing equivalent for GPxs and other GSH-dependent detoxifying enzymes (figure 1).

Beyond its antioxidant activity, GSH exerts several other cellular functions. Glutaredoxins are relatively small GSH-dependent thiol-disulfide oxidoreductases that can reduce protein disulfides or mixed disulfides between proteins and GSH (Holmgren, 1979a, b). Glutathionylation of proteins has emerged as a novel regulatory mechanism of signalling cascades by reversible protein thiol modification. This modification is believed to act as a redox-sensing mechanism under conditions of oxidative stress (Fernandes and Holmgren, 2004). Glutaredoxins are also involved in DNA synthesis by reducing ribonucleotide reductase. Glutathione-S-transferases represent a family of GSH-dependent enzymes that mainly detoxify xenobiotics by GSH conjugation (Hayes and Pulford, 1995; Mannervik and Danielson, 1988). These enzymes have also been implicated in the protection against lipid peroxidation as a second line of defense behind catalases, superoxide dismutases, and GPxs (Sharma et al., 2004). GSH also acts as a reservoir for intracellular Cys, as the free form of Cys is considered to be toxic.

### 1.3.2 The $\gamma$ -glutamyl and the Cys/(Cys)<sub>2</sub> cycle of GSH biosynthesis

GSH is synthesized intracellularly in a two step mechanism by the rate-limiting enzyme  $\gamma$ -glutamylcysteine synthetase ( $\gamma$ -GCS) and glutathione synthase (GSH-S) from cysteine (Cys), glutamate (Glu) and glycine (Gly). The importance of GSH for mammalian life has been demonstrated by targeted deletion of  $\gamma$ -GCS in mice.  $\gamma$ -GCS-deficient mice lack GSH biosynthesis and fail to develop beyond embryonic day 7.5. (Shi et al., 2000). The enzymatic activity of  $\gamma$ -GCS can efficiently be blocked by the chemical inhibitor L-buthionine sulfoximine (BSO). The rate-limiting substrate for GSH biosynthesis is Cys. Reduced Cys can be transported into the cell by the unspecific amino acid transport system ASC (a shared amino acid transporter for Ala, Ser, and Cys), whereas oxidised cystine (Cys)<sub>2</sub> (figure 4) can only be transported by the Glu/(Cys)<sub>2</sub> exchange system, system x<sub>c</sub><sup>-</sup>.

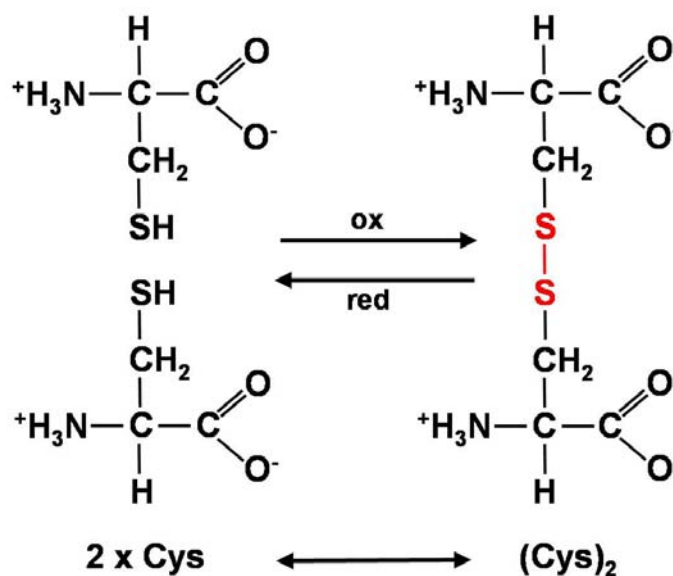


**Figure 4:** The reversible oxidation of cysteine (Cys) to cystine ((Cys)<sub>2</sub>). (Cys)<sub>2</sub> is formed by the oxidation of two molecules Cys.

The Glu/(Cys)<sub>2</sub> antiporter, system x<sub>c</sub><sup>-</sup>, consists of two protein components, xCT light chain and 4F2 heavy chain, whereas xCT mediates transport specificity (Sato et al., 1999). System x<sub>c</sub><sup>-</sup> transports one mole (Cys)<sub>2</sub> into the cell in exchange of one mole Glu (figure 5), which can be inhibited by high concentrations of extracellular Glu (Bannai, 1986). The reducing environment inside the cell rapidly reduces (Cys)<sub>2</sub> to Cys, which is used for GSH or protein biosynthesis. A part of intracellular Cys is released back into the medium via neutral amino acid transport systems, where it is rapidly oxidized to (Cys)<sub>2</sub> by oxygen in the medium. Thus, system x<sub>c</sub><sup>-</sup> is regarded as a major part of the Cys/(Cys)<sub>2</sub> cycle, essential for the maintenance of the Cys/(Cys)<sub>2</sub>

redox balance (Bannai et al., 1989) as well as cellular GSH levels (Bannai and Tateishi, 1986). xCT knockout mice are healthy in appearance and fertile, but isolated fibroblasts die in cell culture, if not supplemented with thiol-containing compounds (Sato et al., 2005). Thus, system  $x_c^-$  seems to be dispensable for mammalian development although it is vitally important for cells cultivated *in vitro*. Of note, certain cell types (e.g. B and T cells) have a very limited  $(Cys)_2$  uptake capacity due to low expression levels of xCT. This renders B cells and Burkitt lymphoma cells dependent on reduced Cys, which must be provided by feeder cells or thiol-containing supplements (Falk et al., 1993). Recently, Sakakura et al., showed that xCT is expressed in activated neutrophils, indicating that system  $x_c^-$  protects neutrophils from generated ROS during host defense (Sakakura et al., 2007).

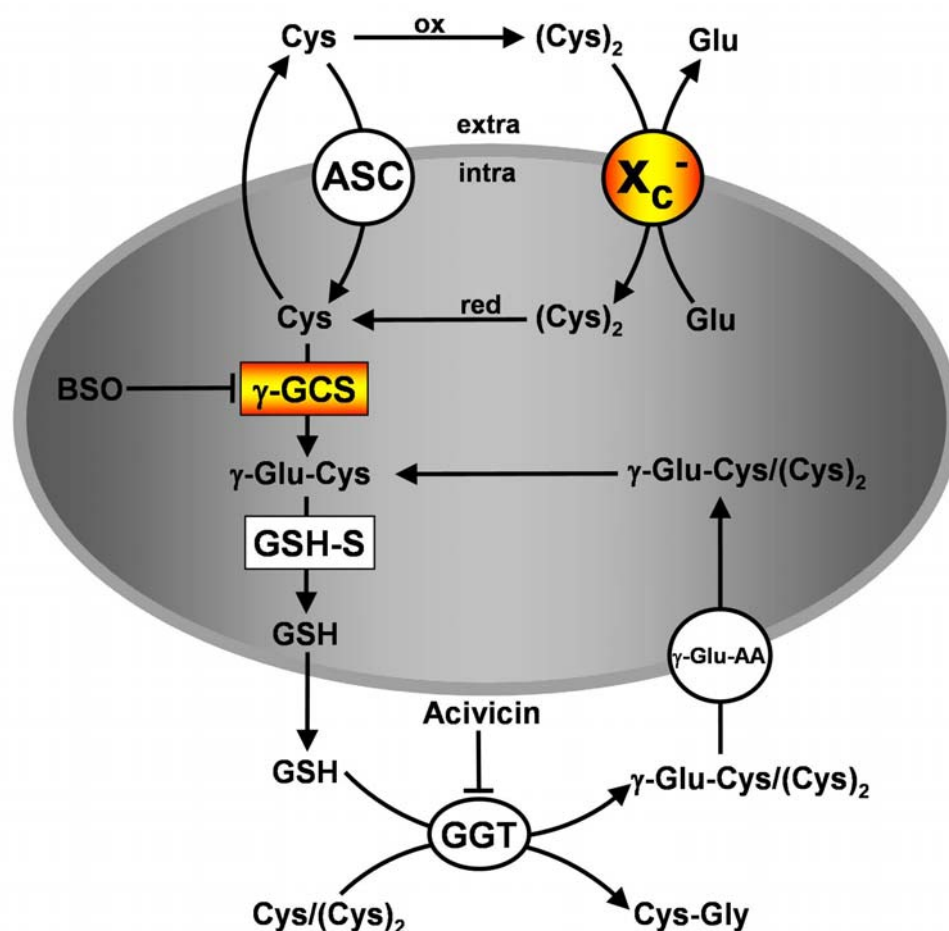


**Figure 5:** The  $\gamma$ -glutamyl and the  $Cys/(Cys)_2$  cycle of glutathione (GSH) biosynthesis. *De novo* GSH biosynthesis is catalysed from Cys, Glu and Gly by the rate-limiting enzyme  $\gamma$ -GCS and GSH-S. The rate limiting substrate of the *de novo* GSH biosynthesis is Cys. Cys is transported into the cell by the transport system ASC and in its oxidized form  $(Cys)_2$  by system  $x_c^-$ , respectively. Intracellular Cys is partially secreted by neutral amino acid transport systems. The salvage pathway of GSH biosynthesis is mediated by GGT and the  $\gamma$ -Glu-AA transport system, bypassing the rate limiting step of  $\gamma$ -glutamylcysteine synthesis. For further details please refer to text.

Extracellular GSH levels are rather low, yet the export of GSH provides a salvage pathway of GSH biosynthesis, bypassing the rate-limiting step of  $\gamma$ -glutamylcysteine synthesis. This pathway recycles secreted GSH, by recovering Cys-containing cleavage products and is independent from system  $x_c^-$ . Synthesized GSH translocates to the membrane bound  $\gamma$ -glutamyl transpeptidase (GGT), which catalyses the transfer of the  $\gamma$ -glutamyl moiety to reduced Cys or its oxidised form (Cys)<sub>2</sub>, forming  $\gamma$ -glutamyl-cysteine/cystine ( $\gamma$ -Glu-Cys/(Cys)<sub>2</sub>) and cysteinylglycine (Cys-Gly). GGT can be blocked by the chemical inhibitor acivicin.  $\gamma$ -Glu-Cys/(Cys)<sub>2</sub> is taken up by a  $\gamma$ -glutamyl amino acid transporter ( $\gamma$ -Glu-AA), whereas Cys-Gly can be cleaved by dipeptidases, releasing Cys.

## **1.4 Phospholipid hydroperoxide glutathione peroxidase (PHGPx, GPx4)**

### **1.4.1 The genetic and molecular structure of PHGPx**

PHGPx was first purified from pig liver in 1982 by Ursini et al. and characterized as a protein efficiently protecting liposomes and biomembranes from peroxidative degradation in the presence of GSH (Ursini et al., 1982). PHGPx shares the least sequence homology with the other GPxs and significantly differs from its family members in terms of its monomeric structure, relatively low substrate specificity, and its necessity for mouse development (Imai and Nakagawa, 2003; Yant et al., 2003).

Three distinct forms of mammalian PHGPx exist, revealing different subcellular localization and distinct tissue-specific expression. Any of these forms is expressed from its own promoter (figure 6). Alternative transcription initiation leads to formation of either the short cytosolic form (20 kDa), the mitochondrial form (23 kDa) with an N-terminal mitochondrial leader sequence, and the 34 kDa nuclear form of PHGPx (nPHGPx), previously referred to as sperm nuclei-specific GPx (SnGPx) (Pfeifer et al., 2001). The alternative exon (Ea) encodes a nuclear targeting sequence. The cytosolic form of PHGPx is ubiquitously expressed, whereas the mitochondrial and the nuclear form are predominantly expressed in testis (Pfeifer et al., 2001; Pushpa-Rekha et al., 1995; Schneider et al., 2006).

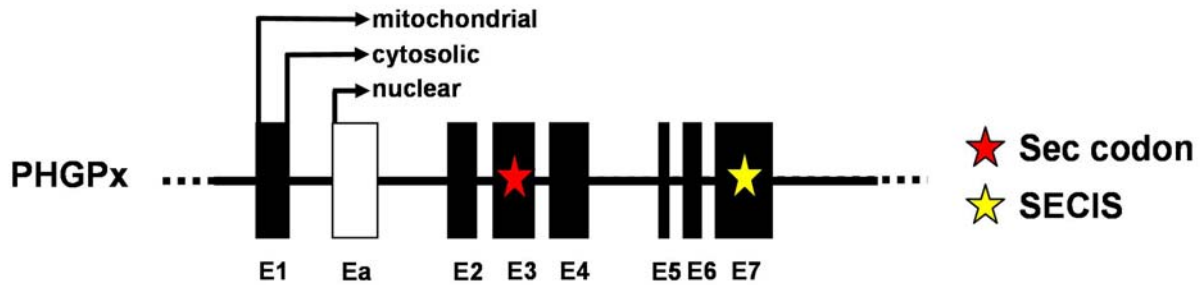


**Figure 6:** Genomic DNA structure of mammalian PHGPx. PHGPx consists of 7 regular exons (E) and one additional exon, located between exon 1 and exon 2. The mitochondrial and cytosolic start codons are encoded by E1. The sperm nuclei specific form of PHGPx is transcribed from the alternative exon (Ea). The Ea encodes a nuclear targeting signal and clusters of basic amino acids, which most probably allow binding of PHGPx to DNA. The Sec codon (red asterisk) is encoded by exon 3. The SECIS element (yellow asterisk) is located on exon 7.

In mice, the amino acid sequence homology of PHGPx compared with the other Sec-containing GPxs is less than 40 %, yet they share conserved motifs that include the catalytic triad of Sec, Gln and Trp. This conserved triad has been shown to form a catalytic centre in which the selenol group of Sec is stabilized and activated by hydrogen bonds, provided by the Gln and Trp residues (Maiorino et al., 1995). An initial mutational and biochemical approach by Maiorino et al. revealed that the conversion of Sec to Cys causes a decrease of PHGPx activity by about three orders of magnitude in the recombinant protein (Maiorino et al., 1995).

#### 1.4.2 The catalytic mechanism of PHGPx

The catalytic mechanism is similar in all GPxs, involving redox shuttling of the Sec residue within the active site (figure 7). The dissociated selenol (-SeH) from Sec is oxidized by hydroperoxides to yield a selenenic acid (-SeOH). The selenenic acid reacts with a free thiol (-SH), typically GSH, to form an intermediate selenodisulfide, which in turn is resolved by a second GSH molecule. In contrast to the other GPxs, PHGPx activity does not solely rely on GSH as a reducing equivalent but also reacts with thiols from proteins, in particular when GSH is limiting as evident in mature spermatozoa (see chapter 1.4.3.2) (Conrad et al., 2005). Whether PHGPx specifically regulates thiol-containing compounds by oxidation is still a matter of debate.

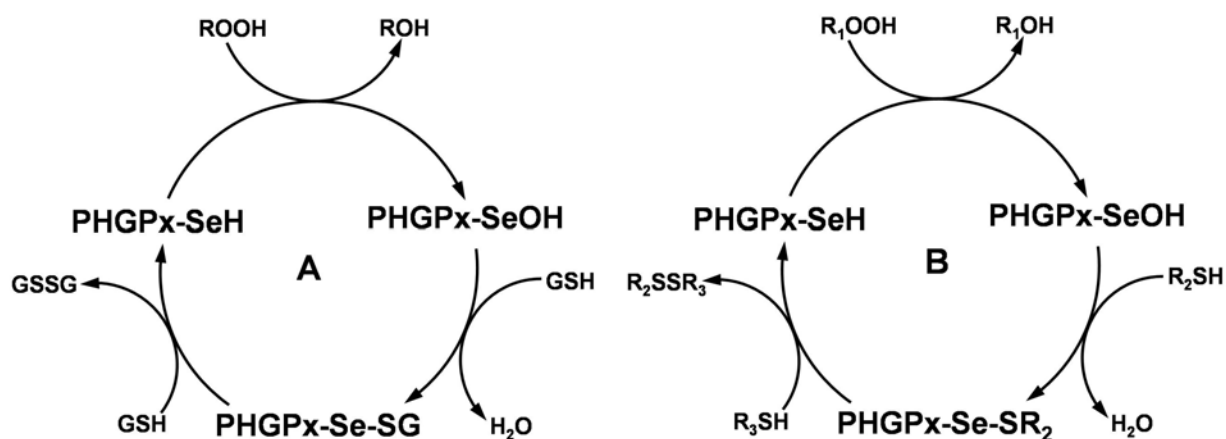


**Figure 7:** The catalytic cycle of PHGPx. The PHGPx selenol (PHGPx-SeH) is oxidized by hydroperoxides to selenenic acid (PHGPx-SeOH), following reduction to an intermediate selenodisulfide with GSH (A) or other thiol containing molecules (B). PHGPx is reconstituted to its active state by a second reducing equivalent, yielding an oxidized GSH dimer (GSSG) or other disulfides.

In view of reducing and oxidising substrates, PHGPx is the least specific GPxs. Hydrogen peroxide and lipid hydroperoxides are both common substrates for all GPxs. In addition, PHGPx can efficiently reduce phospholipid hydroperoxides within biological membranes. Hence, PHGPx has been implicated in the protection of cellular membranes against oxidative damage. Two features may account for the low substrate specificity of PHGPx. Firstly, PHGPx acts as a monomer and the active site selenol is displayed on a hydrophobic surface of the enzyme. Secondly, arginine residues that direct GSH to the active site are present in GPx1, GPx2 and GPx3, but are missing in PHGPx. Instead, two lysine residues (Lys-48, Lys-125), supposedly less specific for GSH, guide the sulphur atom of various thiol-containing molecules to the active site of PHGPx (Mauri et al., 2003; Roveri et al., 2001; Ursini et al., 1999; Ursini et al., 1997).

### 1.4.3 The cellular functions of PHGPx

#### 1.4.3.1 PHGPx as an anti-apoptotic factor

PHGPx was originally described as a protein which protects liposomes and biomembranes from peroxidation and was thus implicated in the protection of biomembranes against oxidative stress (Ursini et al., 1982). Over the last couple of years it became evident that PHGPx protects cells against various apoptotic stimuli, such as prooxidants, DNA damaging agents, glucose depletion, and UV-irradiation



(Arai et al., 1999; Imai et al., 1996; Nomura et al., 1999; Shidoji et al., 2006; Yagi et al., 1996). PHGPx has been cloned by our group in an expression cloning approach as an enzyme protecting Burkitt's lymphoma cells from cell death imposed by seeding cells at low cell density (Brielmeier et al., 2001). Specific inactivation of PHGPx in mice causes early embryonic lethality at E7.5 (Imai et al., 2003; Imai and Nakagawa, 2003; Yant et al., 2003), but the biological reasons are unclear. Studies with primary mouse embryonic fibroblasts (MEFs) isolated from PHGPx knockout mice revealed that heterozygous PHGPx knockout cells (PHGPX<sup>(wt/-)</sup>) are more susceptible to oxidative stress induced cell death, compared to their wild-type counterparts (Yant et al., 2003). However, PHGPx has not only antioxidant functions but plays an important role in other cellular processes, such as sperm maturation and redox regulation.

#### **1.4.3.2 PHGPx and spermatogenesis**

Early studies with Se-depleted rodents demonstrated the importance of Se for male fertility. Severe Se deficiency causes structural abnormalities of sperm, such as broken midpiece of sperm tails, giant heads and reversible testicular atrophy (Behne et al., 1996b; Watanabe and Endo, 1991). Due to its particularly high expression level in testis, PHGPx has been considered to account for most of the structural and morphological defects in the midpiece and head region of mature spermatozoa, as well as reversible testicular atrophy observed under severe Se deficiency.

In fact, PHGPx has been shown to comprise several functions during sperm maturation. Besides its GSH-dependent peroxidase activity during the early phase of spermatogenesis, PHGPx acts as a major structural component (approximately 50% of total protein) of the mitochondrial capsule of the midpiece in mature spermatozoa (Ursini et al., 1999). PHGPx initiates polymerisation of the mitochondrial capsule by oxidising sperm mitochondrion-associated cysteine-rich protein (SMCP) (Maiorino et al., 2005). Due to the lack of remaining reducing equivalents, PHGPx eventually polymerizes by cross-linking between the Sec<sup>46</sup> and Cys<sup>148</sup> on the surface of the protein, but also heteropolymers with SMCP have been reported (Roveri et al., 2001; Ursini et al., 1999). The polymerisation process leads to the loss of PHGPx activity, converting it into a structural protein. PHGPx has also been implicated in chromatin condensation of maturing spermatozoa. The deduced amino acid composition of the

alternative exon (Ea) shows a striking similarity with protamines. This finding suggests a similar binding mechanism of nPHGPx to DNA like protamines and a role in chromatin condensation by thiol oxidation (Pfeifer et al., 2001). Recent experiments with transgenic mice, specifically lacking the nuclear form of PHGPx, revealed that nPHGPx contributes to the structural stability of sperm chromatin. Thereby nPHGPx acts as a protein thiol peroxidase, but this function appeared not to be essential for male fertility (Conrad et al., 2005). Despite its remarkably high expression in testis, final evidence that PHGPx plays an essential role in spermatogenesis, has still been lacking. Final proof will be provided by ongoing studies in our laboratory, in which targeted disruption of the mitochondrial form of PHGPx causes sterility in male mice (Schneider et al., submitted).

#### **1.4.3.3 A regulatory role for glutathione peroxidases in arachidonic acid metabolism**

GPxs and PHGPx have been considered to control the activities of lipoxygenases (LOXs) and cyclooxygenases (COXs), key enzymes of arachidonic acid metabolism (figure 8). Arachidonic acid, mainly released from biomembranes by phospholipase A<sub>2</sub> (PLA<sub>2</sub>), is a common substrate of both types of enzymes. COXs convert arachidonic acid into an unstable hydroperoxide intermediate, prostaglandin G<sub>2</sub> (PGG<sub>2</sub>) and subsequently to PGH<sub>2</sub>, the precursor of various prostanoids (Funk, 2001). LOXs oxygenate arachidonic acid at different positions and the resulting hydroperoxyeicosatetraenoic acids (HPETE) are subsequently reduced either to hydroxyeicosatetraenoic acid (HETE) or transformed into leukotrienes, hepoxilins and lipoxins (Funk and Cyrus, 2001).

Both types of enzymes require peroxides and/or hydroperoxyl-intermediate metabolites for initial activation and full activity (Ivanov et al., 2005). Inactive LOXs contain a single iron in the ferrous oxidation state (Fe<sup>2+</sup>), whereas active LOXs contain an iron in the ferric oxidation state (Fe<sup>3+</sup>). The conversion of the ferrous to the ferric state may be triggered by small amounts of peroxides, including HPETEs (Zhang et al., 1994). Since PHGPx controls the cellular peroxide tone and efficiently reduces alkylhydroperoxides, including HPETEs, PHGPx has been regarded as a key enzyme, antagonizing LOX and COX activities.

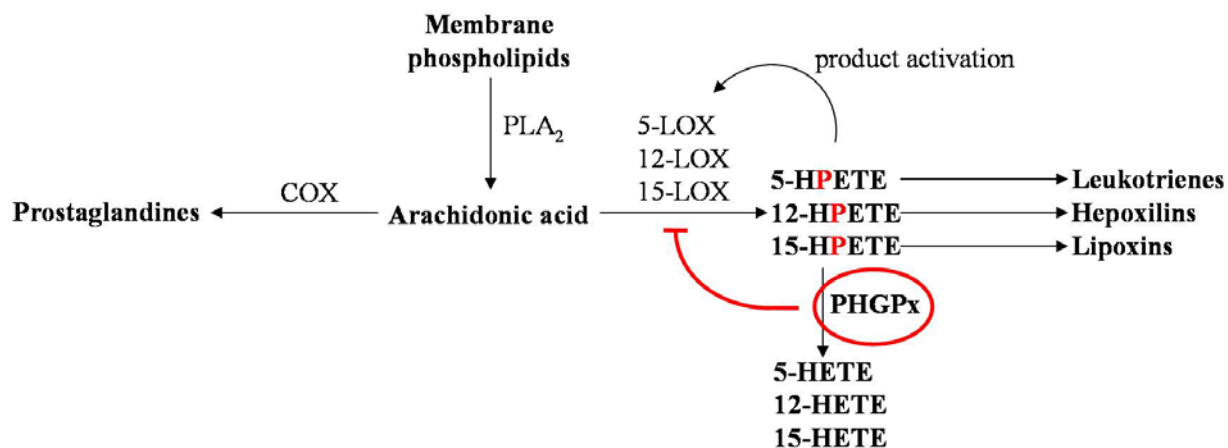


**Figure 8:** Arachidonic acid metabolism. Arachidonic acid is a substrate for COXs and LOXs, which is released from membranes by PLA<sub>2</sub>. LOXs catalyze the production of HPETEs, peroxy intermediates which are either isomerized to leukotrienes, hepoxilins or lipoxins. HPETEs can also be converted to HETEs by the peroxidase activity of GPxs. LOXs and COXs need a certain peroxide tone for initial and full activation, and thus PHGPx has been considered as a counteracting enzyme of eicosanoid production.

Initial evidence for an antagonistic role for PHGPx in arachidonic acid metabolism was provided by Se depletion and repletion studies *in vitro* as well as *in vivo*. Down-regulation of PHGPx by selenium depletion inversely correlated with 5-LOX activity in RBL-1 cells (Weitzel and Wendel, 1993). A similar effect has been reported for human B lymphocytes after GSH depletion (Jakobsson et al., 1992). A reverse effect was observed by PHGPx overexpression in RBL-2H3 cells, causing decreased leukotriene production upon treatment with the Ca<sup>2+</sup>-ionophore A23187 (Imai et al., 1998). Likewise, PHGPx knockdown was associated with up-regulation of 12-LOX and COX1 activity in human epidermoid carcinoma A431 cells (Chen et al., 2003). Moreover, the inactivation of PHGPx by iodoacetate in human platelets inhibited 12-HETE production by 80% (Sutherland et al., 2001). COX1 and COX2 are inhibited in PHGPx overexpressing RBL-2H3 cells, whereas COX activity could be restored by either BSO-mediated inhibition of PHGPx (COX2) or upon the addition of 15-HPETE (COX1) (Sakamoto et al., 2000). A systematic *in vitro* assay with purified LOXs, COXs and PHGPx showed that PHGPx inhibits the activity of any tested arachidonic acid oxidases (5-/12-/15-LOX, COX1/2) to a certain extent. 15-LOX, however, proved to be most sensitive to PHGPx-mediated inactivation (Huang et al., 1999). Interestingly, 12-LOX activity could be restored by the addition of lipid hydroperoxides 13-HPODE, supporting the idea that PHGPx antagonizes the product activation of LOXs and COXs by reducing hydroperoxide products that are produced by the arachidonic acid metabolism itself. Nevertheless, LOX and COX activation may also

be triggered by peroxides from other cellular sources, such as electron leakage from the respiratory chain, or even ROS produced by exogenous stimuli, such as UV-irradiation and oxidising chemicals.

## **1.5 Objectives**

Glutathione is the major scavenger of ROS, by acting as the reducing equivalent for GPxs and other antioxidant enzymes. It is well known that GSH is rapidly consumed under conditions of oxidative stress, leading to severe damage of cells and tissue. However, it has still been a matter of debate, whether oxidative stress-induced cell death is caused by a pleiotropic effect of accumulated ROS or by a distinct signalling cascade. Since PHGPx is considered as one of the most significant GSH-dependent enzymes, targeted PHGPx disruption in cells promised to be an ideal tool to address this question. To bypass early embryonic lethality of PHGPx-deficient mice, the main objective of this work was the production and analysis of an inducible knockout model for PHGPx, including transgenic MEFs and an inducible Cre/loxP system. The physiological functions of PHGPx should then be analysed after targeted PHGPx disruption in cells, with special emphasis on the accumulation of ROS, the impact on arachidonic acid metabolism, as well as the mechanism of oxidative stress-induced cell death.

To gain further insights into the complex system of GSH-dependent enzymes,  $\gamma$ -GCS knockout cells deficient in GSH biosynthesis, should be included in these studies. GSH has long been considered being indispensable for cell survival. Thus it should be addressed, whether cells survive in the absence of GSH, provided that sufficient cysteine is available as an alternative reducing equivalent by overexpressing antiporter system  $x_c^-$ . This experiment should proof the existence of a putative back-up system under conditions of oxidative stress and concomitant GSH depletion. Thus, these studies should reveal the mechanism of oxidative stress-induced cell death, which is a common signature of many degenerative disorders, such as atherosclerosis, Alzheimer's disease, Parkinson's disease, and accounts for ischemia and reperfusion-induced detriment during myocardial infarction and stroke.

## 2 Materials

Chemicals	Company	Catalog-No.
AA-861	Sigma-Aldrich GmbH, Taufkirchen, Germany	A3711
Acivicin	Sigma-Aldrich GmbH, Taufkirchen, Germany	A2295
Acrylamide	Bio-Rad, Munich, Germany	161-0158
Agarose, electrophoresis grade	Invitrogen, Karlsruhe, Germany	15510-027
Agarose, low melting point	Fermentas GmbH, St. Leon-Rot, Germany	R0801
$\alpha$ -Lipoic acid	Sigma-Aldrich GmbH, Taufkirchen, Germany	T1395
Ammonium persulfate	Sigma-Aldrich GmbH, Taufkirchen, Germany	A3678
Ampicillin	Sigma-Aldrich GmbH, Taufkirchen, Germany	A9518
Arachidonic acid	Sigma-Aldrich GmbH, Taufkirchen, Germany	A9673
$\alpha$ -Tocopherol (Toc)	Sigma-Aldrich GmbH, Taufkirchen, Germany	T3251
Baicalein	Sigma-Aldrich GmbH, Taufkirchen, Germany	465119
$\beta$ -Mercaptoethanol (2-ME)	Roth Carl GmbH & Co., Karlsruhe, Germany	4227.1
BODIPY 581/591 C <sub>11</sub>	Invitrogen, Karlsruhe, Germany	D-3861
Bovine Albumin	MP Biomedicals, Eschwege, Germany	840043
Bromophenol Blue Sodium Salt	Merck KGaA, Darmstadt, Germany	111746
Buthionine Sulfoximine (BSO)	Sigma-Aldrich GmbH, Taufkirchen, Germany	B2640
Caffeic acid	Sigma-Aldrich GmbH, Taufkirchen, Germany	C0625
4',6-diamidino-2-phenylindole (DAPI)	Invitrogen, Karlsruhe, Germany	D1306
DCF (CM-H2DCFDA)	Invitrogen, Karlsruhe, Germany	C-6827
dNTP Mix	Fermentas GmbH, St. Leon-Rot, Germany	R0241
DMSO (Dimethylsulfoxide)	Sigma-Aldrich GmbH, Taufkirchen, Germany	D2650
DTNB	Sigma-Aldrich GmbH, Taufkirchen, Germany	D8130
DTT (Dithiothreitol)	Sigma-Aldrich GmbH, Taufkirchen, Germany	D8161
ECL	GE Healthcare, Freiburg, Germany	RPN2106
EDTA	Sigma-Aldrich GmbH, Taufkirchen, Germany	E9884
Ethanol p.a.	Merck, Darmstadt, Germany	1.00983.2500
Ethidiumbromide	Merck, Darmstadt, Germany	70257083
ETYA (Eicosatetraenoic Acid)	Sigma-Aldrich GmbH, Taufkirchen, Germany	E1768
Foetal Bovine Serum	PAA, Pasching, Austria	A15-043
Glutathione (GSH)	Sigma-Aldrich GmbH, Taufkirchen, Germany	G6013
Glutathione reduced ethyl ester (GSH-EE)	Sigma-Aldrich GmbH, Taufkirchen, Germany	G1404
Glycine	MP Biomedicals, Eschwege, Germany	808831
Gelatin from porcine skin	Sigma-Aldrich GmbH, Taufkirchen, Germany	G2500
5(S)-HpETE	Cayman Chemical, ANN Arbor, MI, USA	44230
12(S)-HpETE	Cayman Chemical, ANN Arbor, MI, USA	44570
15(S)-HpETE	Biomol GmbH, Hamburg, Germany	HP-015
Hydroperoxide	Sigma-Aldrich GmbH, Taufkirchen, Germany	H1009
4-Hydroxytamoxifen (Tam)	Sigma-Aldrich GmbH, Taufkirchen, Germany	H7904
Indomethacin	Sigma-Aldrich GmbH, Taufkirchen, Germany	I7378
Iodoacetamide	Sigma-Aldrich GmbH, Taufkirchen, Germany	I6125
Isopropanol p.a.	Merck, Darmstadt, Germany	1.09634.2511
L-Glutamine	Invitrogen, Karlsruhe, Germany	25030

<u>Chemicals</u>	<u>Company</u>	<u>Catalog-No.</u>
LIF (ESGRO)	Millipore, Billerica, MA, USA	ESG1107
Luria Broth Base	Invitrogen, Karlsruhe, Germany	12795-019
MK-886	Biomol GmbH, Hamburg, Germany	EL266
MOPS	Sigma-Aldrich GmbH, Taufkirchen, Germany	M1254
Mounting medium	Dako Cytomation, Hamburg, Germany	S3023
N-Acetyl-L-Cysteine	Sigma-Aldrich GmbH, Taufkirchen, Germany	A9165
NDGA	Sigma-Aldrich GmbH, Taufkirchen, Germany	N2036
Oligonucleotides	Metabion international AD, Martinsried, Germany	
Pareformaldehyde (PFA)	Roth Carl GmbH & Co., Karlsruhe, Germany	0335.3
PD146176	Park-Davis, Pfizer, USA	PD146176
Penicillin-Streptomycin	Invitrogen, Karlsruhe, Germany	15140-122
Phenol : Chloroform	MP Biomedicals, Eschwege, Germany	802520
Propidium Iodide (PI)	Sigma-Aldrich GmbH, Taufkirchen, Germany	P4170
Protease Inhibitor Cocktail Tablets	Roche Diagnostics, Mannheim, Germany	1 697 498
Puromycin	Sigma-Aldrich GmbH, Taufkirchen, Germany	P7255
RO 107 905 1	Keith Walker, Roche, Palo Alto, CA, USA	
Select Agar	Invitrogen, Karlsruhe, Germany	30391-023
Skim Milk Powder	Fluka Chemie GmbH, Buchs, Switzerland	70166
Sodium Chloride	MP Biomedicals, Eschwege, Germany	194848
Sodium Deoxycholate	Sigma-Aldrich GmbH, Taufkirchen, Germany	D6750
Sodium Dodecyl Sulfate (SDS)	Fluka Chemie GmbH, Buchs, Switzerland	71729
Sodium Pyrophosphate Tetrabasic Decahydrate	Sigma-Aldrich GmbH, Taufkirchen, Germany	S6422
TEMED	Fluka Chemie GmbH, Buchs, Switzerland	87689
Tris-Base	Merck, Darmstadt, Germany	1.08382
Triton X-100	GE Healthcare, Freiburg, Germany	17-1315-01
Trypan Blue (0.4%)	Sigma-Aldrich GmbH, Taufkirchen, Germany	T8154
Trypsin-EDTA	Invitrogen, Karlsruhe, Germany	25300
Tween 20	Sigma-Aldrich GmbH, Taufkirchen, Germany	P5927

<u>Radioactive Isotopes</u>	<u>Company</u>	<u>Catalog-No.</u>
[ $\alpha$ - <sup>32</sup> P]-dCTP	GE Healthcare, Freiburg, Germany	PT10165
L-[ <sup>14</sup> C (U)] Cystine	Perkin Elmer Life Sciences Inc., Boston, USA	NEC465050UC

<u>Bacteria</u>	<u>Company</u>
DH5 $\alpha$ <i>E.coli</i> cells	Invitrogen, Karlsruhe, Germany

<b>Enzymes</b>	<b>Company</b>	<b>Catalog-No.</b>
DNA Polymerase I (Klenow)	New England Biolabs GmbH, Frankfurt, Germany	M0210S
Pfu DNA Polymerase	Promega GmbH, Mannheim, Germany	M774A
Phosphatase, alkaline	Roche Diagnostics, Mannheim, Germany	713 023
Proteinase K	Roth Carl GmbH & Co., Karlsruhe, Germany	7528.1
Restriction Endonucleases	New England Biolabs GmbH, Frankfurt, Germany MBI Fermentas GmbH, St. Leon-Rot, Germany	
T4 DNA Ligase	Promega GmbH, Mannheim, Germany	M180A
Taq DNA Polymerase	Invitrogen, Karlsruhe, Germany	18038-026

<b>Antibodies (source)</b>	<b>Company</b>	<b>Catalog-No.</b>
$\alpha$ -AIF D20 (goat)	Santa Cruz, Heidelberg, Germany	SC-9416
$\alpha$ -Bcl2 (mouse)	Roche Diagnostics, Mannheim, Germany	1 624 989
$\alpha$ -HA High Affinity, clone 3F10 (rat)	Roche Diagnostics, Mannheim, Germany	11 867 423 001
$\alpha$ -Mouse-HRP conjugate (goat)	Promega GmbH, Mannheim, Germany	W4021
$\alpha$ -PHGPx mGPx4 1B4 (rat)	Elisabeth Kremmer, GSF, Munich, Germany	
$\alpha$ -Rat-HRP conjugate (goat)	Dianova GmbH, Hamburg, Germany	112-035-062
$\alpha$ -Rat-Cy3 conjugate (mouse)	Jackson Immunoresearch Europe Ltd., UK	212-165-168
$\alpha$ -Tubulin (mouse)	Dianova GmbH, Hamburg, Germany	DLN-09992

<b>Disposables and Kits</b>	<b>Company</b>	<b>Catalog-No.</b>
DC Protein Assay	Bio-Rad, Munich, Germany	500-0112
DMEM	Invitrogen, Karlsruhe, Germany	41966
DMEM* (lacking L-cystine)	Invitrogen, Karlsruhe, Germany	21013
Gel Extraction Kit	QIAGEN GmbH, Hilden, Germany	28704
Hybond-C super membrane	GE Healthcare, Freiburg, Germany	RPN203G
Hybond-N <sup>+</sup> membrane	GE Healthcare, Freiburg, Germany	RPN303B
Hyperfilm	GE Healthcare, Freiburg, Germany	RPN3103K
X-ray film	GE Healthcare, Freiburg, Germany	RPN16778K
JETstar Plasmid purification system	Genomed GmbH, Löhne, Germany	220020
LightCycler Capillaries	Roche Diagnostics, Mannheim, Germany	11 909 339 001
LightCycler FastStart DNA Master <sup>PLUS</sup> SYBR Green I	Roche Diagnostics, Mannheim, Germany	03 515 869 001
Lipofectamine 2000	Invitrogen, Karlsruhe, Germany	11668-027
OPTI-MEM	Invitrogen, Karlsruhe, Germany	31985
Plasmid Maxi Kit	QIAGEN GmbH, Hilden, Germany	12163
PCR Cloning Kit	QIAGEN GmbH, Hilden, Germany	231122
Rediprime II random prime labelling system	GE Healthcare, Freiburg, Germany	RPN1633
Reverse Transcription System	Promega GmbH, Mannheim, Germany	A3500
RNase-Free DNase Set	QIAGEN GmbH, Hilden, Germany	79254
RNeasy Mini Kit	QIAGEN GmbH, Hilden, Germany	74104
Sephadex G-50 columns	GE Healthcare, Freiburg, Germany	27-5330-01
Supelclean LC-18 columns	Sigma-Aldrich, Stockholm, Sweden	57012

<u>Equipment</u>	<u>Company</u>
Bench-top radioisotope counter	Bioscan, Washington D.C., USA
FACS Calibur	BD GmbH, Heidelberg, Germany
GenAmp PCR system 2700	Applied Biosystems, Darmstadt, Germany
Gene Pulser II System	Bio-Rad, Munich, Germany
Gene Pulser Electroporation Cuvettes, 0.4 cm gap	Bio-Rad, Munich, Germany
Heraeus Incubator, Modell B 5060	Heraeus Holding GmbH, Hanau, Germany
Leica DM IRBE confocal microscope	Leica Microsystems GmbH, Wetzlar, Germany
Leica TCS SP2 scanner	Leica Microsystems GmbH, Wetzlar, Germany
Light-Cycler 1.5	Roche Diagnostics, Mannheim, Germany
LS 5000 TA Scintillation Counter	Beckman Coulter GmbH, Krefeld, Germany
Microscope Axiovert 135	Carl Zeiss Jena GmbH, Göttingen, Germany
Microscope Axiovert 200M	Carl Zeiss Jena GmbH, Göttingen, Germany
Mini-PROTEAN 3 Electrophoresis Cell	Bio-Rad, Munich, Germany
Mini-Sub Cell GT Electrophoresis Cell	Bio-Rad, Munich, Germany
OTD Combi Ultracentrifuge	Sorvall, Langenselbold, Germany
Photometer Bio	Eppendorf, Hamburg, Germany
PowerPac 200 Power Supply	Bio-Rad, Munich, Germany
Spectrophotometer DU-64	Beckman Coulter GmbH, Krefeld, Germany
Speed Vac Concentrator SVC100H	Savant Instruments NC, Farmingdale, N.Y. USA
Trans-Blot Semi-Dry	Bio-Rad, Munich, Germany
RF-10A XL Fluorescence Spectrophotometer	Shimadzu, Duisburg, Germany
UZ-PA-38,5-1 Ultracentrifuge Tubes	Kisker GbR, Steinfurt, Germany

<u>Oligonucleotides</u>	<u>Sequence</u>
-------------------------	-----------------

Genotyping

PF for1	5' ACTCCCCGTGGAAGCTGTGAGCTTTGTGC 3'
PF rev1	5' GGATCTAAGGATCACAGAGCTGAGGCTGC3'

Cloning

HA-PHGPx for1	5' AATTAGCTAGCTACCCATACGATGTTCCAGATTACG 3'
HA-PHGPx rev2	5' AATTACTCGAGTTTACACAGATCTTGCTGTACATG 3'
PHGPx complete for1	5' CTGGCAGGCACCATGTGTGCATCC 3'
PHGPx complete rev1	5' AGGCAGCCAGGGTGAAGCTCGAGC 3'
PHGPx HAtag for1	5' AATGGATCCGTCGCCACCATGTACCCATACGATGTTCC AGATTACGCTTGTGCATCCCGCGATGATTGGC 3'
PHGPx E4 rev1	5' CATGTCAAAGTTGACGTTGTAGC 3'
PHGPx UC for1	5' GTGGCCTCGCAATGCGGCAAACTGACGTAAAC 3'
PHGPx UC rev1	5' TTTACGTCAGTTTTGCCGATTGCGAGGCCACG 3'
PHGPx US for1	5' GTGGCCTCGCAAAGCGGCAAACTGACGTAAAC 3'
PHGPx US rev1	5' GTTTACGTCAGTTTTGCCGCTTTGCGAGGCCAC 3'



---

Oligonucleotides	Sequence
------------------	----------

---

RT-PCR

Aldolase A	5' GGTCACAGCACTTCGTGCGCACAG 3'
Aldolase B	5' TCCTTGACAAGCGAGGCTGTTGGC 3'
Alox5 A	5' AGAACCTGGAGGCCATCGTCAGC 3'
Alox5 B	5' GCACCAGCTGCAGGAAGATCGAC 3'
Alox12 A	5' TCCAACCTGCAGGAGCTCCAATTCC 3'
Alox12 B	5' CGCCTCCACCTGTGCTCACTACC 3'
Alox12e A	5' CCGCGAGGTCCTGAGGTTGGAC 3'
Alox12e B	5' GGCAAGGCAACGAGTCCACAATG 3'
Alox15 A	5' CACTGCGCAGCACTCTTCCATCC 3'
Alox15 B	5' CACCATAACAGCCTGGCGTCTGC 3'
Alox15b A2	5' TCCGTTCTGATGCCTGGTTCTGC 3'
Alox15b B2	5' GTC AAGGCAGCGAGGCCAACC 3'
Cox1 A	5' GCACTGGTGGATGCCTTCTCTCG 3'
Cox1 B	5' CTGGCACTTCTCCAGCAGCAACC 3'
Cox2 A	5' TGGAGCCCGTGCTGCTCTGTC 3'
Cox2 B	5' GCCTGGCAAGTCTTTAACCTCACAGC 3'
PHGPx A	5' GCAACCAGTTTGGGAGGCAGGAG 3'
PHGPx B	5' CCTCCATGGGACCATAGCGCTTC 3'
xCT for1	5' GGCACCGTCATCGGATCAGGCATC 3'
xCT rev1	5' CACGAGCTTGATTGCAAGTTCAGG 3'

Sequencing

T7 promoter	5' TAATACGACTCACTATAGGG 3'
Sp6 promoter	5' ATTTAGGTGACACTATAGAA 3'
LTR 3'-for1	5' GCTCACAACCCCTCACTC 3'
IRES rev1	5' CTTCCGGCCAGTAACGTTAGG 3'

siRNA knockdown

control siRNA:	5' AAGAGAAAAAGCGAAGAGCCA 3'
AIF-12:	5' ACAGAGAAGAGCCAUUGCC-dTdT 3'
AIF-20:	5' GAGAAACAGAGAAGAGCCA-dTdT 3'
AIF-22:	5' AUGUCACAAAGACACUGCA-dTdT 3'

All DNA-oligonucleotides were obtained from Metabion GmbH, Martinsried, Germany. siRNA-oligonucleotides were obtained from Dharmacon, Inc. (part of Fisher Scientific GmbH, Schwerte, Germany).

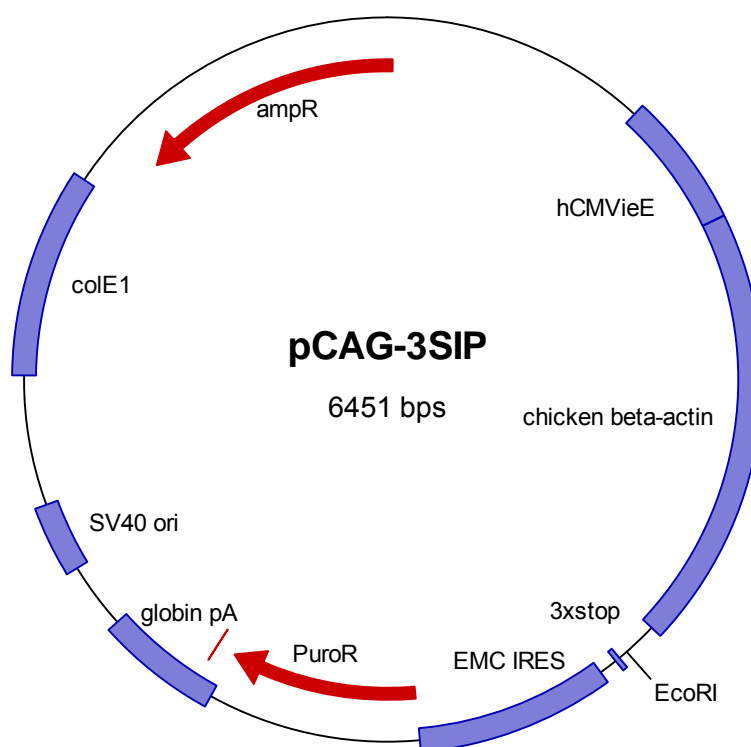
---

 Expression Vectors
 

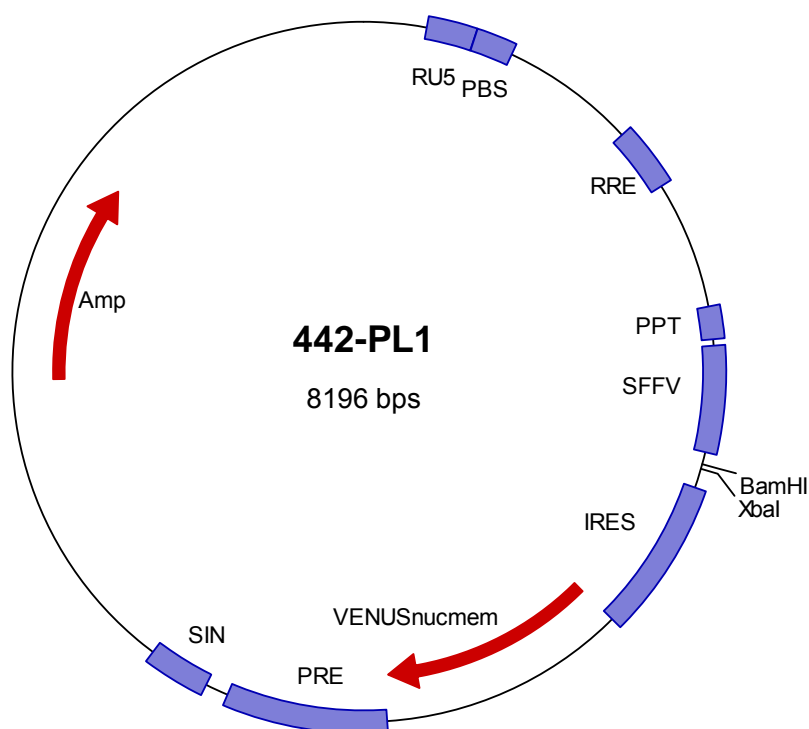
---

Depicted are the expression vector pCAG-3SIP (figure 9) and the lentiviral vector p442-PL1 (figure 10). All cloned plasmids are based on these two vectors. Cloning steps and packaging plasmids used for lentivirus production are described in chapter 3.4 and 3.1.6.3, respectively.

pCAG-3SIP



**Figure 9:** Map of expression vector pCAG-3SIP. hCMVieE (human cytomegalovirus immediate early-enhancer), modified chicken beta-actin promoter, *EcoRI* (restriction site used for cloning), 3 x Stop (3 Stop codons in all three open reading frames), EMC IRES (encephalomyocarditis IRES), PuroR (puromycin N-acetyltransferase gene), globin pA (globin poly A signal), SV40 ori (simian virus 40 origin), colE1 (colE1 origin), ampR (ampicillin resistance gene).

p442-PL1

**Figure 10:** Map of lentiviral vector p442-PL1. ampR (ampicillin resistance gene), RU5 (RU5 LTR), PBS (primer binding site), RRE (Rev responsive element), PPT (poly-purine tract), SFFVp (spleen focus forming virus promoter), *BamHI/XbaI* (restriction sites used for cloning), IRES (internal ribosome entry site), VENUSnucmem (fluorescent protein with nuclear membrane anchor), PRE (post regulatory element), SIN (self-inactivating 3' LTR).

Cell lines

$\gamma$ -GCS<sup>(-/-)</sup> **ES cell like cells** were a kind gift from Michael Lieberman, Houston, Texas, USA [1]. Cells were transfected with pCAG-3SIP, pCAG-3SIP-eGFP, and pCAG-3SIP-xCT, yielding single cell clone mock, eGFP, and xCT-5/7, respectively.

**HEK293 T cells** were used as packaging cell line for the production of lentiviral particles, based on the third generation lentiviral vector p442-PL1.

**Primary MEFs** were isolated from PF transgenic mice, yielding PFa1<sup>(flox/flox)</sup>, PFa24<sup>(flox/flox)</sup>, PFa37<sup>(flox/flox)</sup>, and PFa43<sup>(flox/flox)</sup> cells, which contain either one or two floxed PHGPx alleles. MEFs were transfected with pCAG-3SIP-MCM, yielding cell line PFa1<sup>(flox/flox)</sup>-MCM, PFa24<sup>(flox/flox)</sup>-MCM, PFa37<sup>(flox/flox)</sup>-MCM, and PFa43<sup>(flox/flox)</sup>-MCM, respectively.

## **3 Methods**

### **3.1 Cell culture and related techniques**

#### **3.1.1 Murine embryonic fibroblasts (MEFs)**

Male and female PHGPx (wt/flox or flox/flox) mice were mated, yielding homozygous and heterozygous offspring. Females were checked daily for vaginal plugs. A vaginal plug was considered as embryonic day 0.5. Pregnant mice were sacrificed at E12.5 by cerebral dislocation. Uteri were dissected under sterile conditions and stored in PBS. Embryos were removed from the uterus and washed three times in PBS to remove maternal blood cells. Subsequently, the embryos were dissected off the uterus, organs and the head were removed and the body trunk was minced in a 6 cm cell culture dish with two forceps. Tissue pieces were suspended in 1 ml trypsin and incubated at 37°C for 15 min. The suspension was homogenized by vigorous pipetting and washed in Standard DMEM to remove trypsin. Cell pellets were resuspended in 4 ml Standard DMEM and plated on a 6 cm cell culture dish. Cells were cultivated at 37°C in a 7% CO<sub>2</sub> water-saturated atmosphere. When cell lines reached confluency, they were split at a ratio of 1:3 onto larger cell culture dishes. Cells from early passage numbers were harvested by trypsinization and aliquots were stored by cryo conservation in liquid nitrogen (see chapter 3.1.4). Primary cells grow relatively slow during first passage numbers (P2-P5) until they undergo a senescence-like crisis after approximately 20 passage numbers. This is eventually overcome by outgrowing immortalized cells. Immortalized cells grew faster and were easier to manipulate by electroporation and lentiviral infection (see chapter 3.1.6). Immortalized MEFs were cultivated in Standard DMEM and were routinely split by trypsinization at a ratio of 1:5 every 2<sup>nd</sup> to 3<sup>rd</sup> day.

**PBS:** 80.0 g NaCl, 2.0 g KCL, 14.4 g Na<sub>2</sub>HPO<sub>4</sub>, 2.4 g KH<sub>2</sub>PO<sub>4</sub> in 1 l H<sub>2</sub>O, pH 7.4

**Standard DMEM:** DMEM, 10 % FCS, 1 % glutamine, 50 U/ml penicillin G, 50 µg/ml streptomycin

#### **3.1.2 ES cell like $\gamma$ -GCS knockout cells**

ES cell like  $\gamma$ -GCS knockout cells were obtained from Michael Lieberman, Houston, Texas, USA (Shi et al., 2000). The cells were cultivated in Standard DMEM

containing 15 % FCS and 5 mM NAC, and were routinely split at a ratio of 1:3 every 2<sup>nd</sup> or 3<sup>rd</sup> day.  $\gamma$ -GCS knock out ES cell like cells only adhere weakly to the cell culture dish and are rather sensitive to trypsinization. Thus, cells were detached from the cell culture dish by rinsing the dish with a pipette.

**Standard DMEM:** DMEM, 15 % FCS, 1 % glutamine, 50 U/ml penicillin G, 50  $\mu$ g/ml streptomycin

### **3.1.3 Determination of cell number**

Cells were harvested from cell culture dishes by trypsinization and suspended by adding 5 volumes of Standard DMEM. 30  $\mu$ l of the cell suspension was mixed with an equal volume of 0.4 % trypan blue solution and cells were counted using a Fuchs-Rosenthal haemocytometer. Trypan blue is excluded from viable cells, whereas dead cells stain blue due to plasma membrane disruption.

**Standard DMEM:** DMEM, 10 % FCS, 1 % glutamine, 50 U/ml penicillin G, 50  $\mu$ g/ml streptomycin

### **3.1.4 Cryo conservation and thawing of cells**

Stocks of all cell lines were stored in liquid nitrogen. Cells were grown in 10 cm cell culture dishes until they reached approximately 80 % confluency, trypsinized, and collected by centrifugation. The cell pellets were resuspended in FCS containing 10% DMSO, transferred to cryo vials in 1 ml aliquots and frozen in propanol containers at -80°C over night. Subsequently, vials were transferred to a liquid nitrogen tank. If needed, frozen cells were defrosted in a water bath at 37°C, immediately transferred to 5 ml Standard DMEM and collected by centrifugation. Cell pellets were resuspended in 10 ml Standard DMEM and seeded onto a 10 cm cell culture dish.

**Standard DMEM:** DMEM, 10 % FCS, 1 % glutamine, 50 U/ml penicillin G, 50  $\mu$ g/ml streptomycin

### **3.1.5 Microscopy pictures and time-lapse videos**

Pictures and time-lapse videos of cells were taken with Axiovert Microscopes and Improvision Openlab 3.0.8 software.

### **3.1.6 Genetic transfer methods**

#### **3.1.6.1 Transfection of siRNA**

$3 \times 10^5$  primary MEFs were transfected with siRNA in a 3.5 cm cell culture dish with Lipofectamine 2000. Cells were pre-incubated with 600  $\mu$ l OPTI-MEM for 60 min. 150  $\mu$ l OPTI-MEM were mixed with 10  $\mu$ l Lipofectamine 2000 and 10  $\mu$ l siRNA solution (20  $\mu$ M), respectively. Both solutions were incubated for 3 min at room temperature. The solutions were mixed, vortexed for 10 sec, and incubated for additional 15 min to allow formation of siRNA-Lipofectamine 2000 complexes. The complex solution was added to the cell culture dish and cells were incubated for 5 h at 37°C. Subsequently, cells were washed with PBS and cultivated over night in standard DMEM containing 15 % FCS. The same lipofection procedure was repeated the next day in order to increase transfection efficiency.

#### **3.1.6.2 Electroporation**

Cells were harvested by trypsinization, washed twice in PBS and resuspended in 250  $\mu$ l FCS-free DMEM. Primary MEFs ( $1 \times 10^6$  cells) were electroporated with a Gene Pulser II (Bio Rad, Munich, Germany) in cuvettes with 0.4 cm gap width. For each transfection, 20  $\mu$ g plasmid DNA were transfected into cells with an electric pulse of 230 V and a capacitance of 1,000  $\mu$ F. FCS (500  $\mu$ l) was applied to the cells immediately after the pulse. The cell suspension was gently mixed by pipetting and cells were seeded on a 10 cm cell culture dish in Standard DMEM. Selection for antibiotic resistance was initiated 48 h after electroporation with 0.5  $\mu$ g/ml puromycin, gradually increasing to 2  $\mu$ g/ml over a period of 1 to 3 weeks.

#### **3.1.6.3 Lentiviral infection**

Lentiviral vectors mediate an efficient gene transfer into primary cells. The lentiviral infection method proved to be the most efficient technique to introduce DNA/RNA into primary MEFs due to integration and stable expression of transgenes in dividing as well as resting cells. Lentiviral particles were produced in HEK293 T packaging cells with a third generation lentiviral packaging system, which provides maximal biosafety but is more laborious, involving the transfection of four different plasmids into the

producer cell line. Three plasmids encode all necessary structural proteins for lentivirus production, including pEcoEnv-IRES-puro (contains glycoprotein Env), plasmid pMDLg\_pRRE (contains the main structural protein Gag and the enzyme cluster Pol) and pRSV\_Rev (contains the post-transcriptional regulator Rev). Third generation packaging systems are Tat independent, as the transfer vector pRRL.PPT.SF.IRES-VENUSnucmem (p442) contains an additional SFFV promoter.

$5 \times 10^6$  HEK293 T packaging cells were seeded in Standard DMEM on 10 cm cell culture dishes and incubated for 24 h. Plasmids (2  $\mu$ g pEcoEnv-IRES-puro, 5  $\mu$ g pMDLg\_pRRE, 10  $\mu$ g pRSV\_Rev, 5  $\mu$ g p442-PL1-based vectors) were diluted in 500  $\mu$ l 12.5 mM CaCl<sub>2</sub> solution and mixed with 500 ml HBS by air bubbling. Cell culture medium was replaced with TF medium, and chloroquine was added to a final concentration of 25  $\mu$ M. For calcium phosphate transfection, the plasmid mix was vortexed, applied to the cell culture dish, and cells were incubated for 8-12 h. The transfection medium was replaced with fresh TF medium and the transfected packaging cells were incubated for further 36 h. Virus-enriched TF medium was recovered from the cell culture dish, filtrated through a 0.22 mm sterile filter and centrifuged in a swing rotor ultracentrifuge for at least 16 h at 10,000 x g. The virus containing pellet was resuspended in 200  $\mu$ l Standard DMEM and stored at -80°C.

$3 \times 10^5$  MEFs were infected in a 3.5 cm cell culture dish by adding 50  $\mu$ l of the virus concentrate and a subsequent incubation for 48 h. Infection efficiency was monitored by fluorescence microscopy, screening for VENUSnucmem expression and quantification was performed by FACS analysis.

**Chloroquine (1000x):** 25 mM chloroquine in PBS

**HBS (2x):** 50 mM HEPES, 280 mM NaCl, 1.5 mM Na<sub>2</sub>HPO<sub>4</sub>, pH 7.05 adjusted with NaOH

**PBS:** 80.0 g NaCl, 2.0 g KCL, 14.4 g Na<sub>2</sub>HPO<sub>4</sub>, 2.4 g KH<sub>2</sub>PO<sub>4</sub> in 1 l H<sub>2</sub>O, pH 7.4

**Standard DMEM:** DMEM, 10 % FCS, 1 % glutamine, 50 U/ml penicillin G, 50  $\mu$ g/ml streptomycin

**TF medium:** Standard DMEM, 20 mM HEPES

### **3.2 Genotyping**

The genotyping of isolated MEFs was performed by PCR with purified DNA samples. Cells were harvested from 10 cm cell culture dishes with a cell scraper, washed in PBS and lysed in 300 µl Lysis Buffer. Cells were incubated at 55°C for 12 h with shaking. To remove proteins and lipids, equal volumes of phenol-chloroform were added to the lysate, vortexed and centrifuged for 6 min at 10,000 x g. The upper, DNA-containing phase was recovered and DNA was precipitated by adding 2.5 x volumes of ethanol with 50 mM NaCl. The DNA was recovered by centrifugation at 4°C with 10,000 x g, subsequently washed with 70 % ethanol and centrifuged again at 10,000 x g. The DNA pellet was air dried for 30 min and dissolved in 100 µl TE. Genomic DNA samples were stored at 4°C.

For each PCR, a 25 µl reaction mix was prepared as described in the manufacturers' instructions. The PHGPx (flox/wt) PCR was performed with oligonucleotides PFfor1 and PFrev1 with an annealing temperature of 68°C, elongation time of 40 sec, and 35 cycles. The PCR products were resolved in a 2 % agarose gel in TAE buffer at 120 V.

**Lysis Buffer:** 10 mM Tris pH 7.6; 10 mM EDTA; 0.5 % SDS; 10 mM NaCl, 300 µg/ml Proteinase K

**50x TAE:** 2 M Tris-acetate (2 M Tris-base and 5.71 % v/v acetic acid); 50 mM EDTA/NaOH pH 8.0

**TE:** 10 mM Tris pH 7,5; 1 mM EDTA

### **3.3 Cloning techniques**

#### **3.3.1 Preparation of plasmid DNA**

After transformation, single colonies were picked from LB plates and used to inoculate 2 ml LB medium, containing 50 µg/ml ampicillin. The inoculum was incubated at 37°C for 12-20 h with shaking. Cells were harvested by centrifugation at 10,000 x g for 20 sec and resuspended in 200 µl buffer E1 by vortexing. 200 µl of denaturing buffer E2 was added to the cell suspension, mixed by inverting the tube and incubated for 5 min at room temperature. To stop the denaturation reaction, 200 µl of buffer E3 was added, mixed by inverting and centrifuged for 6 min at 10,000 x g. To extract proteins and lipids, 400 µl of phenol-chloroform was added, vortexed and centrifuged for 3 min at 10,000 x g. Plasmid DNA dissolves in the aqueous upper



phase, which was recovered and added to 500 ml isopropanol for DNA precipitation. The precipitated DNA was harvested by centrifugation for 12 min at 4°C at 10,000 x g. The DNA pellet was washed with 70 % ethanol, air dried for 30 min at room temperature and resuspended in 50 µl TE.

The purified plasmids were subjected to analytic restriction digestions to identify the correct construct and orientation of the insert. After evaluation of the individual clones and their respective plasmid DNA, selected single cell clones were used to augment plasmid DNA, according to *Qiagen Plasmid Maxi Kit* instructions. Plasmid concentrations were quantified by measuring the absorbance at 260 nm in a spectrophotometer.

**E1:** 50 mM Tris, 10 mM EDTA, pH 8,0

**E2:** 200 mM NaOH, 1,0 % w/v SDS

**E3:** 3.1 M potassium acetate, adjust to pH 5.5 with acetic acid

**TE:** 10 mM Tris pH 7,5; 1 mM EDTA

### **3.3.2 Restriction digestion**

DNA restriction digestion was performed with respective endonucleases according to manufacturers' instructions (New England Biolabs GmbH or MBI Fermentas GmbH). DNA fragments were separated by electrophoresis in a 0.8 % low melting point (LMP) agarose gel at 60 V in 1x TAE buffer. The desired fragment was isolated from the gel with a scalpel and processed with a *Qiagen Gel Extraction Kit*, according to the manufacturers' instructions.

**50x TAE:** 2 M Tris-acetate (2 M Tris-base and 5.71 % v/v acetic acid); 50 mM EDTA/NaOH pH 8.0

### **3.3.3 Phenol-chloroform extraction and ethanol precipitation of DNA**

Linearized fragments, obtained from single cutter digestions, were purified by phenol-chloroform treatment and subsequent ethanol precipitation. Therefore, an equal volume of phenol-chloroform was added to the digestion reaction, briefly mixed and centrifuged for 6 min at 10,000 x g. The upper aqueous phase was recovered and DNA was precipitated by adding 2.5 x volumes of ethanol and 50 mM NaCl, followed

by centrifugation at 4°C with 10,000 x g. The DNA precipitate was washed with 70 % ethanol, centrifuged as above and air dried for 30 min. The dried DNA pellet was dissolved in 30 µl TE and stored at -20°C.

### **3.3.4 DNA ligation**

Ligation reactions were prepared with T4 DNA ligase according to standard procedures, described in the manufacturers' instructions (Promega GmbH). The solutions contained 2 µl vector and 2 µl insert DNA and were incubated at 16°C for 12-24 hours. To quantify the specificity of the ligation reaction, respective backbone and insert DNA were subjected to separate control ligations. The ligation reactions were used for subsequent heat shock transformation of competent bacteria.

**50x TAE:** 2 M Tris-acetate (2 M Tris-base and 5.71 % v/v acetic acid); 50 mM EDTA/NaOH pH 8.0

**TE:** 10 mM Tris pH 7,5; 1 mM EDTA

### **3.3.5 Klenow fragment fill-in reaction**

For blunt end clonings, DNA fragments were treated with DNA Polymerase I (Klenow fragment) according to the manufacturers' instructions (New England Biolabs GmbH). The Klenow fragment retains polymerization fidelity and 3'-5' exonuclease activity but is devoid of 5'-3' exonuclease activity. Hence, the Klenow fragment forms blunt ends by either filling-in 5'-overhangs or by removing 3'-overhangs. DNA fragments were purified by phenol-chloroform extraction as described above.

### **3.3.6 Dephosphorylation of linearized plasmid DNA**

Vector DNA was dephosphorylated with alkaline phosphatase according to manufacturers' instructions (Roche Diagnostics). Dephosphorylation of backbone DNA favours the integration of DNA inserts since religation of the backbone is prevented. After dephosphorylation, DNA fragments were purified by phenol-chloroform extraction as described above.

### **3.3.7 Preparation of competent cells**

Competent cells were prepared by the rubidium chloride procedure with DH5 $\alpha$  *E. coli* cells. 250 ml LB medium, containing 20 mM MgSO<sub>4</sub> was inoculated with a single colony from an LB plate and incubated over night at 37°C with shaking until the OD<sub>600</sub> reached 0.4-0.6. Cells were pelleted at 4,500 x g for 5 min at 4°C. All subsequent steps were performed in a 4°C cold room with pre-chilled pipettes, tubes and flasks. Cells were resuspended in 100 ml of ice cold TFB1, incubated on ice for 5 min and pelleted at 4,500 x g for 5 min at 4°C. Cells were resuspended gently in 10 ml TFB2, incubated on ice for 30 min and 200  $\mu$ l aliquots were snap-frozen in liquid nitrogen. Aliquots of competent cells were stored at -80°C. Cells were used no longer than 4 months after preparation.

### **3.3.7 Heat shock transformation**

For transformation, 200  $\mu$ l aliquots were defrosted on ice and 10  $\mu$ l of the ligation mix or 10 ng purified plasmid DNA were added to the cell suspension. Cells were incubated for 15 min on ice, heated to 42°C for 90 sec and replaced on ice for 2 min. 800  $\mu$ l LB medium were added to the cell suspension and incubated for 45 min at 37°C with vigorous shaking. All plasmids used in this work contained an ampicillin resistance cassette for selection. 100  $\mu$ l of the transformation mixture was plated on a LB plate containing 50  $\mu$ g/ml ampicillin. Remaining cells were harvested by brief centrifugation at 10,000 x g for 20 sec to remove excess LB. The pellet was resuspended in 100  $\mu$ l LB and plated onto a second LB plate with ampicillin. Agar plates were incubated for 12-20 h at 37°C until single cell colonies became visible.

**TFB1:** 30 mM potassium acetate; 10 mM CaCl<sub>2</sub>; 50 mM MnCl<sub>2</sub>; 100 mM RbCl; 15 % glycerol; pH 5.8

**TFB2:** 10 mM 3-(N-morpholino) propansulfonic acid (MOPS); 75 mM CaCl<sub>2</sub>; 10 mM RbCl; 15 % glycerol; pH 6.5

## **3.4 Cloning of expression vectors**

### **3.4.1 pCAG-3SIP-based vectors (MCM, eGFP, xCT)**

Plasmid pCAG-3SIP drives gene expression from a highly efficient CAG promoter and encodes an IRES-linked bicistronic sequence, including the puromycin N-

acetyltransferase gene (*purR*) for stable selection. pCAG-3SIP was used for stable expression of the fusion protein MerCreMer, consisting of Cre recombinase (Cre) flanked by two mutated oestrogen receptors (Mer) (Verrou et al., 1999). The MerCreMer cassette was recovered from pBluescript-MerCreMer by *EcoRI* digestion and cloned into *EcoRI* digested and dephosphorylated pCAG-3SIP, yielding pCAG-3SIP-MerCreMer (figure 11). The insert orientation was controlled by analytic digestion with *Sall* and *NheI/XhoI*, respectively.

eGFP was isolated from pEGFP-N1 (Clontech, Saint-Germain-en-Laye, France) by *BamHI/XbaI* digestion. The 751 bp fragment was blunted by Klenow fill-in reaction and cloned into *EcoRI* digested, blunted and dephosphorylated pCAG-3SIP, yielding pCAG-3SIP-eGFP (figure 11). The correct orientation of the insert was verified by *EcoRI/EcoRV* and *XmnI* digestion, respectively.

pCAG-3SIP-xCT (figure 11) was provided by Ana Banjac, encoding the murine DNA sequence of xCT light chain (Banjac Ana, PhD thesis, 2005).

### **3.4.2 p442-PL1-based PHGPx expression vectors**

The 3<sup>rd</sup> generation lentiviral vector p442-PL1 (kind gift from Tim Schröder, GSF, Munich, Germany) was used for efficient gene transfer and expression in MEFs by viral infection. Gene expression in p442-PL1 is regulated by an SFFV promoter, synthesizing a bicistronic mRNA sequence that is linked by an internal ribosome entry site (IRES). The fluorescence marker VENUSnucmem including a nuclear membrane anchor (nucmem) is encoded at the 3' position of the bicistronic expression cassette. As described below, various genes were cloned into the 5' position of the expression cassette, upstream of the IRES.

### **3.4.4 Cloning of tagged PHGPx**

The PHGPx gene was amplified from murine testis cDNA by RT-PCR with primers "PHGPx complete for1" and "PHGPx complete rev1". The purified 721 nucleotide product was cloned into pDrive according to manufacturers' instructions (Qiagen PCR Cloning Kit). pDrive-PHGPx was used as template for a PCR with primers

“PHGPx HAtag for1” and “PHGPx E4 rev1”, synthesizing an N-terminal HA-tagged fusion of PHGPx. The 351 bp PCR product was digested with *BamHI* and *BssHII* and the 72 bp fragment was used to replace the N-terminal part of PHGPx in pDrive-PHGPx, yielding pDrive-HA-PHGPx. The pDrive-HA-PHGPx clones were tested by analytic restriction digestion with *EcoRI* and sequenced with primers “T7 promoter” and “SP6 promoter”. The HA-tagged PHGPx sequence was transferred from pDrive-HA-PHGPx to the lentiviral expression vector p442-PL1 by restriction digestion with *BamHI* and *XbaI*. p442-HA-PHGPx clones (figure 11) were analyzed by restriction digestion (*EcoRI* and *BamHI/XbaI*) and sequenced with primers “5'-LTR for1” and “IRES rev1”.

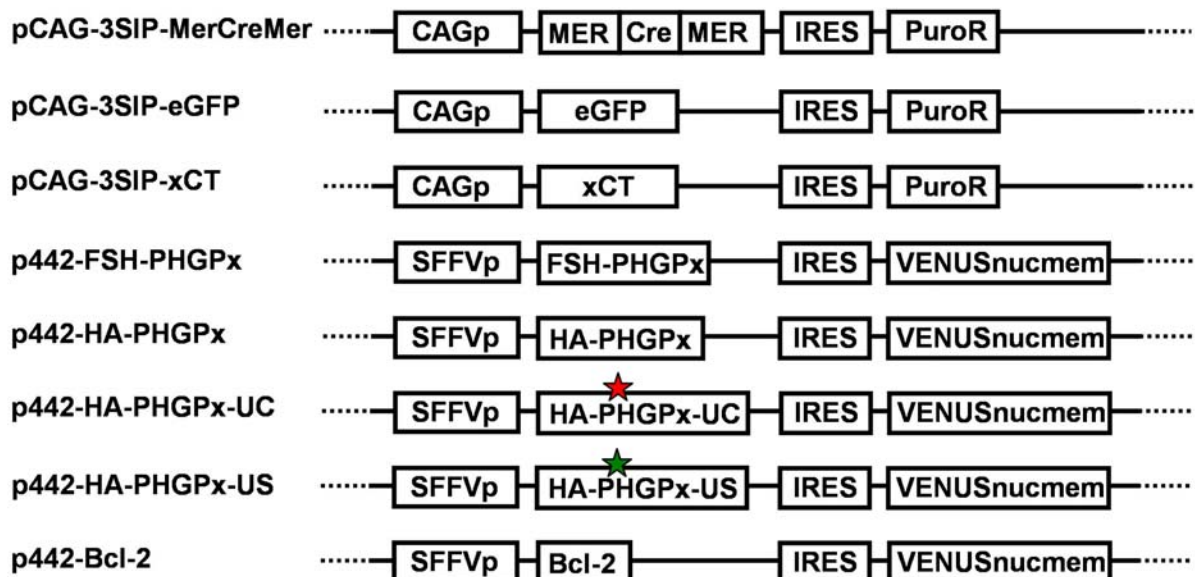


**Figure 11:** Schematic representation of all cloned expression vectors. Depicted are the pCAG-3SIP-based vectors, containing an efficient CAG promoter and a PuroR cassette (puromycin N-acetyltransferase). The p442-PL1-based lentiviral vectors contain a SFFVp (spleen focus forming virus promoter) and a VENUSnucmem fluorescence marker. The cloned PHGPx contains an N-terminal HA-tag and FSH-tag (Flag-, Strep-, HA-tag), respectively. The two mutant forms of HA-PHGPx have a Cys (red asterisk) and Ser (green asterisk) instead of Sec.

For future studies, HA-PHGPx was additionally tagged with an optimised TAPe- (enhanced tandem affinity purification) tag, which has been developed and functionally tested for B-raf and C-Raf (Raf1) in Marius Ueffing’s laboratory at the GSF (kind gift from Dr. Johannes Gloeckner, GSF, Munich, Germany). This tag was specifically designed for the purification of native protein complexes from mammalian cells. The TAPe-tag facilitates rapid and native purification of protein complexes for subsequent identification of PHGPx binding partners by LC-MS/MS as well as functional assays. The combination of two medium-affinity binding epitopes (tandem

Strep-tag II and a FLAG-tag) reduces the tag size to approximately 5 kDa. Hence, the N-terminal TAP-tag/PHGPx fusion protein is only marginally larger than wild type PHGPx. The N-terminal part of HA-PHGPx (lacking the start codon) was amplified with primers “HA-PHGPx for1” and “HA-PHGPx rev2”, introducing a 5' *NheI* and a 3' *XhoI* restriction site. The 349 bp PCR product was purified and cloned into pcDNA3-NTAPe with *NheI/XhoI*. The N-terminal part of PHGPx, now including the TAPe-tag, was replaced in pDrive-HA-PHGPx by *BamHI/BssHIII*, yielding a Flag, Strep (2x), and HA-tagged PHGPx gene, designated pDrive-FSH-PHGPx (figure 11). The constructs were analysed by restriction digestion with *BamHI/BglII* and sequenced with primers “T7 promoter” and “SP6 promoter”. The FSH-PHGPx sequence was transferred to p442-PL1 with *BamHI/XbaI* as described above, yielding p442-FSH-PHGPx.

### **3.4.5 PHGPx Mutagenesis**

Mutations of single amino acids within PHGPx were performed by PCR mutagenesis with pDrive-HA-PHGPx in a volume of 50 µl. Primers of 33 nucleotides were designed, such that the primer sequence consists of a mutated codon, flanked by wild type sequences of at least 10 nucleotides. Mutated codons were chosen according to the highest murine codon usage of the respective amino acid. The Sec codon (UGA) at position 46 of murine PHGPx was mutated to Cys (UGC) and Ser (AGC) with primers “PHGPx UC for1/rev1” and “PHGPx US for1/rev1”, respectively. The PCR-reactions were performed with reduced primer annealing temperature (-6°C), due to the mismatch of primer and wild type PHGPx sequence. Prior to the transformation of competent cells, PCR reactions were digested with *DpnI* for 60 min to remove methylated template DNA. Mutations were verified by sequencing in pDrive with primers “T7 promoter” and “SP6 promoter”. The mutated sequences were transferred to the lentiviral expression vector p442-PL1 as described above, yielding p442-HA-PHGPx-UC and p442-HA-PHGPx-US, respectively (figure11).

### **3.4.5 Bcl-2 expression vectors**

The sequence for wild type Bcl-2 was recovered from pBabe-Bcl-2-puro (kind gift from Gerard Evan, London, UK; (Fanidi et al., 1992)) by restriction digestion with *EcoRI*. The purified 948 bp fragment was cloned into *EcoRI*-digested and

dephosphorylated vector p442-PL1, yielding p442-Bcl-2 (figure 11). Single clones were checked for correct orientation of the insert by restriction digestion with *BamHI* and *XmaI*, respectively.

Plasmid pIRES-neo3-Bcl-2-ActA is based on the CMV promoter-driven expression vector pIRESneo3 (Clontech), containing an IRES and a neomycin resistance cassette (NeoR) for stable selection of expressing cell clones with G418. The plasmid encodes a mutated Bcl-2 in which the membrane anchor was replaced by the mitochondrial insertion sequence of ActA (Bcl-2-ActA) (Zhu et al., 1996), targeting Bcl-2 localisation to the outer mitochondrial membrane. Plasmid pIRES-neo3-Bcl-2-ActA was a kind gift from Prof. Peter Daniel (University Medical Centre Charité, Berlin-Buch, Germany).

### **3.5 Immunoblotting and Immunocytochemistry**

#### **3.5.1 Western blot**

For whole cell lysate preparation, cells were lysed in LCW Lysis Buffer, containing Protease Inhibitor Cocktail (Roche Diagnostics), and incubated for 15 min on ice. The cell debris was removed by centrifugation for 15 min at 4°C at 10,000 x g. The protein concentration of the supernatant was determined by the DC Protein Assay (Bio-Rad), according to manufacturers' instructions. Equal amounts of protein lysates were mixed with Sample Loading Buffer, boiled for 5 min at 95°C, and proteins were separated by 12 % SDS-PAGE at 160 V in a Mini-PROTEAN 3 Electrophoresis Cell. Proteins were transferred from the gel onto a Hybond-C super nitrocellulose membrane in Blotting Buffer with a Trans-Blot Semi-Dry Blotter at 20 V for 30 min. Membranes were blocked with 5 % skim milk powder in TBST for 60 min and hybridized with a primary antibody at 4°C for at least 12 h. Membranes were washed three times in TBST for 5 min, following HRP-conjugated secondary antibody incubation for 90 min. The nitrocellulose membranes were repeatedly washed in TBST (3x 5 min) and proteins were visualized by ECL detection on Hyperfilm. Efficient stripping of Hybond-C super membranes was performed with 0.4 M NaOH for 10 min. Prior to second hybridisation (usually with primary antibody  $\alpha$ -Tubulin),

membranes were blocked with 5 % skim milk powder in TBST for 60 min. All following steps were performed as described above.

**Blotting Buffer:** 10 % Running Buffer (10x), 20 % Methanol

**Sample Loading Buffer (2x):** 100 mM Tris, 4 % SDS, 20 % Glycerol, 0.1% Bromophenol Blue, 100 mM DTT, pH 6.8

**LCW Lysis Buffer:** 0.5 % TritonX-100, 0.5 % Sodium Deoxycholate Salt, 150 mM NaCl, 20 mM TRIS, 10 mM EDTA, 30 mM Na-Pyrophosphate, pH 7.5

**Running Buffer (10x):** 250 mM TRIS-Base, 1 % SDS, 2.5 M Glycine

**TBST:** 25 mM TRIS, 125 mM NaCl, 0.1 % Tween-20, pH 8.0

### **3.5.2 The production of antibodies for murine PHGPx**

The production of antibodies, specific for murine PHGPx, was performed by Elisabeth Kremmer, GSF, Munich, Germany. Antibodies were raised in rat against a PHGPx-specific peptide sequence, homologue to the C-terminal part of PHGPx (PQVIEKDLPCYL). The Cys of the PHGPx sequence was replaced by butyric acid (Ba) and an additional Cys was added at the C-terminal end. The peptide sequence was coupled to ovalbumin (OVA) or keyhole limpet hemocyanin (KLH) at the C-terminus (PQVIEKDLPBaYLC-OVA/KLH). The peptides were obtained from Peptide Specialty Laboratories, Heidelberg, Germany. Five positive clones of hybridoma cells were identified (mGPx 1B4, 7E2, 6G8, 7E8, 8A5). The antibody-containing supernatant of clone mGPx4 1B4 (IgG1) was used in this work.

### **3.5.3 Immunocytochemistry and confocal microscopy**

MEFs were seeded onto UV-sterilized cover slips in 6-well cell culture dishes. Cells were cultivated to semi-confluency in standard DMEM. For fixation of adherent cells, medium was aspirated from the cell culture dish, and cover slips were rinsed with PBS. Cells were fixed for 10 min in a 4% PFA solution. Cover slips were washed 3x with PBS and permeabilized for 15 min with 0.1% Triton X-100 in PBS. Subsequently, cells were blocked for 2 h with 10% FCS in PBS. For detection of HA-tagged PHGPx, cover slips were incubated over night with primary antibody  $\alpha$ -HA High Affinity (clone 3F10) at 4°C in a humidified chamber. Glasses were washed 3x with PBS/Tween and subsequently incubated with secondary antibody  $\alpha$ -rat-Cy3



conjugate protected from light (45 min). Cover slips were washed 3 x with PBS/Tween and then incubated for 2 min in DAPI solution. Glasses were briefly rinsed in PBS and mounted onto microscope slides, using mounting medium. Slides were dried over night at 4°C, protected from light and eventually sealed with nail polish. Pictures were taken by confocal microscopy with Leica DM IRBE microscope, Leica TCS SP2 scanner and Leica Confocal software.

**α-HA (clone 3F10) antibody solution:** 1/10 dilution of 3F10 hybridoma supernatant in PBS/10% FCS

**α-rat-Cy3 solution:** 1/1000 dilution in PBS/10% FCS

**DAPI-solution:** 1 µg/ml DAPI diluted in PBS (5mg/ml stock solution in H<sub>2</sub>O)

**PBS:** 80.0 g NaCl, 2.0 g KCL, 14.4 g Na<sub>2</sub>HPO<sub>4</sub>, 2.4 g KH<sub>2</sub>PO<sub>4</sub> in 1 l H<sub>2</sub>O, pH 7.4

**PBS/Tween:** 0.1% (v/v) Tween 20 in PBS

**PFA solution:** 4% (w/v) PFA in PBS, pH 7.4 adjusted with HCl

**Standard DMEM:** DMEM, 10 % FCS, 1 % glutamine, 50 U/ml penicillin G, 50 µg/ml streptomycin

**Triton X-100 solution:** 0.1% (v/v) Triton X-100 in PBS

### **3.6 Determination of mRNA levels**

#### **3.6.1 RNA isolation and cDNA synthesis**

Total RNA from cells was isolated with RNeasy Mini Kit (Qiagen) according to manufacturers' instructions. MEFs were harvested from 10 cm cell culture dishes with a cell scraper. Cells were disrupted by the addition of 600 µl Buffer RLT, containing 10 µl/ml 2-ME. To process samples simultaneously during time course experiments, cell extracts were temporarily stored at -80°C, which did not affect the quality and yield of total RNA. To avoid DNA contamination, on-column DNase digestion with the accessory RNase-Free DNase Set (Qiagen) was performed. RNA was eluted from the column with 30 µl elution buffer. Final RNA concentrations were determined by measuring the absorbance at 260 nm in a spectrophotometer. Single-stranded cDNA was synthesized from 1 µg of isolated mRNA by Reverse Transcription System (Promega) according to manufacturers' instructions. The incubation time, however, was extended to 45 min to obtain more abundant transcripts. The cDNA amplification was performed with random primers at 42°C. The 20 µl first-strand cDNA synthesis reaction mix was finally diluted to 100 µl with nuclease-free water and subjected to RT-PCR.

### **3.6.2 Quantitative RT-PCR**

The synthesized cDNA was amplified and detected with LightCycler FastStart DNA MasterPLUS SYBR Green I Kit in combination with LightCycler 1.5 System (Roche). For each RT-PCR reaction, 6 µl H<sub>2</sub>O, 1 µl primer mix, 1 µl Master Mix and 2 µl cDNA were mixed in a LightCycler Capillary, pre-cooled in a centrifuge adapter. RT-PCR primers were designed with software Primer3 (Rozen and Skaletsky, 2000), standardizing optimal T<sub>M</sub> of approximately 70°C and a product size of 200-300 nucleotides. If possible, primer pairs hybridizing on different exons were used to prevent unspecific amplification of possible genomic DNA contaminations. Gene expression levels were normalized to *aldolase* expression levels. To control the specificity of the RT-PCR reaction, the synthesized PCR product was correlated to a specific melting point, which was assessed by running a melting curve program.

**Primer mix:** 5 µl of 100 µM primer A, 5 µl of 100 µM primer B, 90 µl H<sub>2</sub>O (5 µM each primer)

**TE:** 10 mM Tris pH 7,5; 1 mM EDTA

### **3.7 Northern blot**

The specific DNA-probe for murine xCT was a kind gift from Ana Banjac (Banjac Ana, PhD thesis, 2005). The DNA fragments were labelled using Rediprime II random prime labelling system and 50 µCi [ $\alpha$ -<sup>32</sup>P]-dCTP (3000 Ci/mmol, 10 mCi/ml) according to manufacturers' instructions. Non-incorporated nucleotides were separated from the labelled probe by using Sephadex G-50 columns. Labelling efficiency was detected by using a bench-top radioisotope counter. Just before hybridisation, the probe was heat-denatured at 95°C for 5 min.

Total RNA was isolated with RNeasy Mini Kit (Qiagen) according to manufacturers' instructions. MEFs were harvested from 10 cm cell culture dishes with a cell scraper. Total RNA was dissolved in 100 µl RNase-free water and samples were stored at -80°C. 10 µg of total RNA was lyophilised in a speed vac, dissolved in 15 µl RNA loading buffer and incubated at 70°C for 10 min to minimize RNA secondary structures. RNA was separated in a 1 % formaldehyde agarose gel in the presence of 2.2 M formaldehyde in MOPS buffer overnight at 40 V. RNA was transferred to a Hybond-N<sup>+</sup> membrane by capillary forces using 10 x SSC solution. The gel was placed on a glass plate covered with two Whatman filter papers (dipped in reservoirs

with 10 x SSC solution) and overlaid with a Hybond-N<sup>+</sup> membrane and several layers of blotting paper. The transfer of RNA was controlled by UV light. Subsequently, RNA was covalently cross-linked to the membrane by baking at 80°C for 1 hour. The membrane was pre-hybridised at 65°C for 2 hours in Church buffer. Hybridisation was performed at 68°C overnight in 15-20 ml of fresh Church buffer, containing approximately 1x10<sup>7</sup> dpm of radioactively labelled probe. Membranes were washed twice for 15 min at 68°C with 2 x SSC, 1 % SDS and then twice for 10 min at 68°C with 0.1 x SSC, 0.5 % SDS. Membranes were dried and exposed to an X-ray film overnight at -80°C.

**Church buffer:** 200 mM NaH<sub>2</sub>PO<sub>4</sub>, 400 mM Na<sub>2</sub>HPO<sub>4</sub>, 7 % (w/v) SDS, 1 mM EDTA, pH 7.1-7.2

**Formaldehyde agarose gel:** 2.2 M formaldehyde, 1x MOPS buffer, 1 % (w/v) agarose

**MOPS buffer:** 0.4 M MOPS (free acid), 100 mM Na-acetate, 10 mM EDTA/NaOH pH 8.0, pH 7.0 adjusted with 10 N NaOH

**RNA loading buffer:** 50 % (v/v) formamide, 2.2 M formaldehyde, 1 x MOPS buffer, 50 µg/ml ethidium bromide, 0.2 % (w/v) bromophenol blue

**SSC (20 x):** 3 M NaCl, 300 mM Tris-sodium citrate/NaOH pH 7.0

### **3.8 Flow cytometry (FACS analysis)**

#### **3.8.1 Intracellular peroxide detection**

Intracellular peroxide levels were detected by DCF staining. The acetylated forms of DCF, such as CM-H<sub>2</sub>DCFDA, are non-fluorescent until the acetyl groups are removed by intracellular esterases and oxidation occurs inside the cell. Cells (1 x 10<sup>6</sup> cells) were loaded with 1 µM CM-H<sub>2</sub>DCFDA for 60 min at 37°C in Standard DMEM. Cells were washed with PBS and detached from the cell culture dish by trypsinization. Subsequently, cells were harvested by centrifugation (600 x g, 5 min), washed in PBS (3x) and resuspended in 200 µl PBS. Samples were applied to a flow cytometer (BD FACSCalibur) in which cells were excited with 488 nm UV line argon ion laser. The DCF emission was recorded on channel FL1 at 530 nm. Data were collected from at least 20,000 cells.

**DCF solution:** 1 µM CM-H<sub>2</sub>DCFDA in ethanol

**PBS:** 80.0 g NaCl, 2.0 g KCL, 14.4 g Na<sub>2</sub>HPO<sub>4</sub>, 2.4 g KH<sub>2</sub>PO<sub>4</sub> in 1 l H<sub>2</sub>O, pH 7.4

**Standard DMEM:** DMEM, 10 % FCS, 1 % glutamine, 50 U/ml penicillin G, 50 µg/ml streptomycin

### **3.8.2 Detection of lipid peroxidation**

Cellular lipid peroxidation was detected by BODIPY staining. The fluorophore BODIPY intercalates in biomembranes where its fluorescence shifts from red to green upon oxidation. Cells ( $1 \times 10^6$  cells) were loaded with  $2 \mu\text{M}$  BODIPY 581/591  $\text{C}_{11}$  for 60 min at  $37^\circ\text{C}$  in Standard DMEM. Cells were washed with PBS and detached from the cell culture dish by trypsinization. Subsequently, cells were harvested by centrifugation ( $600 \times g$ , 5 min), washed in PBS (3x) and resuspended in  $200 \mu\text{l}$  PBS. Samples were applied to a flow cytometer (BD FACSCalibur), in which cells were excited with 488 nm UV line argon ion laser and BODIPY emission was recorded on channels FL1 at 530 nm (green) and FL2 at 585 nm (red). Data were collected from at least 20,000 cells.

**BODIPY solution:** 2 mM BODIPY 581/591  $\text{C}_{11}$  in DMSO

**PBS:** 80.0 g NaCl, 2.0 g KCL, 14.4 g  $\text{Na}_2\text{HPO}_4$ , 2.4 g  $\text{KH}_2\text{PO}_4$  in 1 l  $\text{H}_2\text{O}$ , pH 7.4

**Standard DMEM:** DMEM, 10 % FCS, 1 % glutamine, 50 U/ml penicillin G, 50  $\mu\text{g}/\text{ml}$  streptomycin

### **3.8.3 Cell viability detection by flow cytometry**

Cell viability was determined by propidium iodide (PI) staining. Adherent cells were washed with PBS and detached by trypsinization. Subsequently, cells were harvested by centrifugation ( $600 \times g$ , 5 min), washed in PBS (3x) and resuspended in  $200 \mu\text{l}$  PBS. PI was added to a final concentration of  $1 \mu\text{g}/\text{ml}$ . The fluorogenic dye PI enters only dead cells and intercalates into double stranded DNA. PI can not cross the intact membrane of viable cells, thus its fluorescence of above 630 nm can be used for cell viability screening. Cell suspensions were excited with 488 nm UV line argon ion laser and PI emission was recorded on channel FL3 at 661 nm.

**PI solution:** 1 mg/ml PI in PBS

**PBS:** 80.0 g NaCl, 2.0 g KCL, 14.4 g  $\text{Na}_2\text{HPO}_4$ , 2.4 g  $\text{KH}_2\text{PO}_4$  in 1 l  $\text{H}_2\text{O}$ , pH 7.4

**Standard DMEM:** DMEM, 10 % FCS, 1 % glutamine, 50 U/ml penicillin G, 50  $\mu\text{g}/\text{ml}$  streptomycin

### **3.9 Detection of HETE/HPETE and LTB<sub>4</sub> detection by HPLC**

Cells were harvested by trypsinization and cell number was determined in a haemocytometer by trypan blue exclusion.  $2.5 \times 10^6$  cells were washed and resuspended in 500  $\mu$ l prewarmed PBS containing 1 mM CaCl<sub>2</sub> and 1 mg/ml glucose. To activate arachidonic acid metabolism and enrich its metabolites, cells were incubated for 10 min with 40  $\mu$ M arachidonic acid and 2.5  $\mu$ M A23187 Ca<sup>2+</sup>-ionophore. The incubation was stopped by addition of 1 ml of -20°C methanol to the cell suspension, concurrently extracting lipids from the cell extract. Solid phase extraction was performed on Supelclean LC-18 columns (Sigma) according to manufacturers' instructions.

Lipid extracts were applied to an HPLC machine equipped with C18 reverse-phase NovaPak HPLC column and connected to a UV-detector. Protocol A resolved 5-HETE/HPETE, 12-HETE/HPETE and 15-HETE/HPETE in a mobile phase containing 60% acetonitrile, 40% H<sub>2</sub>O and 0.01% acetic acid at a wavelength of 235 nm. Protocol B resolved LTB<sub>4</sub> in a mobile phase containing 35 % methanol, 35% H<sub>2</sub>O, 30% acetonitrile and 0,0001% acetic acid at 270 nm.

### **3.10 Detection of Cys/(Cys)<sub>2</sub> and GSH**

#### **3.10.1 Cys and GSH detection by HPLC**

The HPLC system consisted of a System Gold 126 pump, connected to a System Gold 508 autosampler (both Beckman Coulther GmbH, Krefeld, Germany) and a RF-10A XL fluorescence spectrophotometer (Shimadzu, Duisburg, Germany). The mobile phase consisted to 95 % of 30 mM ammonium-formiate, 40 mM ammonium-nitrate buffer (adjusted to pH 3.65 with formic acid) and to 5 % of acetonitrile. The column effluent was monitored by fluorescence detection with an excitation wavelength of 385 nm and an emission of wavelength of 515 nm.

Cellular Cys and GSH levels were measured in extra- and intracellular fractions of  $\gamma$ GCS knockout cells. Cells were incubated in FCS-free cell culture medium for 90 min. Subsequently, medium was recovered for extracellular and cells for intracellular Cys and GSH measurements. Cells were harvested from cell culture dishes by

vigorous pipetting, washed twice in PBS, resuspended in 500  $\mu$ l Borate Buffer 1 and homogenized by sonication.

For GSH and Cys/(Cys)<sub>2</sub> measurement, samples (200  $\mu$ l) were treated on ice with 20  $\mu$ l 100 ml/l tri-*n*-butylphosphine in dimethylformamide for 30 min in order to reduce thiols and liberate them from proteins. This reducing step was omitted for free Cys detection, to avoid (Cys)<sub>2</sub> reduction. 200  $\mu$ l perchloric acid was added to the samples, mixed and incubated on ice for 10 min. Proteins were removed by centrifugation at 10,000 x g for 10 min at 0°C. 100  $\mu$ l supernatant, 250  $\mu$ l Borate Buffer 2 and 100  $\mu$ l SBDF were mixed and incubated at 60°C for 60 min. To terminate the SBDF derivatization step, the solutions were snap-cooled on ice and transferred to a cooled autosampler vial. Aliquots of 50  $\mu$ l were injected into the column. Standard samples of L-cysteine (3 to 250  $\mu$ M) and GSH (1 to 50  $\mu$ M) were prepared by serial dilution in Borate Buffer 1.

**Borate Buffer 1:** 0.2 M boric acid, containing 2 mM Na<sub>2</sub>EDTA, pH 9.5

**Borate Buffer 2:** 0.2 M boric acid, containing 5 mM Na<sub>2</sub>EDTA, pH 10.5

**PBS:** 80.0 g NaCl, 2.0 g KCL, 14.4 g Na<sub>2</sub>HPO<sub>4</sub>, 2.4 g KH<sub>2</sub>PO<sub>4</sub> in 1 l H<sub>2</sub>O, pH 7.4

**Perchloric acid:** 0.5 M perchloric acid, containing 1 mM Na<sub>2</sub>EDTA

**SBDF:** 1.0 g/l 7-fluoro- benzo-2-oxa-1.3-diazole-4- sulphonate in 0.1 M Borate Buffer 1

### **3.10.2 Determination of cellular L-cystine uptake capacity**

The uptake capacity for L-cystine was determined by measuring the time-dependent increase of radioactive labelled L-[<sup>14</sup>C(U)] cystine in the cell. 1x10<sup>6</sup> cells were seeded per 6 cm cell culture dish in DMEM, containing 5 mM NAC, and incubated for 24 h. The cellular monolayer was washed with prewarmed PBS(+) (3x), following the addition of 500  $\mu$ l Uptake Solution and incubation in a water bath at 37°C for 90 sec. To control the specificity of antiporter x<sub>c</sub><sup>-</sup>-mediated cystine uptake, 2.5 mM glutamate was added to the Uptake Solution. The Uptake Solution was aspirated, cells were washed with ice cold PBS and lysed in 500  $\mu$ l 0.5 M NaOH over night. The protein concentration of the recovered samples was determined by DC Protein Assay (Bio Rad). 200  $\mu$ l cell lysate, 3 ml scintillation cocktail and 100  $\mu$ l 0.2 M Tris-HCl were mixed in a scintillation tube. Radioactivity was determined by a LS 500 TA Scintillation Counter. To correlate cystine concentration and radioactivity, 5  $\mu$ l Uptake

Solution (50  $\mu$ M cystine) was mixed with 500  $\mu$ l 0.5 M NaOH and the “specific activity” was measured. The cellular cystine uptake activity is stated as nmol cystine  $\text{min}^{-1} \text{mg}^{-1}$ .

**Uptake Solution:** 50  $\mu$ M L-cystine, 0.2  $\mu$ Ci/ml L-[ $^{14}$ C(U)] cystine, 10 % glucose, 1 %  $\text{CaCl}_2$ , 1 %  $\text{MgCl}_2$  in PBS. 5 mM L-cystine stock solution was dissolved in 0.05 M HCL with stirring for several hours at room temperature.

**PBS:** 80.0 g NaCl, 2.0 g KCL, 14.4 g  $\text{Na}_2\text{HPO}_4$ , 2.4 g  $\text{KH}_2\text{PO}_4$  in 1 l  $\text{H}_2\text{O}$ , pH 7.4

**PBS(+):** PBS, 10 % glucose, 1 %  $\text{CaCl}_2$ , 1 %  $\text{MgCl}_2$

### **3.10.3 Determination of extracellular mercaptans**

Levels of extracellular mercaptans were measured with DTNB, also called Ellman’s reagent. This aromatic disulfide reacts with aliphatic thiol groups to form a mixed disulfide. DTNB has little absorbance, but upon reaction with free sulfhydryl groups it gives an intense yellow colour, which can be detected with a photometer at 412 nm.  $\gamma$ -GCS knockout cells were incubated in FCS-free DMEM and medium was recovered at different time points. 50  $\mu$ l DTNB solution was added to 500  $\mu$ l medium, mixed and incubated for 2 min. Absorbance was measured with a DU-64 Spectrophotometer at 412 nm. Control cells were incubated in DMEM\*, lacking component cystine. Fresh DMEM was used as blank control. Standard samples of reduced GSH (10 to 40  $\mu$ M) were prepared by serial dilution in DMEM.

**DTNB Solution:** 10 mM DTNB in K-Phosphate Buffer

**K-Phosphate Buffer:** 0.2 M K-Phosphate, 10 mM EDTA, pH 7.2

## **4. Results**

### **4.1 Inducible inactivation of PHGPx in primary MEFs**

To bypass early embryonic lethality of PHGPx null mice, the Cre/loxP system was employed to create mice with targeted conditional disruption of gene PHGPx (Conrad Marcus, PhD thesis, 2001) (figure 12-A). These transgenic mice were used in this work to generate individual cell lines of primary MEFs. To achieve inducible inactivation of PHGPx, cells with one or two loxP flanked (floxed) PHGPx alleles were stably transfected with the tamoxifen-inducible Cre fusion protein MerCreMer. MerCreMer was used instead of constitutively active Cre, since it was unknown whether loss of PHGPx in MEFs might affect cell proliferation or even cause cell death. Cells were transfected with the bicistronic expression vector pCAG-3SIP-MerCreMer (figure 12-D).

The CAG promoter of pCAG-3SIP is a strong promoter consisting of the chicken  $\beta$ -actin promoter and elements of the CMV enhancer. The bicistronic expression cassette, containing MerCreMer and puromycin N-acetyltransferase, ensures stable expression of MerCreMer (a kind gift from T. Schroeder, GSF, Munich) (Verrou et al., 1999), due to the possibility to select for transfected cells by puromycin. A point mutation in the oestrogen receptors of MerCreMer prevents binding of endogenous  $17\beta$ -oestradiol in the mouse but retains binding capacity for tamoxifen. In the absence of tamoxifen, MerCreMer is retained in the cytosol by forming a complex with heat shock protein 90 (Hsp90) via its two mutated oestrogen receptor domains. The knockout of PHGPx can be induced by the addition of 4-hydroxytamoxifen to the cell culture medium. 4-hydroxytamoxifen binds to the mutated oestrogen receptors of fusion protein MerCreMer, whereupon MerCreMer is released from Hsp90 and translocates to the nucleus where Cre-mediated recombination between two adjacent loxP sites takes place. Since Cre activation causes the deletion of exon five to seven of the PHGPx gene, including the crucial SECIS element, PHGPx activity is abolished.



The following nomenclature for mice and cell lines was adopted from Marcus Conrad's work (Conrad Marcus, PhD thesis, 2001). Transgenic PHGPx mice are designated with the abbreviation PF (PHGPx, flipped) and isolated fibroblasts with the abbreviation PFa. To isolate primary MEFs, male PF (wt/flox or flox/flox) mice were mated with PF (wt/flox or flox/flox) females. At 12.5 days *post coitum*, females were sacrificed, and embryos were dissected. In total, 56 primary MEF cell lines were isolated from E12.5 embryos and the respective genotypes were determined from 40 outgrowing cell lines by PCR. The isolated MEF cell lines contain either one or two floxed PHGPx alleles. Embryos obtained from matings of heterozygous PF (wt/flox) male and PF (wt/flox) female mice gave rise to 7 PFa<sup>(wt/wt)</sup> (21 %), 16 PFa<sup>(wt/flox)</sup> (49 %), and 10 PFa<sup>(flox/flox)</sup> (30%) cell lines, whereas breeding of homozygous PF<sup>(flox/flox)</sup> parents gave rise to 7 homozygous PFa<sup>(flox/flox)</sup> cell lines. Four independent PFa cell lines were used for further studies. These include the homozygous cell lines PFa1<sup>(flox/flox)</sup> and PFa24<sup>(flox/flox)</sup>, which contain two floxed PHGPx alleles, and the hemizygous cell lines PFa37<sup>(wt/flox)</sup> and PFa43<sup>(wt/flox)</sup>, each harbouring one floxed and one wild type allele (figure 12-B).

Plasmid pCAG-3SIP-eGFP (figure 12-D) was included in these studies to monitor transfection efficiency and puromycin selection of stably transfected MEFs by fluorescence microscopy and flow cytometry analysis. Primary MEFs with early passage number grew slowly and transfection efficiency by electroporation did not exceed 5 %. At least 6 weeks were necessary to accomplish puromycin selection with low passage number MEFs, transfected with pCAG-3SIP-eGFP (figure 12-C). Primary MEFs that overcame replicative senescence after 20-30 passages grew faster and transfection efficiency increased notably to more than 50 %. These cells were clearly reduced in size, which correlated with a significantly faster cell division rate. When immortalized cell lines were used, the selection of stably transfected clones by puromycin was already accomplished after 2 weeks. Thus, immortalized cells were used for all subsequent transfections. After optimisation of the transfection and selection procedure with plasmid pCAG-3SIP-eGFP, PFa<sup>(wt/flox)</sup> and PFa<sup>(flox/flox)</sup> cell lines were stably transfected with pCAG-3SIP-MerCreMer by electroporation and subsequent puromycin selection, yielding PFa-MerCreMer cell lines. PFa-MerCreMer cells were maintained under selection pressure (2 µg/ml puromycin) to assure stable expression of MerCreMer.

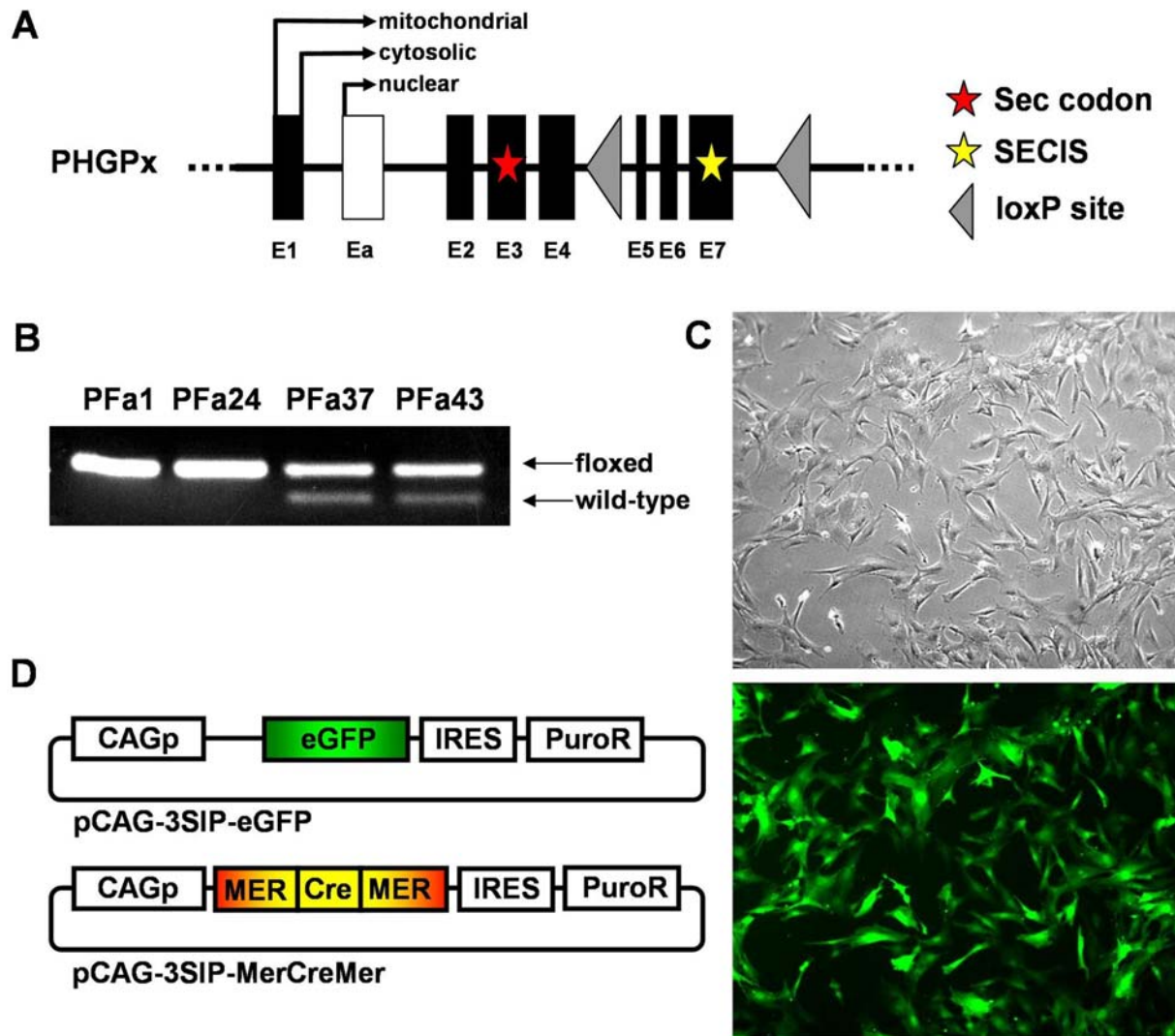


**Figure 12:** The inducible Cre/loxP system for PHGPx deletion in MEFs. **(A)** Depicted is the genomic structure of a transgenic PHGPx allele in PFa cells. Exons 5 to 7 were flanked by loxP sites (for further details see figure 6). **(B)** The genotyping of isolated MEFs by PCR shows wild type PHGPx (170 bp) and floxed PHGPx (240 bp) alleles. PFa1<sup>(floxed/floxed)</sup> and PFa24<sup>(floxed/floxed)</sup> were identified as homozygous cell lines, whereas PFa37<sup>(wt/floxed)</sup> and PFa42<sup>(wt/floxed)</sup> cells contain one wild type and one floxed PHGPx allele. **(C)** Fluorescence microscopy of pCAG-3SIP-eGFP-transfected MEFs, after selection with puromycin. **(D)** Schematic representation of the bicistronic expression vectors, used for stable expression of MerCreMer or eGFP.

The Cre-mediated disruption of PHGPx was assessed by quantitative RT-PCR and Western blot in PFa<sup>(floxed/floxed)</sup>-MerCreMer cells (figure 13). The antioxidant  $\alpha$ -tocopherol had to be included in the cell culture medium during the course of the experiments, for reasons as outlined below (refer to chapter 4.4). RT-PCR was performed with primers specifically binding to the exon 3 to 4 boundary and exon 6. cDNA was synthesized from total cellular mRNA, isolated from PFa1<sup>(floxed/floxed)</sup>-MerCreMer cells. 24 hours after the addition of 4-hydroxytamoxifen to the cell culture medium, PHGPx mRNA levels decreased to approximately 4 % compared to total PHGPx mRNA in

non-treated cells. The mRNA levels remained below 10 %, at least during the 96 hours after addition of 4-hydroxytamoxifen (figure 13-A). PHGPx protein levels were assessed by immunoblotting, using antibody  $\alpha$ -PHGPx (mGPx4 1B4) (figure 13-B). The PHGPx protein levels drastically decreased 48 hours after the induction of the PHGPx knockout.

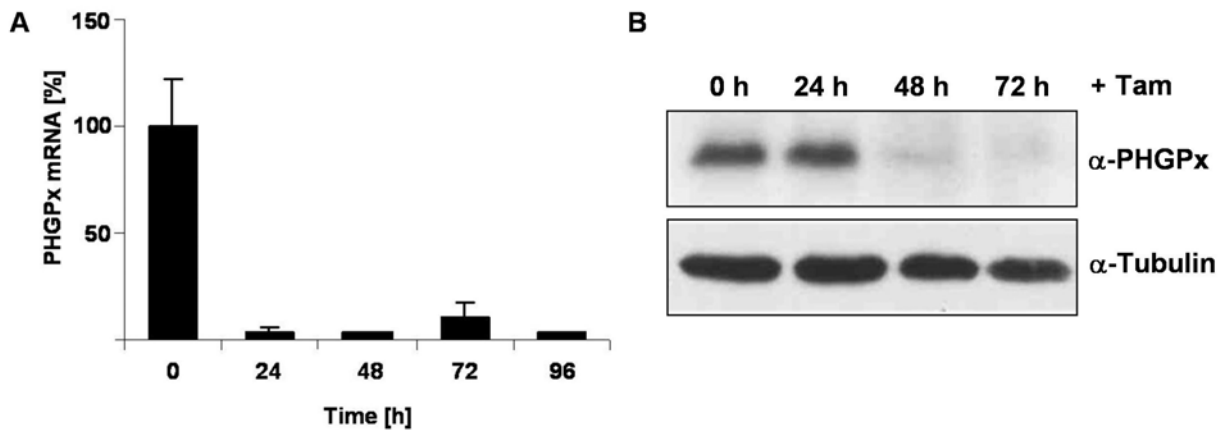


**Figure 13:** Inducible disruption of PHGPx in primary MEFs. **(A)** Endogenous PHGPx mRNA levels in PFA1<sup>(flox/flox)</sup>-MerCreMer cells were determined by quantitative RT-PCR before and after 4-hydroxytamoxifen (Tam)-induced activation of MerCreMer. **(B)** PHGPx protein levels were determined by western blot, using  $\alpha$ -PHGPx antibody mGPx4-1B4, before and after the induction of the PHGPx knockout.

#### 4.2 PHGPx depletion causes rapid cell death

To study the effects of PHGPx abolition, PFA<sup>(flox/flox)</sup>-MerCreMer cells and the hemizygous control cell lines PFA37<sup>(wt/flox)</sup>-MerCreMer and PFA43<sup>(wt/flox)</sup>-MerCreMer were treated with 4-hydroxytamoxifen (figure 14). The deletion of PHGPx in PFA1<sup>(flox/flox)</sup>-MerCreMer and PFA24<sup>(flox/flox)</sup>-MerCreMer cells caused massive cell death, already 48 hours after the addition of 4-hydroxytamoxifen to the cell culture medium. By contrast, no obvious phenotype could be observed in 4-hydroxytamoxifen-treated PFA43<sup>(wt/flox)</sup>-MerCreMer cells (figure 14-A). PFA37<sup>(wt/flox)</sup>-MerCreMer cells showed only a transient retardation in cell growth, but eventually recovered from 4-hydroxytamoxifen-treatment (data not shown).

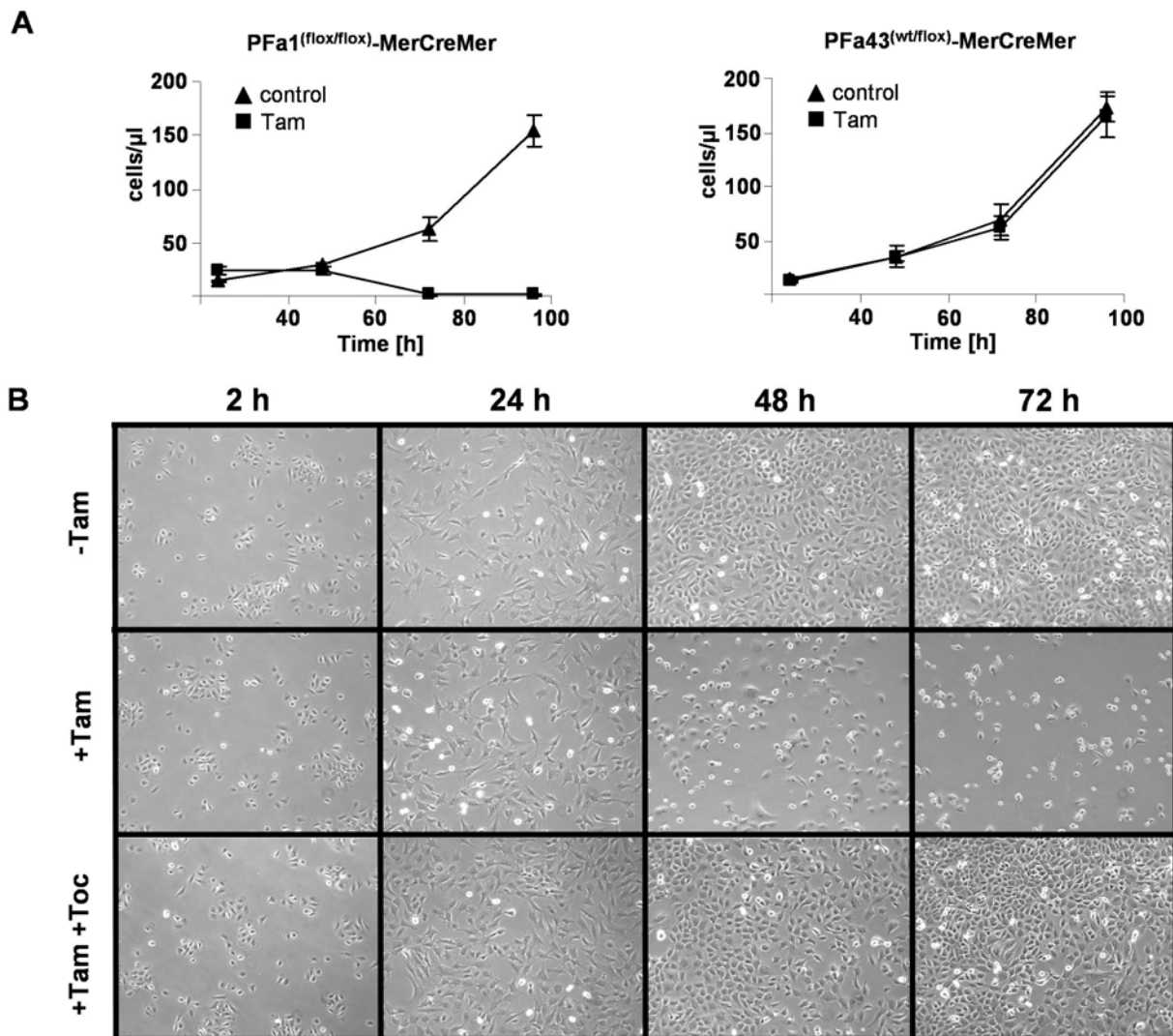


**Figure 14:** PHGPx disruption causes massive cell death in MEFs. **(A/B)** Cell growth after Cre-mediated PHGPx depletion in PFa1<sup>(flox/flox)</sup>-MerCreMer and PFa43<sup>(wt/flox)</sup>-MerCreMer cells. **(B)** 4-hydroxytamoxifen (Tam) treated PFa1<sup>(flox/flox)</sup>-MerCreMer cells underwent rapid cell death. The lipophilic antioxidant  $\alpha$ -tocopherol (Toc) fully rescued PHGPx depletion.

Of note, 4-hydroxytamoxifen-treated PFa<sup>(flox/flox)</sup>-MerCreMer cells, seeded at high cell density, grew until confluence and did not undergo cell death. Subsequent passaging at low cell density, however, caused rapid cell death within 24 hours, indicating that only proliferating cells depend on functional PHGPx (data not shown). The morphological features of cell death progression in PHGPx-deficient cells were observed by time-lapse videos (see supplementary data on CD). PHGPx-deficient cells shrunk, showed deformation, and lost contact to the cell culture dish and adjacent cells, morphological features reminiscent to those observed in apoptotic

cells. Heterozygous control cells with one functional PHGPx allele could be cultivated indefinitely in cell culture after 4-hydroxytamoxifen-treatment, without showing any signs of increased cell death.

### **4.3 The reconstitution of PHGPx expression with a lentiviral add-back system rescues PHGPx knockout cells**

The activation of MerCreMer by 4-hydroxytamoxifen caused massive cell death within 48 hours in PFa<sup>(flox/flox)</sup>-MerCreMer cells. To rule out any unspecific detrimental side effects, e.g. by Cre activation or by 4-hydroxytamoxifen, PHGPx was ectopically expressed in these cells. The coding region of the PHGPx gene was amplified from murine testis cDNA and cloned into the pDrive vector. The coding sequences for an HA-tag or a Flag-Strep-HA-tag (FSH-tag) were cloned in frame in the 5'-end of PHGPx cDNA. The tagged PHGPx constructs were transferred into the lentiviral vector p442-PL1, yielding expression vectors p442-HA-PHGPx (figure 15-A) and p442-FSH-PHGPx, respectively. The lentiviral infection system, including vector p442-PL1, was chosen for several reasons. First, lentiviruses comprise high infection efficiency rates due to their ability to infect also non-proliferating cells. Second, lentiviruses are retroviruses that stably integrate into the hosts' genome, and thus replicate non-episomally. Moreover, p442-PL1 comprises a strong SFFV promoter and a bicistronic IRES-VENUSnucmem element for monitoring simultaneous expression of the gene of interest and VENUSnucmem in infected cells.

Ecotropic lentivirus particles were produced in HEK293 T packaging cells. The CaCl<sub>2</sub> transfection efficiency of HEK293 T cells was observed by fluorescence microscopy 24 hours after transfection (figure 15-B). The virus particles were harvested from HEK293 T cell culture medium and used for subsequent infection of PFa1<sup>(flox/flox)</sup>-MerCreMer cells. PFa1<sup>(flox/flox)</sup>-MerCreMer cells, infected with p442-HA-PHGPx and p442-FSH-PHGPx, could be detected by fluorescence microscopy and FACS analysis due to VENUSnucmem expression. The lentiviral infection efficiency was quantified by FACS analysis and ranged between 75-99 % of positive cells (figure 15-C).

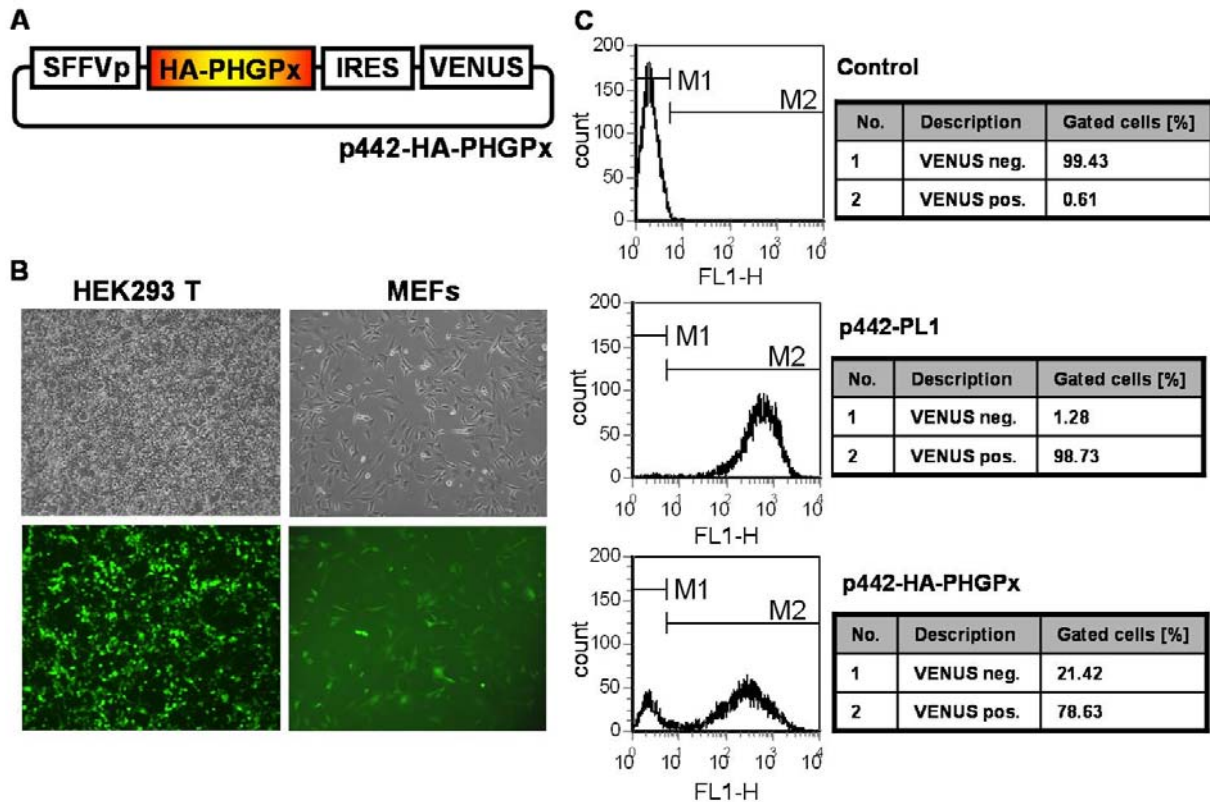


**Figure 15:** Strategy for add-back of exogenous HA-tagged wild type PHGPx with a lentiviral transduction system. **(A)** Schematic illustration of the lentiviral expression vector, including HA-tagged PHGPx and VENUSnucmem expression cassette. **(B)** Fluorescence microscopy of lentiviral VENUSnucmem expression. Depicted are HEK293 T packaging cells (left) and PFA1<sup>(flox/flox)</sup>-MerCreMer MEFs, after the infection with lentiviral supernatants (right). **(C)** Quantification of VENUSnucmem-expressing PFA1<sup>(flox/flox)</sup>-MerCreMer cells, infected with vector p442-PL1 or p442-HA-PHGPx, by FACS analysis.

The expression levels of PHGPx in PFA1<sup>(flox/flox)</sup>-MerCreMer cells, infected with p442-HA-PHGPx or p442-FSH-PHGPx, were quantified by RT-PCR and by immunoblotting. Cellular localization was visualized by immunocytochemistry. Total mRNA was isolated from wild type and p442-HA-PHGPx infected PFA1<sup>(flox/flox)</sup>-MerCreMer cells. PHGPx transcripts increased 5-fold in p442-HA-PHGPx infected cells compared to non-infected wild type cells (figure 16-A). The protein levels of tagged PHGPx (~20 kDa) were analyzed by immunoblotting with  $\alpha$ -HA-tag antibody 3F10 in p442-HA-PHGPx and p442-FSH-PHGPx-infected cells (figure 16-B). A distinct band was detected with both variants of tagged PHGPx, whereas the FSH-tagged PHGPx expression appeared to be much more prominent.

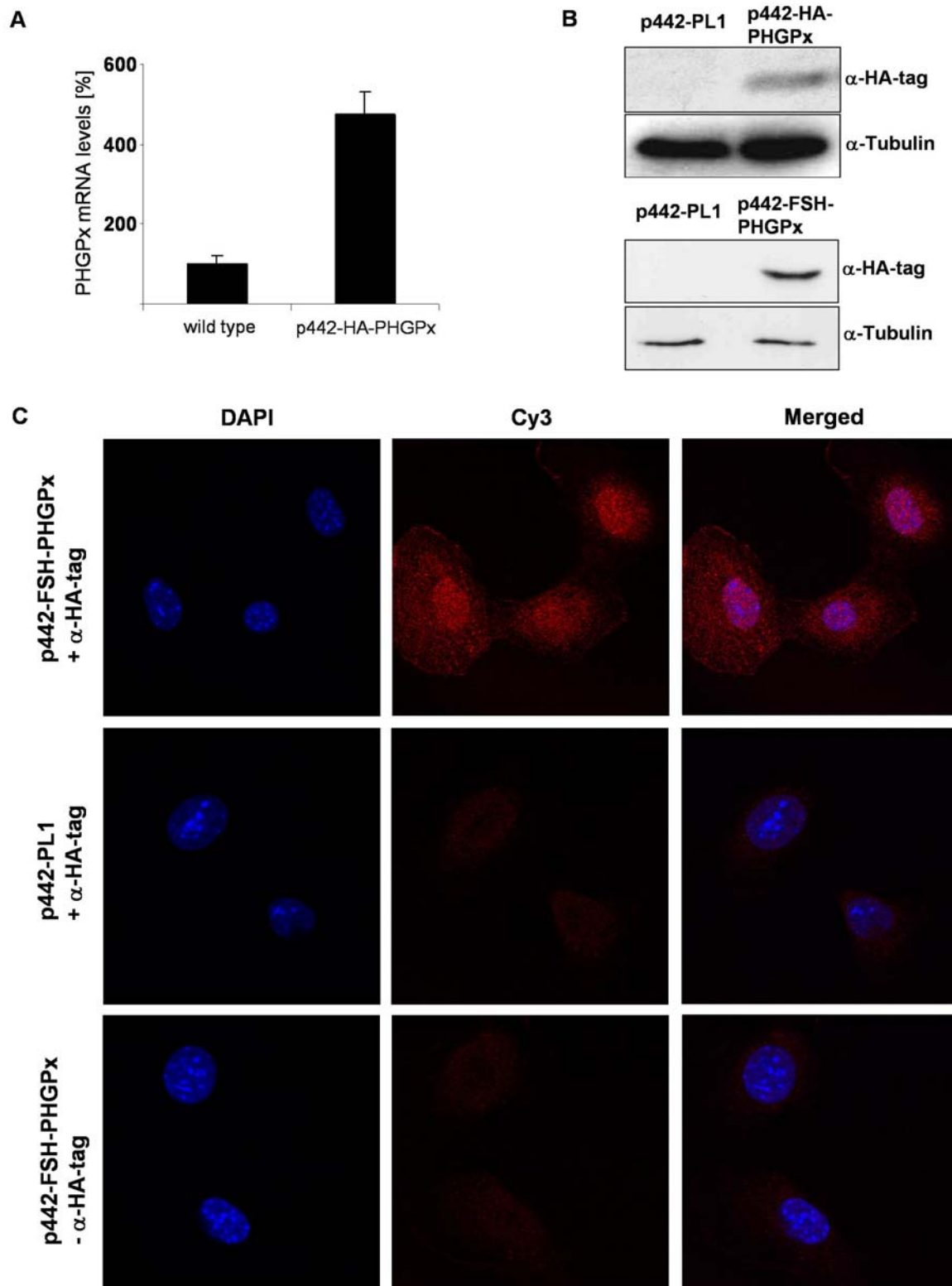


**Figure 16:** Reconstitution of PHGPx expression in PHGPx null cells. HA-tagged or FSH-tagged wild type PHGPx were introduced into PFa1<sup>(flox/flox)</sup>-MerCreMer cells by a lentiviral infection system. **(A)** PHGPx mRNA levels were analyzed by quantitative RT-PCR. PHGPx mRNA levels increased approximately 5-fold in p442-HA-PHGPx-infected cells. PHGPx mRNA levels were normalized to *aldolase* transcription levels. **(B)** Western blot with an  $\alpha$ -HA-tag antibody revealed HA-PHGPx and FSH-PHGPx expression in PFa1<sup>(flox/flox)</sup>-MerCreMer cells. **(C)** Immunocytochemistry with a primary  $\alpha$ -HA antibody and a Cy3-labeled secondary antibody, showing FSH-PHGPx expression in PFa1<sup>(flox/flox)</sup>-MerCreMer cells. Cy3 staining was visualized by confocal microscopy.



The  $\alpha$ -HA-tag antibody 3F10 was also used to visualize FSH-tagged PHGPx expression by immunocytochemistry in paraffin-fixed PFa1<sup>(flox/flox)</sup>-MerCreMer cells. Mock-infected PFa1<sup>(flox/flox)</sup>-MerCreMer cells and control cells, only stained with the secondary antibody ( $\alpha$ -rat-Cy3), revealed a faint Cy3 background. In contrast, p442-FSH-PHGPx infected PFa1<sup>(flox/flox)</sup>-MerCreMer cells yielded a strong Cy3 signal (figure 16-C). The exact localization of PHGPx inside the cell could not be determined by these studies, requiring further co-localization experiments with organelle specific dyes. A very similar, but significantly weaker Cy3 signal was obtained with p442-HA-PHGPx-infected PFa1<sup>(flox/flox)</sup>-MerCreMer cells (data not shown), which is most probably due to weaker expression of the HA-tagged fusion protein, as already observed by immunoblotting.

To examine, whether cell death of PHGPx knockout cells could be rescued by expression of HA-PHGPx in PFa1<sup>(flox/flox)</sup>-MerCreMer cells, proliferation assays were performed after the deletion of endogenous PHGPx expression (figure 17). The number of viable cells was assessed over a period of 96 hours after 4-hydroxytamoxifen treatment.

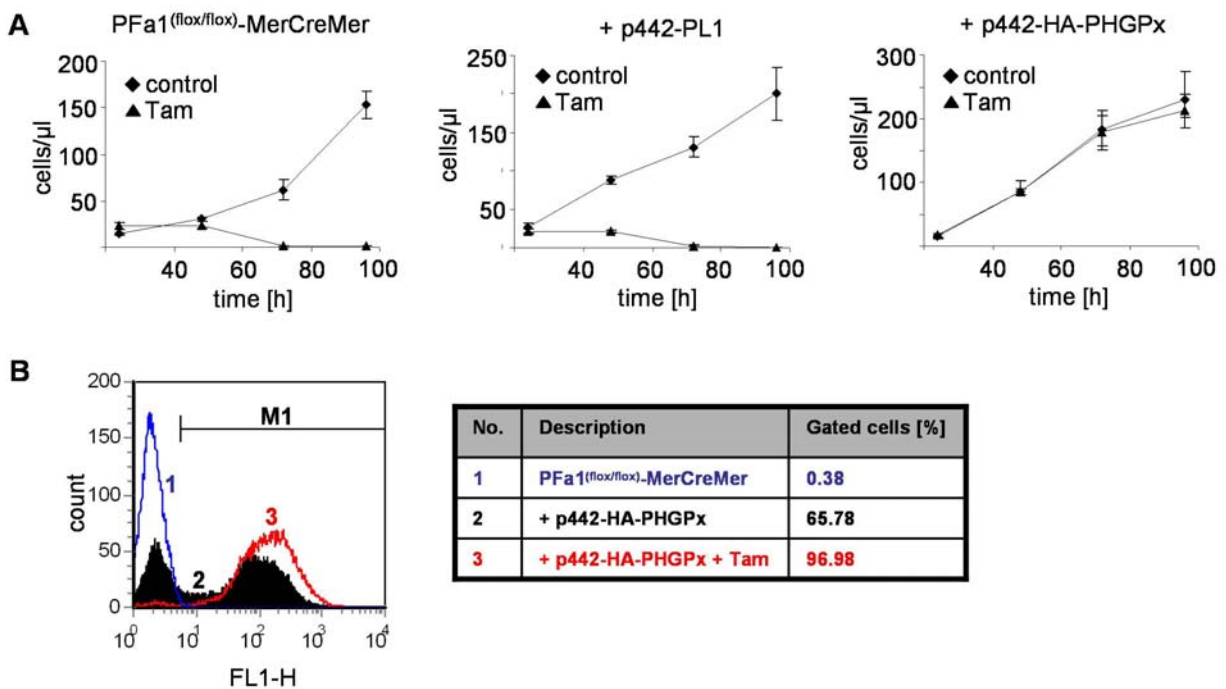


**Figure 17:** The reconstitution of PHGPx expression in PHGPx knockout cells rescued MEFs from cell death. **(A)** Growth curve after deletion of endogenous PHGPx in non-infected PFa1<sup>(flox/flox)</sup>-MerCreMer cells, p442-PL1 mock-infected cells, and p442-HA-PHGPx-infected cells. **(B)** FACS analysis of VENUSnucmem-positive PFa1<sup>(flox/flox)</sup>-MerCreMer cells after p442-HA-PHGPx infection. Quantification was performed before (blue, black) and 72 hours after 4-hydroxytamoxifen (Tam) treatment (red).



As shown in figure 17-A, the reconstitution of PHGPx expression by lentiviral infection with vector p442-HA-PHGPx fully rescued PFa1<sup>(flox/flox)</sup>-MerCreMer cells from cell death. The lentiviral infection itself had no effect on proliferation in the absence of 4-hydroxytamoxifen. When treated with 4-hydroxytamoxifen, p442-PL1-infected control cells died within 48 hours, like non-infected parental PFa1<sup>(flox/flox)</sup>-MerCreMer cells.

Since HA-PHGPx and VENUSnucmem expression is coordinated by a bicistronic expression cassette, VENUSnucmem expression could be used to track cell survival of infected and non-infected cells. The quantification of VENUSnucmem expressing cells was performed by FACS analysis. 66 % of PFa1<sup>(flox/flox)</sup>-MerCreMer cells were positive for VENUSnucmem expression immediately after lentiviral infection with p442-HA-PHGPx. The treatment with 4-hydroxytamoxifen caused an increase from 66 % to 97 % of VENUSnucmem-positive cells after 72 hours (figure 17-B), indicating that non-infected cells died during this period, while exogenous HA-PHGPx expression rescued the deletion of endogenous PHGPx expression.

#### **4.4 Vitamin E, but not water-soluble antioxidants rescue PHGPx-deficient cells from cell death**

PHGPx has been initially identified as an enzyme, efficiently protecting liposomes and biomembranes from peroxidative degradation (Ursini et al., 1982). Hence antioxidant supplements were considered to protect MEFs from cell death, induced by PHGPx disruption. Various concentrations of lipophilic and hydrophilic antioxidants were added to the cell culture medium 12 hours after the addition of 4-hydroxytamoxifen. The number of viable cells was determined 48 hours later by trypan blue exclusion (figure 18).

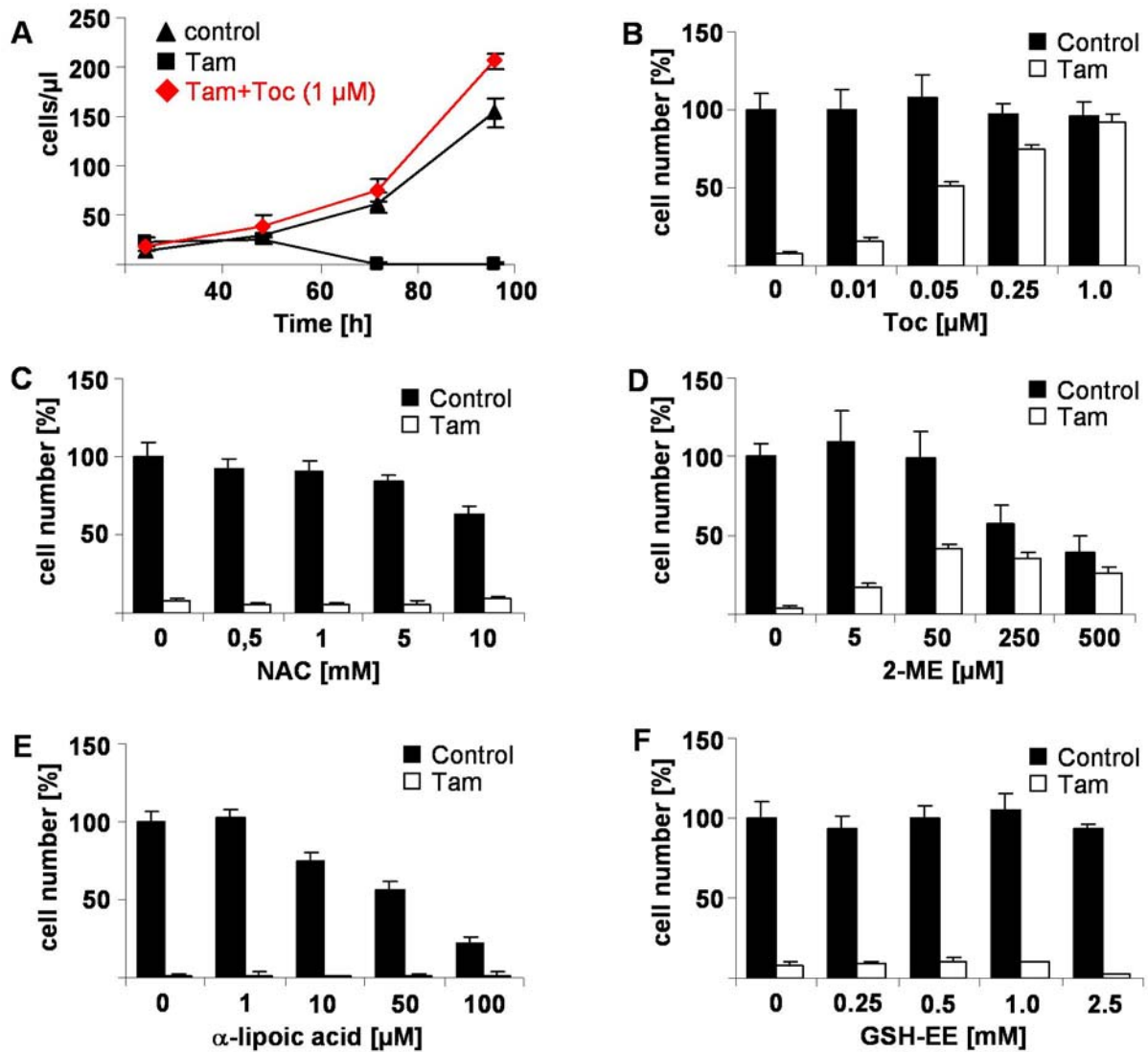


**Figure 18:** The lipophilic antioxidant  $\alpha$ -tocopherol (Toc) rescued PHGPx deficiency *in vitro*. (A/B) The addition of 1  $\mu$ M  $\alpha$ -tocopherol fully rescued cells from cell death, (C) whereas NAC, (D) 2-ME, (E)  $\alpha$ -lipoic acid, (F) and GSH-EE did not protect PHGPx knockout cells. Cell numbers are depicted in per cent, related to the cell number of non-treated wild type cells.

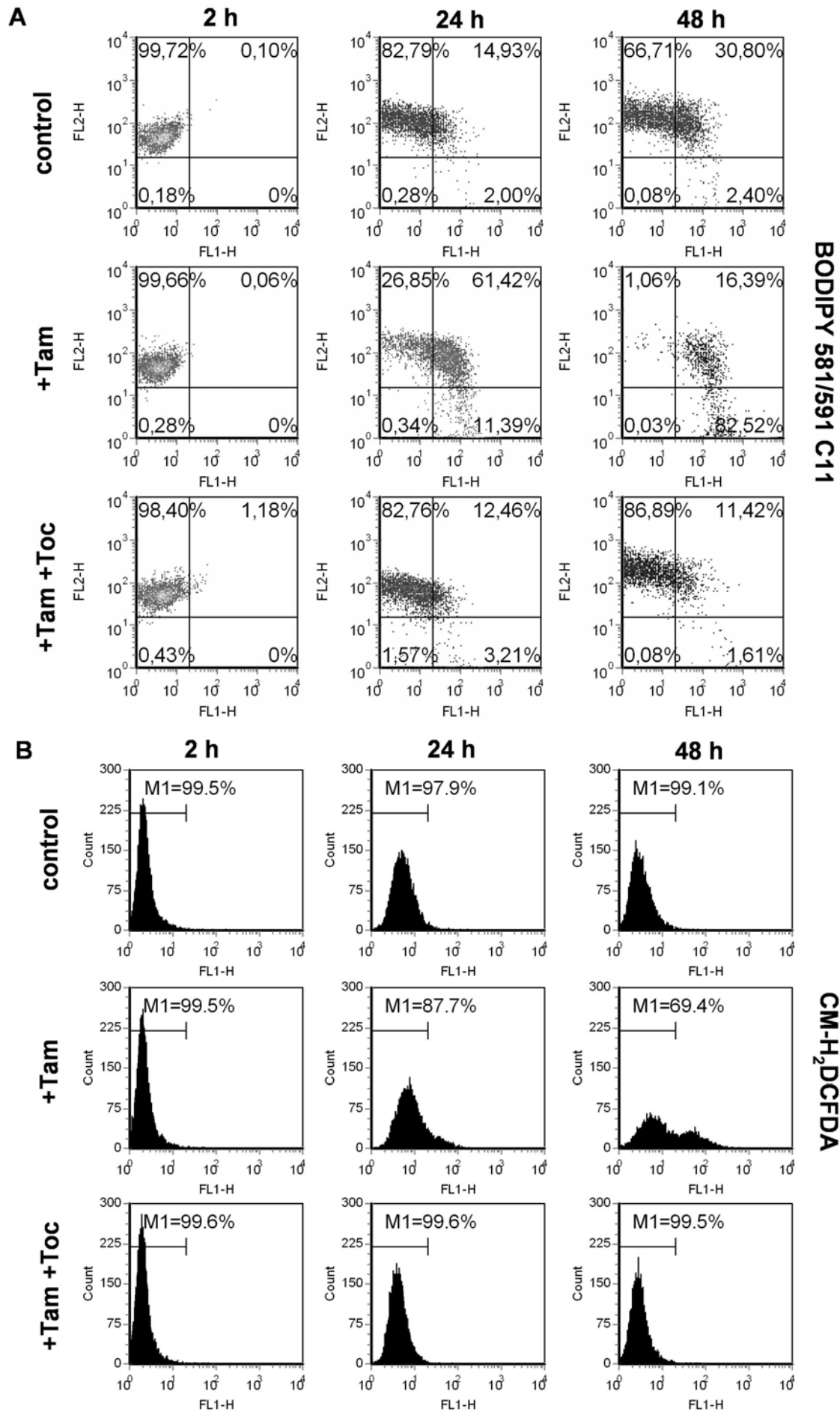
None of the hydrophilic antioxidants [NAC (0.5-10 mM), 2-ME (5-500  $\mu$ M), and GSH-EE (0.25-2.5 mM)] protected PHGPx knockout cells from cell death over a wide range of different concentrations. Only 2-ME, at a concentration of 50  $\mu$ M, showed a weak protective effect but higher concentrations were toxic as shown with control cells. While  $\alpha$ -lipoic acid (1-100  $\mu$ M) proved to be ineffective, the lipophilic antioxidant  $\alpha$ -tocopherol (0.01-1  $\mu$ M) efficiently protected cells from cell death at concentrations of 1  $\mu$ M and higher (figure 14 and 18). Of note, 4-hydroxytamoxifen-treated cells could be indefinitely cultivated in cell culture, when supplemented with  $\alpha$ -tocopherol. A subsequent passaging in the absence of  $\alpha$ -tocopherol, however, caused massive cell death within 24 hours (data not shown).

#### **4.5 Deletion of PHGPx causes cell death, resulting from massive lipid peroxidation**

To address whether PHGPx deficiency may lead to the accumulation of detrimental oxygen radicals, cells were stained with different redox-sensitive dyes. This allowed the quantification and discrimination of cytosolic (CM-H<sub>2</sub>DCFDA) and lipid-associated (BODIPY 581/591 C<sub>11</sub>) ROS.

The lipophilic compound BODIPY 581/591 C<sub>11</sub> is a specific indicator for lipid peroxidation that intercalates in lipid bilayers and shifts its fluorescence from red to green upon oxidation. CM-H<sub>2</sub>DCFDA has been frequently used for the detection of cytosolic ROS, emitting green fluorescence upon oxidation inside the cell. Viable and dead cells were discriminated by PI staining. Cells were subjected to FACS analysis, 2, 24 and 48 hours after 4-hydroxytamoxifen treatment as shown in figure 19.

An increase of lipid peroxidation was detected in more than 70 % of PFa1<sup>(flox/flox)</sup>-MerCreMer cells, already 24 hours after the addition of 4-hydroxytamoxifen. Lipid peroxidation clearly preceded the onset of cell death and arose when cells still maintained cell integrity, as shown by PI exclusion (figure 19-A/C). Cytosolic ROS levels were only slightly increased 24 hours after 4-hydroxytamoxifen treatment, but were more pronounced at 48 hours (figure 19-B). Likewise, PI staining revealed substantial cell death only 48 hours after the induction of the PHGPx knockout (figure 19-C). The addition of  $\alpha$ -tocopherol fully prevented lipid peroxidation, the accumulation of cytosolic ROS, and cell death.



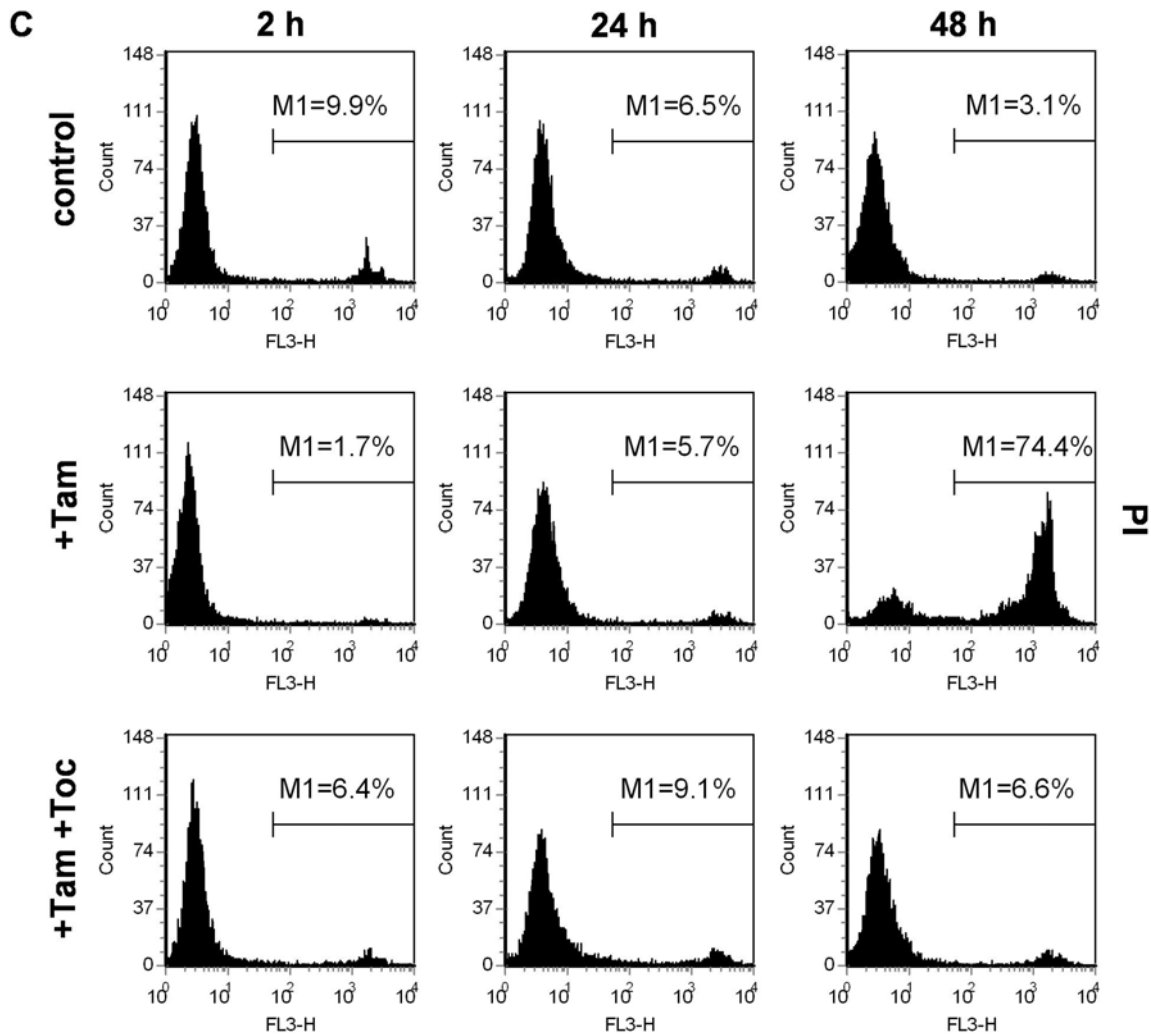


**Figure 19:** Lipid peroxidation is an early event in PHGPx knockout cells, preceding the accumulation of soluble ROS and cell death. (A) Lipid peroxidation was assessed by BODIPY 581/591 C<sub>11</sub> staining. (B) Soluble ROS were detected by CM-H<sub>2</sub>DCFDA staining. (C) Viable and dead cells were discriminated by PI staining. The deletion of PHGPx was induced by 4-hydroxytamoxifen (Tam) and cells were stained with respective fluorophores at indicated time points. Lipid peroxidation, increase of cytosolic ROS, and cell death could be entirely prevented by  $\alpha$ -tocopherol (Toc).

#### 4.6 The crosstalk between PHGPx and arachidonic acid metabolism

PHGPx, along with other GPxs, has been considered to control the activities of LOXs and COXs. In the first catalytic step, LOXs and COXs oxygenate arachidonic acid to the hydroperoxyl-intermediates HPETE and PGG<sub>2</sub>, respectively. (Chen et al., 2003; Imai et al., 1998; Jakobsson et al., 1992). Both types of enzymes require a certain peroxide tone for initial activation and full activity, mediated by oxidation of the catalytically essential ferrous iron to ferric iron (Ivanov et al., 2005). Since PHGPx controls the cellular peroxide tone and efficiently reduces alkylhydroperoxides to its corresponding alcohols, PHGPx has been regarded as a key regulator antagonizing

LOX and COX activities. Since lipid peroxidation was identified as very early event triggering cell death in PHGPx-deficient cells, it was conceivable that PHGPx depletion in PFA1<sup>(flox/flox)</sup>-MerCreMer cells may cause an increase in COX and LOX activities. The accumulation of LOX- and COX-derived hydroperoxyl-intermediates may thus lead to unspecific detrimental lipid peroxidation and eventually cell death in PHGPX-deficient cells.

RT-PCR analysis was used to examine, whether LOXs and COXs are in fact expressed in MEFs. It was shown that COX1, COX2, and various isoforms of the lipoxygenase family, including 5-LOX, 12-LOX, 15-LOX are expressed in MEFs, whereas no expression of 8-LOX and epidermis-type 12-LOX could be detected (figure 20-A).

To test the hypothesis of aberrant arachidonic acid metabolism in PHGPx knockout cells, PFA1<sup>(flox/flox)</sup>-MerCreMer cells were treated with various concentrations of arachidonic acid and cell viability was observed 36 hours later (figure 20-B). Arachidonic acid clearly accelerated cell death in a concentration dependent manner in PHGPx-deficient cells, whereas wild type cells were not affected by arachidonic acid.

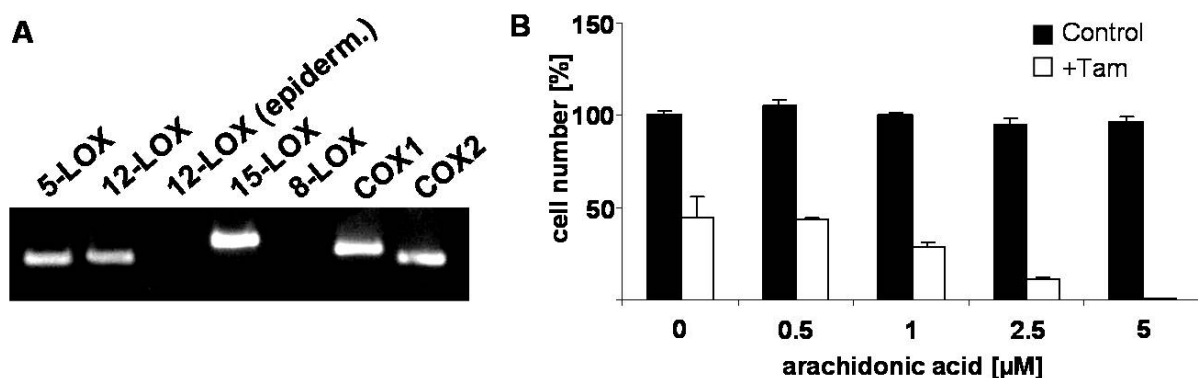


**Figure 20:** (A) The expression of various LOXs and COXs in PFA1<sup>(flox/flox)</sup>-MerCreMer cells was examined by RT-PCR. (B) Arachidonic acid significantly accelerated cell death in PHGPx knockout cells. Depicted are the numbers of viable cells, 36 hours after the treatment with 4-hydroxytamoxifen (Tam). The cell number is depicted in per cent, related to the number of non-treated wild type cells.

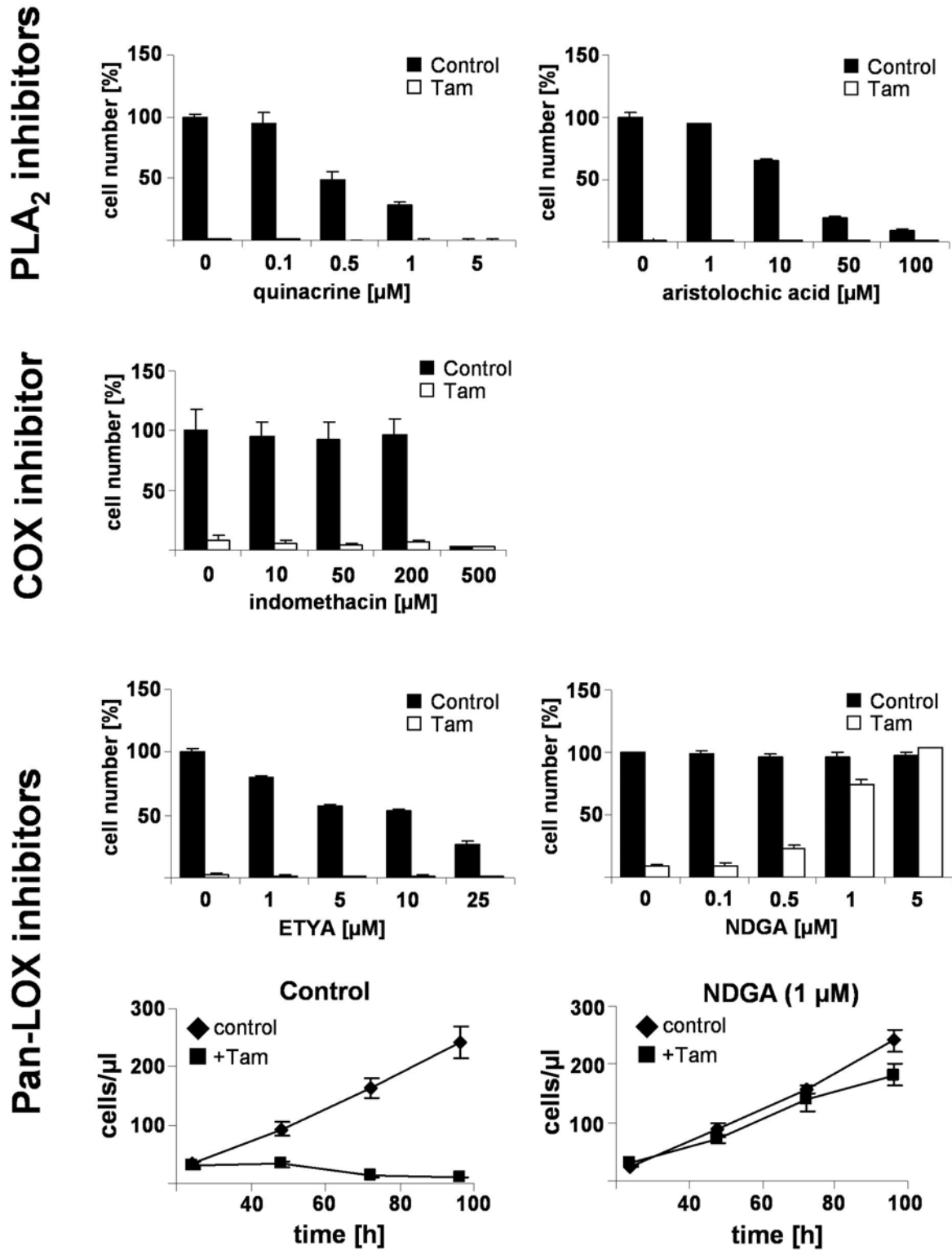


**Figure 21:** The inhibition of LOXs, but not COXs rescued PHGPx-deficient cells from cell death. PHGPx knockout cells were treated with inhibitors of PLA<sub>2</sub>, COXs, and LOXs. Cell number was determined 48 hours after 4-hydroxytamoxifen (Tam) treatment. Only the general LOX inhibitor NDGA rescued PHGPx-deficient cells from cell death. Cell number is depicted in per cent, related to the number of non-treated wild type cells.

If deregulated LOXs and/or COXs activities lead to the detrimental increase of lipid-associated peroxides, inhibitors of enzymes involved in arachidonic acid metabolism were considered to protect PHGPx-deficient cells from cell death. 12 hours after 4-hydroxytamoxifen treatment, various inhibitors were added to PFa1<sup>(flox/flox)</sup>-MerCreMer cells at different concentrations and cell viability was determined 48 h later (figure 21).

Arachidonic acid, the major substrate for LOXs and COXs, is mainly released from biomembranes by PLA<sub>2</sub>, hence the inhibition of PLA<sub>2</sub> by quinacrine (0.1–5 µM) and aristolochic acid (1-100 µM) was considered to cause an indirect inhibition of LOXs and COXs. Yet, in this cellular system, no protective effect was observed with any PLA<sub>2</sub> inhibitor. Indomethacin was used as specific COX inhibitor, but did not rescue cell death at any tested concentration (10-500 µM). Two non-specific pan-LOXs inhibitors, ETYA and NDGA, were tested on 4-hydroxytamoxifen-treated PFa1<sup>(flox/flox)</sup>-MerCreMer cells. ETYA (1-25 µM) did not have any protective effect, whereas NDGA (0.1-5 µM) fully rescued PHGPx-deficient cells in a concentration dependent manner.

Since the general LOX inhibitor NDGA proved to be effective in preventing cell death upon PHGPx depletion, the contribution of individual LOXs was more thoroughly evaluated. A set of specific inhibitors of distinct LOX isoforms was employed to verify the role of various LOXs (figure 22).

MK886, AA-861 and caffeic acid were used to inhibit 5-LOX activity. MK886 inhibits 5-LOX indirectly by inhibiting 5-LOX-activating protein (FLAP). AA-861 has also been reported to inhibit mouse epidermis-type 12-LOX (Nakadate et al., 1985) and 15-LOX (Yamazaki et al., 1996). Baicalein was used as 12-LOX inhibitor, but it has also been reported to block 5-LOX, 15-LOX and COX activity (Butenko et al., 1993; Deschamps et al., 2006; Sekiya and Okuda, 1982). PD146176 (Sendobry et al., 1997) and RO1079051 (Gillmor et al., 1997) were used as specific 15-LOX inhibitors. RO1079051 has been shown to be highly effective against human 15-LOX, but rather ineffective against murine 15-LOX. Of note, PD146176 has been shown to be a highly specific 15-LOX inhibitor, lacking significant antioxidant activity (Sendobry et al., 1997), which does not always account for most other inhibitors.



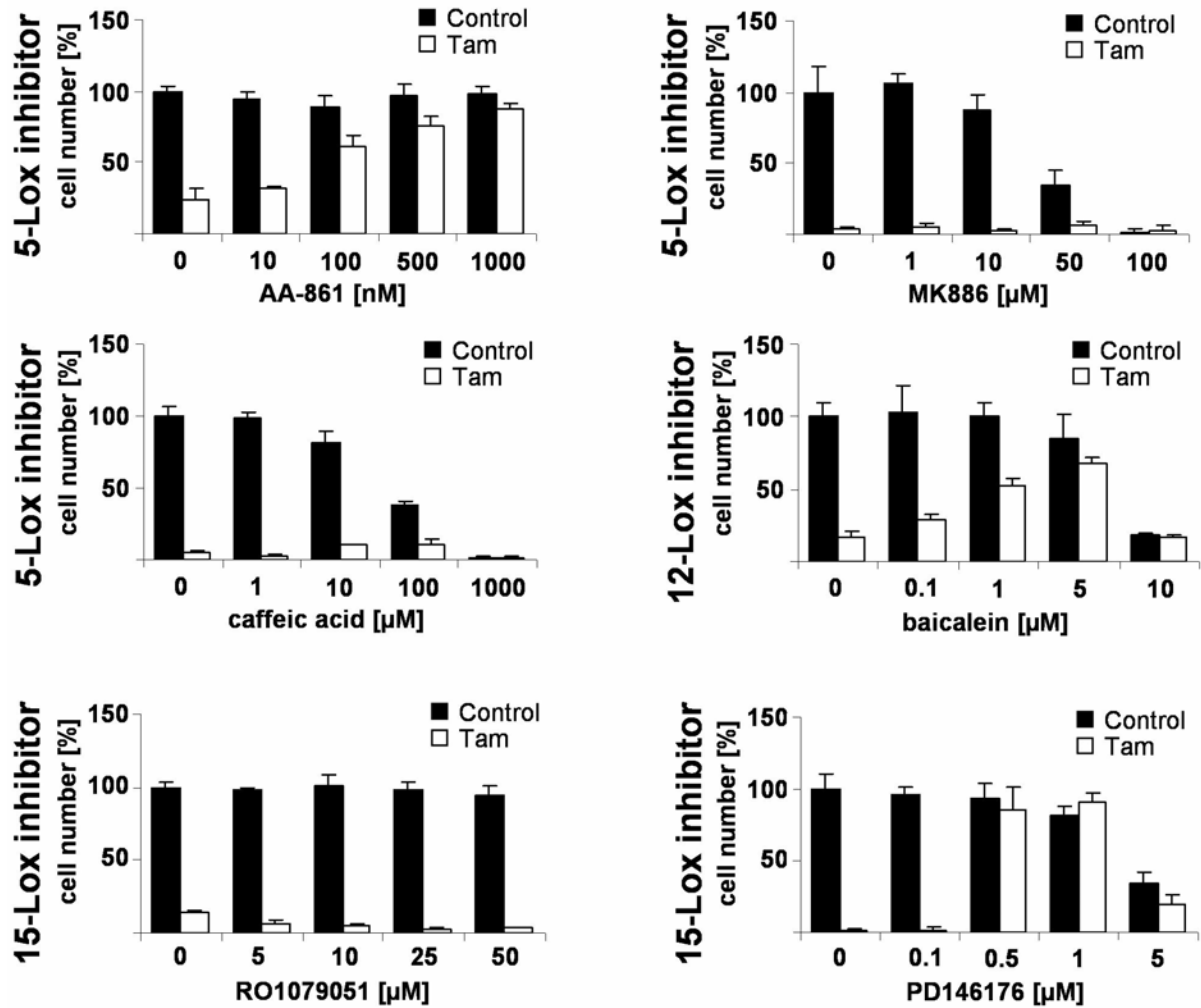


**Figure 22:** 15-LOX is a major player of lipid peroxidation-induced cell death in PHGPx knockout cells. PHGPx-deficient cells were treated with 5-LOX, 12-LOX, and 15-LOX inhibitors. Cell number was determined 48 hours after the treatment with 4-hydroxytamoxifen (Tam). 5-LOX inhibitor AA-861 and the 15-LOX inhibitor PD146176 fully rescued PHGPx-deficient cells. The number of viable cells is depicted in per cent, related to the number of non-treated wild type cells.

The 5-LOX inhibitor AA861 efficiently protected PHGPx knockout cells in a dose dependent manner (0.01-1 µM). As little as 1 µM AA861 was sufficient for a full rescue of PHGPx-deficient cells. The FLAP inhibitor MK886 (1-100 µM) and 5-LOX inhibitor caffeic acid (1-1000) did not have any protective effect over a broad range of different concentrations. Higher concentrations of MK886 and caffeic acid (> 10 µM) caused toxic effects also in control cells. 0.1–5 µM of the 12-LOX inhibitor baicalein rescued 4-hydroxytamoxifen-treated cells to some extent, while higher baicalein concentrations proved to be toxic for both wild type and knockout cells. The 15-LOX inhibitor RO1079051 (5-50 µM) did not have any effect at any tested concentrations. In contrast, the 15-LOX-specific inhibitor PD146176, efficiently protected cells from cell death at concentrations of only 0.5-1 µM. These findings point to 15-LOX as a

central player for the increased lipid peroxidation and cell death in PHGPx knockout cells, whereas 5-LOX, 12-LOX and COX seem to play a negligible role.

To investigate whether uncontrolled 15-LOX may lead to substantial accumulation of peroxy-intermediates, various arachidonic acid metabolites were measured by HPLC (figure 23). Purified HETE/HPETE isoforms, 5-HETE/HPETE, 12-HETE/HPETE and 15-HETE/HPETE, could be detected and distinguished due to distinct retention times. In general HETEs elute earlier than their respective HPETEs, whereas 15-HETE/HPETE elutes before 12-HETE/HPETE and 5-HETE/HPETE.

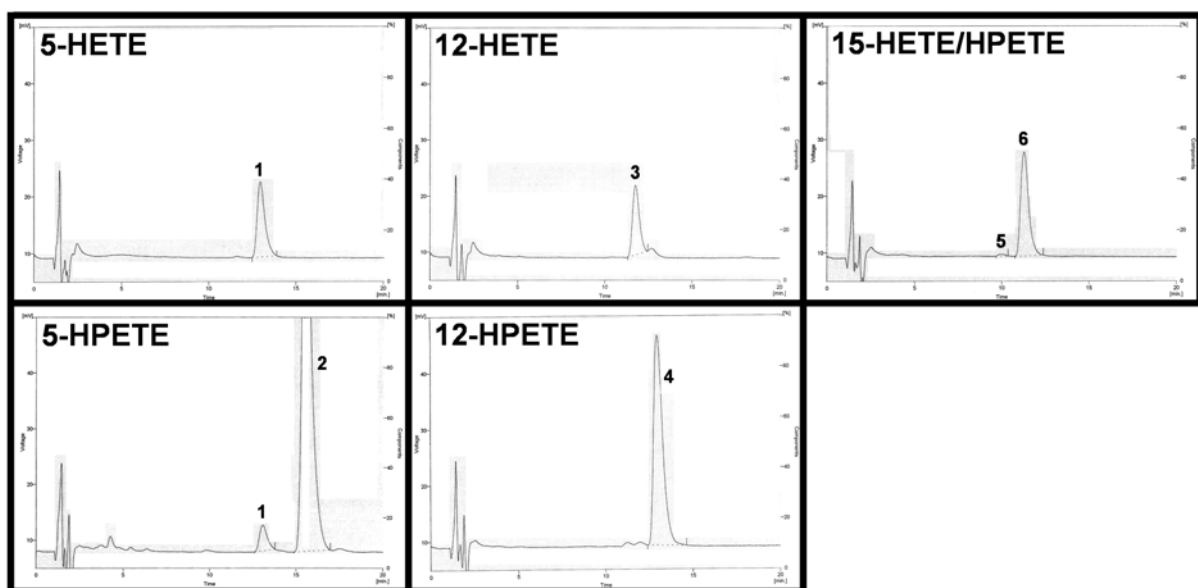


**Figure 23:** HETE/HPETE-HPLC profiles (protocol A) with purified HETE and HPETE isoforms, which could be distinguished by specific retention times. 15-HETE (**5**; 10.0 min), 15-HPETE (**6**; 11.3 min), 12-HETE (**3**; 11.8 min), 12-HPETE (**4**; 13.0 min), 5-HETE (**1**; 13.1 min), 5-HPETE (**2**; 15.5 min).

Throughout the analysis, untreated PFA1<sup>(flox/flox)</sup>-MerCreMer control cells were compared with 4-hydroxytamoxifen-treated knockout cells. 24 and 48 hours after the addition of 4-hydroxytamoxifen, cells were harvested and arachidonic acid metabolism was stimulated for 10 minutes with arachidonic acid and the ionophore A23187. Only low HETE/HPETE levels were detected in PFA1<sup>(flox/flox)</sup>-MerCreMer cells and no significant difference in intracellular HETE/HPETE concentrations was observed either at 24 or 48 h after the induction of the knockout (figure 24).

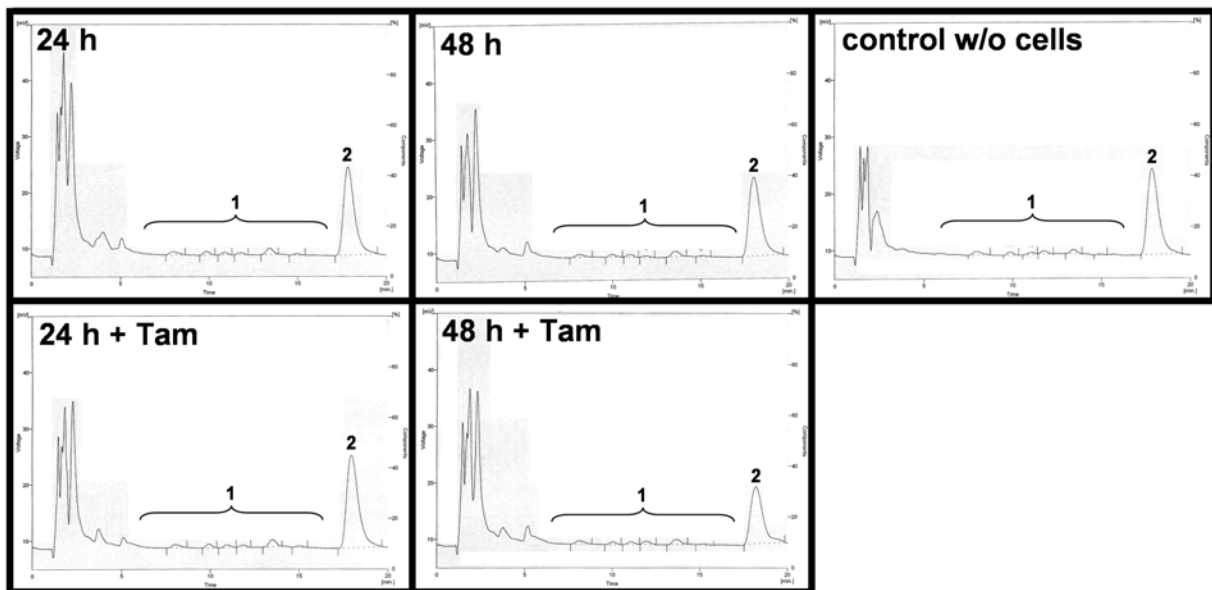


**Figure 24:** HETE/HPETE-HPLC analysis (protocol A) of cellular lipid fractions from 4-hydroxytamoxifen-treated and wild type Pfa1<sup>(flox/flox)</sup>-MerCreMer cells. No significant difference in HETE/HPETE concentrations (1) could be observed 24 and 48 h after the knockout induction, as compared to uninduced cells. 17-OH-22:3 (2) was used as internal standard.

Since HPETEs might be reduced to HETEs by other peroxidatic enzymes, e.g. GPx1, catalase, peroxiredoxins or glutathione-S-transferases, PHGPx knockout cells were incubated with 3  $\mu$ M 5-HPETE for 5 min at 37°C, and the conversion of 5-HPETE to 5-HETE was determined by HPLC. No significant accumulation of intracellular 5-HPETE could be detected in PHGPx knockout versus wild type cells. By contrast, 5-HPETE was completely converted to 5-HETE in 4-hydroxytamoxifen-treated as well as non-treated Pfa1<sup>(flox/flox)</sup>-MerCreMer cells (figure 25).

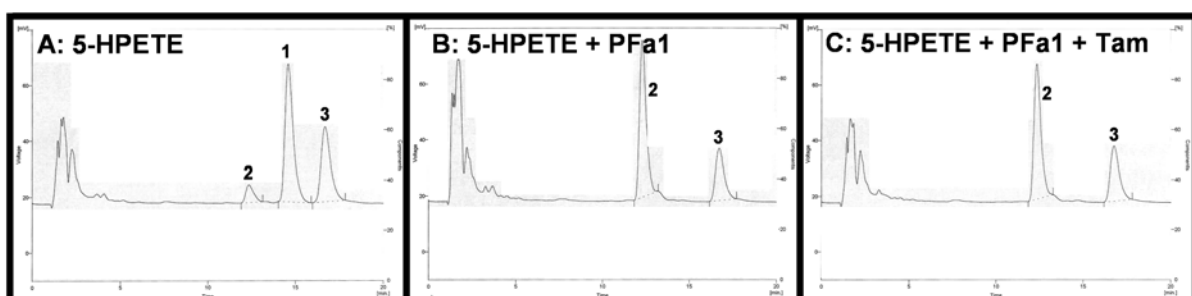


**Figure 25:** HETE/HPETE-HPLC analysis (protocol A) of lipid fractions from Pfa1<sup>(flox/flox)</sup>-MerCreMer cells co-incubated with 5-HPETE. (A) Purified 5-HPETE (1; 14.6 min) with auto-reduced 5-HETE (2; 12.3 min) and internal standard 17-OH-22:3 (3; 16.7 min). (B/C) Wild type and PHGPx knockout cells (+ Tam) converted 5-HPETE to 5-HETE in a similar manner.

Since no significant difference in HPETE and HETE levels could be detected in PHGPx wild type versus knockout cells, an additional approach was performed to assess possible changes in arachidonic acid metabolism. Leukotriene B<sub>4</sub> (LTB<sub>4</sub>), an end product of 5-LOX metabolism, was measured in PFa1<sup>(flox/flox)</sup>-MerCreMer cells. Human neutrophils express high levels of 5-LOX, and thus have been used as a positive control.

48 hours after the addition of 4-hydroxytamoxifen, cells were stimulated with arachidonic acid and the ionophore A23187. Prostaglandine B<sub>2</sub> (PGB<sub>2</sub>) was used as an internal standard during the entire purification process. Yet, no cellular LTB<sub>4</sub> production could be detected in PHGPx wild type and knockout fibroblasts, whereas control cells produced high levels of LTB<sub>4</sub> after induction of the arachidonic acid metabolism (Figure 26).

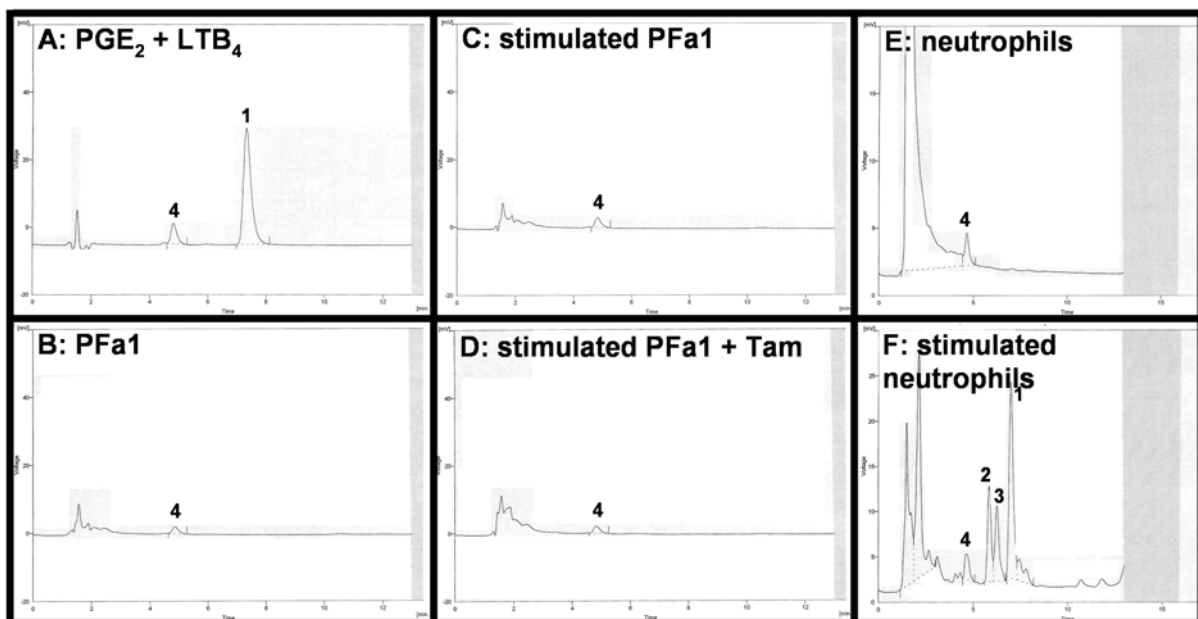


**Figure 26:** LTB<sub>4</sub>-HPLC analysis (protocol B) with lipid fractions from PFa1<sup>(flox/flox)</sup>-MerCreMer cells and human neutrophils. (A) HPLC-setup with purified PGB<sub>2</sub> (4; 4.8 min) and LTB<sub>4</sub> (1; 7.3 min). (B) Lipid fraction from wild type MEFs. (C) Lipid fraction from wild type MEFs, stimulated with arachidonic acid and the ionophore A23187. (D) 4-hydroxytamoxifen-treated, PHGPx knockout cells, stimulated with arachidonic acid and the ionophore A23187. (E) Unstimulated human neutrophils. (F) Human neutrophils, stimulated with arachidonic acid and the ionophore A23187, produced high levels of LTB<sub>4</sub> (1), which is typically accompanied by the non-enzymatic hydrolysis products of LTB<sub>4</sub>, compound A (2) and compound B (3).

#### 4.7 Cell death is mediated by AIF translocation in PHGPx knockout cells

LOX activation and lipid peroxidation were shown to be one of the earliest events triggering cell death in PHGPx-deficient cells. Arachidonic acid metabolites such as HPETEs and HPODEs, have been linked to apoptosis (Shureiqi et al., 2003; Sordillo et al., 2005), and lipid peroxidation is considered a common mediator of programmed cell death through the mitochondrial death pathway (Buttke and Sandstrom, 1994; Kagan et al., 2005; Sarafian and Bredesen, 1994). In this respect, overexpression of the anti-apoptotic molecule Bcl-2 or downregulation of the pro-apoptotic molecule AIF were thought to prevent cell death in PHGPx-deficient cells (figure 27 and 28).

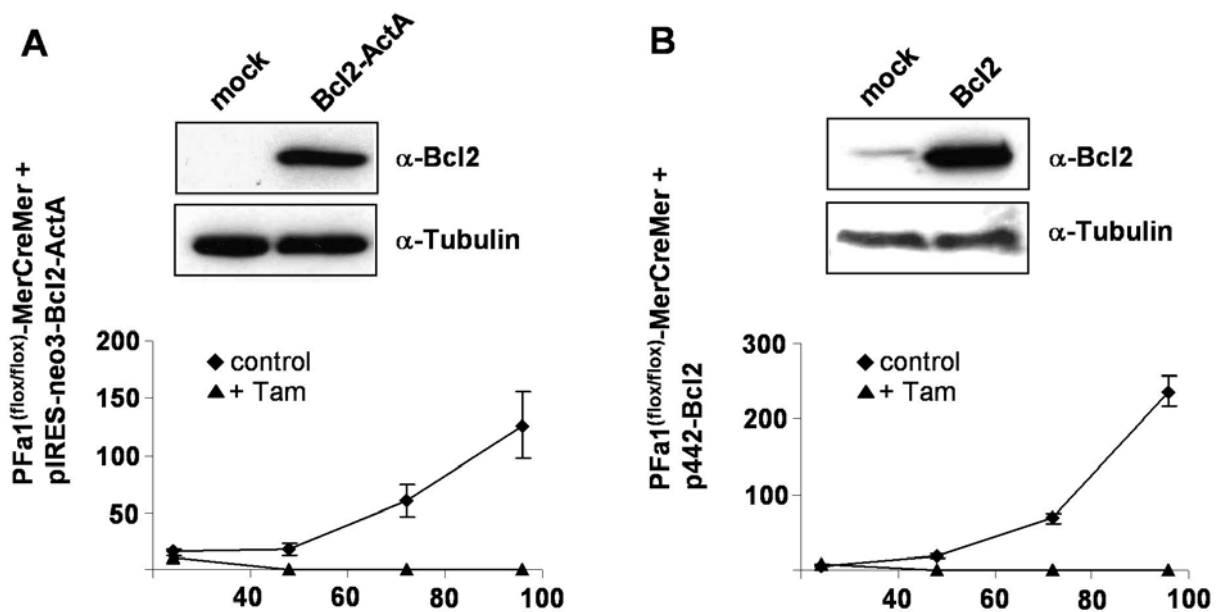


**Figure 27:** Bcl-2 overexpression did not protect PHGPx-deficient cells from cell death. **(A)** Immunoblotting and growth curve of PFA1<sup>(flox/flox)</sup>-MerCreMer cells, transfected with pIRES-neo3-Bcl2-ActA. **(B)** Immunoblotting and growth curve of PFA1<sup>(flox/flox)</sup>-MerCreMer cells, transfected with p442-Bcl2. The deletion of PHGPx was induced by 4-hydroxytamoxifen (Tam).

PFA1<sup>(flox/flox)</sup>-MerCreMer cells were transfected with pIRES-neo3-Bcl-2-ActA and p442-Bcl-2, respectively. Bcl2-ActA includes the mitochondrial membrane targeting sequence of ActA. pIRES-neo3-Bcl-2-ActA transfected cells were selected for neomycin resistance with G418 for 2 weeks. p442-Bcl-2 lentiviral infection was quantified by FACS analysis due to VENUSnucmem expression, yielding approximately 50 % positive cells (data not shown).

The protein levels of Bcl-2 were analyzed by immunoblotting, revealing a strong expression in both cell lines when compared to mock-transfected cells (figure 27). Yet, the deletion of PHGPx in Bcl-2- and Bcl-2-ActA- overexpressing cells caused massive cell death within 24-48 hours. Hence neither ActA-tagged Bcl2 nor wild type Bcl-2 protected PHGPx-deficient cells from cell death.

A caspase-independent apoptosis pathway includes the translocation of cleaved apoptosis-inducing factor (AIF) (activation) from mitochondria to the nucleus upon mitochondrial outer membrane permeabilization (MOMP). Activated AIF induces chromatin condensation and DNA fragmentation (Modjtahedi et al., 2006; Yuste et al., 2005). To examine, whether AIF depletion in PFA1<sup>(flox/flox)</sup>-MerCreMer cells might prevent cell death, gene silencing of AIF was performed with AIF-specific siRNAs. Silencing of gene expression by siRNA is only transient and rapidly recovers after siRNA molecules are used up. Thus, the knockout of PHGPx was induced before siRNA transfection in the presence of  $\alpha$ -tocopherol. Since removal of  $\alpha$ -tocopherol causes rapid cell death within 24-48 hours, this time window was sufficient to explore the effects of siRNA-mediated knockdown of AIF.

AIF expression levels were determined by immunoblotting, revealing a substantial reduction in AIF-12 and AIF-22 siRNA-transfected cells, whereas AIF-20 siRNA was rather inefficient (figure 28-A). After siRNA-treatment, cells were seeded in the presence and absence of  $\alpha$ -tocopherol and the number of viable cells was determined 30 hours later.

Control cells, supplemented with  $\alpha$ -tocopherol, showed a weak retardation in cell growth after transfection with AIF siRNA, compared to control siRNA transfected cells. This is in line with previous findings by other groups, suggesting that AIF has both pro- and anti-apoptotic functions (Modjtahedi et al., 2006). Which and how these antagonizing mechanisms prevail under certain conditions is still unclear. Yet, AIF knockdown with AIF-12 and AIF-22 siRNA clearly reduced cell death in PHGPx-deficient cells, 30 hours after the withdrawal of  $\alpha$ -tocopherol (figure 28-B). AIF-20 siRNA only marginally protected cells from cell death, which is in line with no detectable reduction of the AIF protein level. These findings demonstrate that cell death caused by PHGPx inactivation involves the AIF death pathway.

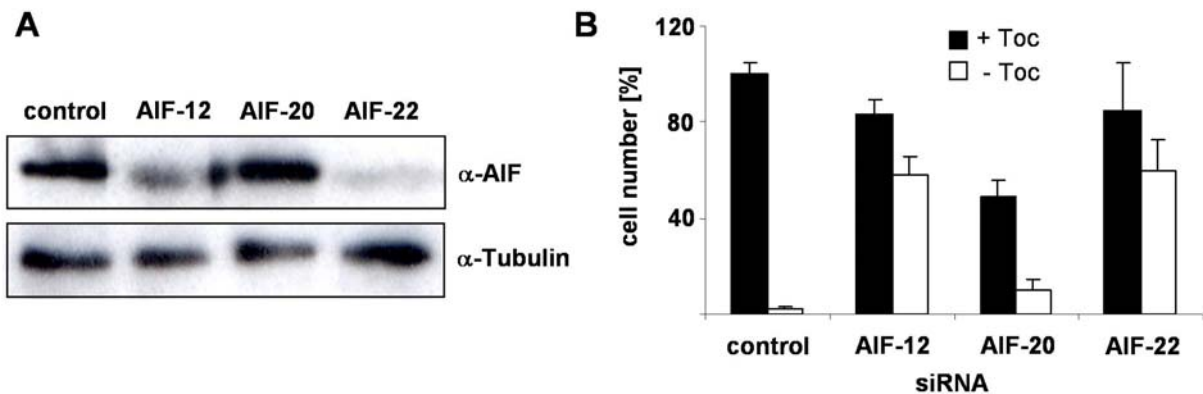


**Figure 28:** AIF gene-silencing prevented cell death in PHGPx knockout cells. **(A)** Immunoblotting of PFA1<sup>(flox/flox)</sup>-MerCreMer cells, 48 hours after the transfection of AIF siRNA. **(B)** AIF knockdown significantly reduced cell death in PHGPx knockout cells. Number of viable cells was determined 30 hours after the removal of  $\alpha$ -tocopherol and is depicted in per cent, related to control cells.

#### 4.8 The physiological role of catalytically important amino acids of PHGPx

In the past, some of the catalytically important amino acids of PHGPx as well as its biochemistry have been studied in great detail. The physiological relevance of specific amino acids, such as the catalytic triad (Sec<sup>46</sup>, Gln<sup>81</sup>, Trp<sup>136</sup>), the nine Cys residues, and some highly conserved amino acids, has remained unclear (figure 29).

The amino acid sequence of PHGPx is highly conserved within mammals (>90%), shares significant identity with vertebrates, and homologues are even found in insects, plants, and yeast (figure 30-A). Of note, only PHGPx from vertebrates contains Sec, whereas insects, plants, and yeast express a Cys-containing homologue.

To investigate the biological significance of Sec in the catalytic centre, two PHGPx mutants were generated by PCR mutagenesis in plasmid pDrive-HA-PHGPx. The Sec codon (UGA) at position 46 of the cytosolic protein sequence was mutated to Cys (UGC) and Ser (AGC), respectively. Both HA-PHGPx mutant sequences were cloned into the lentiviral vector p442-PL1, yielding plasmids p442-HA-PHGPx-UC and p442-HA-PHGPx-US. Like the reconstitution experiment with HA-tagged wild type PHGPx (see chapter 4.3), both mutants were introduced into PFA1<sup>(flox/flox)</sup>-MerCreMer cells by lentiviral infection. The infection efficiency was determined by

FACS analysis, ranging from 79-99% (figure 31-A). No alterations in morphology or proliferation rates was observed in Pfa1<sup>(flox/flox)</sup>-MerCreMer cells, overexpressing any of the HA-PHGPx mutants.

Species:	Sequence:
	<p style="text-align: center;"> <span style="margin-right: 40px;">C2</span> <span style="margin-right: 40px;">C10</span> <span style="margin-right: 40px;">C28</span> <span style="margin-right: 40px;">Y32</span> <span style="margin-right: 40px;">C37</span> <span style="margin-right: 40px;">U46</span> </p>
Mus_musculus	MCASRDDWRCA <sup>C2</sup> RS <sup>C10</sup> MHEFS <sup>C28</sup> SAK <sup>Y32</sup> DI <sup>C37</sup> DGHM <sup>U46</sup> VCLDKY <sup>C28</sup> RGFV <sup>C37</sup> CIVTNVAS <sup>U46</sup> QUGKTD 50
Rattus_norvegicus	MCASRDDWRCA <sup>C2</sup> RS <sup>C10</sup> MHEFAAKDIDGHM <sup>C28</sup> VCLDKY <sup>Y32</sup> RG <sup>C37</sup> VCIVTNVAS <sup>U46</sup> QUGKTD 50
Sus_scrofa	MCASRDDWRCA <sup>C2</sup> RS <sup>C10</sup> MHEFS <sup>C28</sup> SAK <sup>Y32</sup> DIDGHM <sup>C37</sup> VNLDKY <sup>Y32</sup> RGY <sup>C37</sup> VCIVTNVAS <sup>U46</sup> QUGKTE 50
Bos_taurus	MCASRDDWRCA <sup>C2</sup> RS <sup>C10</sup> MHEFS <sup>C28</sup> SAK <sup>Y32</sup> DIDGRM <sup>C37</sup> VNLDKY <sup>Y32</sup> RGH <sup>C37</sup> VCIVTNVAS <sup>U46</sup> QUGKTD 50
Homo_sapiens	MCASRDDWRCA <sup>C2</sup> RS <sup>C10</sup> MHEFS <sup>C28</sup> SAK <sup>Y32</sup> DIDGHM <sup>C37</sup> VNLDKY <sup>Y32</sup> RGF <sup>C37</sup> VCIVTNVAS <sup>U46</sup> QUGKTE 50
Gallus_gallus	MCAQADEWR.SATS <sup>C2</sup> SIYDFHARDIDGRDVSLE <sup>C37</sup> QY <sup>Y32</sup> RGFV <sup>C37</sup> CIITNVASK <sup>U46</sup> UGKTA 50
Drosophila_melanogaster	MSAN-GDYKNAASIYEFY <sup>C2</sup> TKV <sup>C10</sup> TDTHGNDVSLE <sup>C37</sup> KY <sup>Y32</sup> KGKVV <sup>C37</sup> LVVNIASK <sup>U46</sup> CGLTK 49
Saccharomyces_cerevisiae	-----MSEFYK <sup>C2</sup> LAPV <sup>C10</sup> DKK <sup>C28</sup> Q <sup>Y32</sup> PF <sup>C37</sup> FD <sup>U46</sup> QLK <sup>C28</sup> GKVV <sup>C37</sup> LIVNASK <sup>U46</sup> GFTP 40
	<p style="text-align: center;"> <span style="margin-right: 40px;">Y53</span> <span style="margin-right: 40px;">Y63</span> <span style="margin-right: 40px;">C66</span> <span style="margin-right: 40px;">C75</span> <span style="margin-right: 40px;">Q81</span> <span style="margin-right: 40px;">Y96</span> </p>
Mus_musculus	VNYTQLVDLHARYAEC <sup>C75</sup> GLRILAF <sup>Y53</sup> PC <sup>Y63</sup> NQ <sup>C66</sup> FR <sup>C75</sup> QEPGSN--QEIKEFAAG-YN 97
Rattus_norvegicus	VNYTQLVDLHARYAEC <sup>C75</sup> GLRILAF <sup>Y53</sup> PC <sup>Y63</sup> NQ <sup>C66</sup> FR <sup>C75</sup> QEPGSN--QEIKEFAAG-YN 97
Sus_scrofa	VNYTQLVDLHARYAEC <sup>C75</sup> GLRILAF <sup>Y53</sup> PC <sup>Y63</sup> NQ <sup>C66</sup> FR <sup>C75</sup> QEPGSD--AEIKEFAAG-YN 97
Bos_taurus	VNYTQLVDLHARYAEC <sup>C75</sup> GLRILAF <sup>Y53</sup> PC <sup>Y63</sup> NQ <sup>C66</sup> FR <sup>C75</sup> QEPGSN--AEIKEFAAG-YN 97
Homo_sapiens	VNYTQLVDLHARYAEC <sup>C75</sup> GLRILAF <sup>Y53</sup> PC <sup>Y63</sup> NQ <sup>C66</sup> FG <sup>C75</sup> KQEPGSN--EEIKEFAAG-YN 97
Gallus_gallus	VNYTQLVDLHARYAEC <sup>C75</sup> GLRILAF <sup>Y53</sup> PC <sup>Y63</sup> NQ <sup>C66</sup> FG <sup>C75</sup> KQEPGDD--AQIKAF <sup>Y96</sup> AEG-YG 97
Drosophila_melanogaster	NNYEKLTDLKEKYGERGLVILNF <sup>C75</sup> PC <sup>Y63</sup> NQ <sup>C66</sup> FGS <sup>C75</sup> QMP <sup>Y96</sup> EADGEAMV <sup>C75</sup> HLRDS-KA 98
Saccharomyces_cerevisiae	-QYKELEALYKRYKDEGFTIIG <sup>C75</sup> FP <sup>Y53</sup> PC <sup>Y63</sup> NQ <sup>C66</sup> FGH <sup>C75</sup> QEPGSD--EEI <sup>Y96</sup> AQ <sup>C75</sup> FC <sup>Y96</sup> QLNYG 87
	<p style="text-align: center;"> <span style="margin-right: 40px;">C107</span> <span style="margin-right: 40px;">W136</span> </p>
Mus_musculus	VKFDMSK <sup>C107</sup> ICVNGDDAHPLWK <sup>C107</sup> WMK <sup>W136</sup> VQPKGRGMLGN-AIK <sup>W136</sup> WNFTKFLIDKN 146
Rattus_norvegicus	VRFDMSK <sup>C107</sup> ICVNGDDAHPLWK <sup>C107</sup> WMK <sup>W136</sup> VQPKGRGMLGN-AIK <sup>W136</sup> WNFTKFLIDKN 146
Sus_scrofa	VKFDMSK <sup>C107</sup> ICVNGDDAHPLWK <sup>C107</sup> WMK <sup>W136</sup> VQPKGRGMLGN-AIK <sup>W136</sup> WNFTKFLIDKN 146
Bos_taurus	VKFDLFSK <sup>C107</sup> ICVNGDDAHPLWK <sup>C107</sup> WMK <sup>W136</sup> VQPKGRGMLGN-AIK <sup>W136</sup> WNFTKFLIDKN 146
Homo_sapiens	VKFDMSK <sup>C107</sup> ICVNGDDAHPLWK <sup>C107</sup> WMK <sup>W136</sup> IQPKGKILGN-AIK <sup>W136</sup> WNFTKFLIDKN 146
Gallus_gallus	VKFDMSK <sup>C107</sup> IEVNGDGAHPLWK <sup>C107</sup> WLKEQPKGRGTLGN-AIK <sup>W136</sup> WNFTKFLINRE 146
Drosophila_melanogaster	DIGEVFAKVDVNGDNAAPLYKYLKAKQTG--TLGS-GIK <sup>W136</sup> WNFTKFLVNKE 145
Saccharomyces_cerevisiae	VTFPIMKKIDVNGNEDPVYKFLKSQKSG--MLGLRGIK <sup>W136</sup> WNFEKFLVDKK 135
	<p style="text-align: center;"> <span style="margin-right: 40px;">C148</span> <span style="margin-right: 40px;">Y153</span> <span style="margin-right: 40px;">C168/Y169</span> </p>
Mus_musculus	GCVVKRYGPMEE <sup>C148</sup> PQVIEKDL <sup>Y153</sup> PCYL---- 170
Rattus_norvegicus	GCVVKRYGPMEE <sup>C148</sup> PQVIEKDL <sup>Y153</sup> PCYL---- 170
Sus_scrofa	GCVVKRYGPMEE <sup>C148</sup> PQVIEKDL <sup>Y153</sup> PCYL---- 170
Bos_taurus	GCVVKRYGPMEE <sup>C148</sup> PLVIEKDL <sup>Y153</sup> PCYL---- 170
Homo_sapiens	GCVVKRYGPMEE <sup>C148</sup> PLVIEKDL <sup>Y153</sup> PHYF---- 170
Gallus_gallus	GQVVKRYSPMED <sup>C148</sup> PVIEKDL <sup>Y153</sup> PAYL---- 170
Drosophila_melanogaster	GVPINRYAPT <sup>C148</sup> TDPMDIAK <sup>Y153</sup> DIKLL---- 169
Saccharomyces_cerevisiae	GKVYERYSSLTKPSSLSETIEELLKEVE 163

**Figure 29:** Sequence alignment of murine PHGPx and its homologues from other species, using ClustalW V1.82. Highlighted are the catalytic triad (red), consisting of Sec (U), Gln (Q), and Trp (W), all Cys residues (green), and particularly conserved Tyr residues (blue). The positions of all highlighted amino acids within the PHGPx sequence of *mus musculus* are indicated in detail.



The expression levels of wild type PHGPx and both mutant forms were evaluated by immunoblotting, using the antibody  $\alpha$ -HA-tag 3F10 (figure 30-B). While, the expression level of HA-tagged wild type PHGPx was similar as described in chapter 4.3, the expression of both PHGPx mutants (Sec/Cys and Sec/Ser) was dramatically higher than that of wild type PHGPx (figure 30-B).

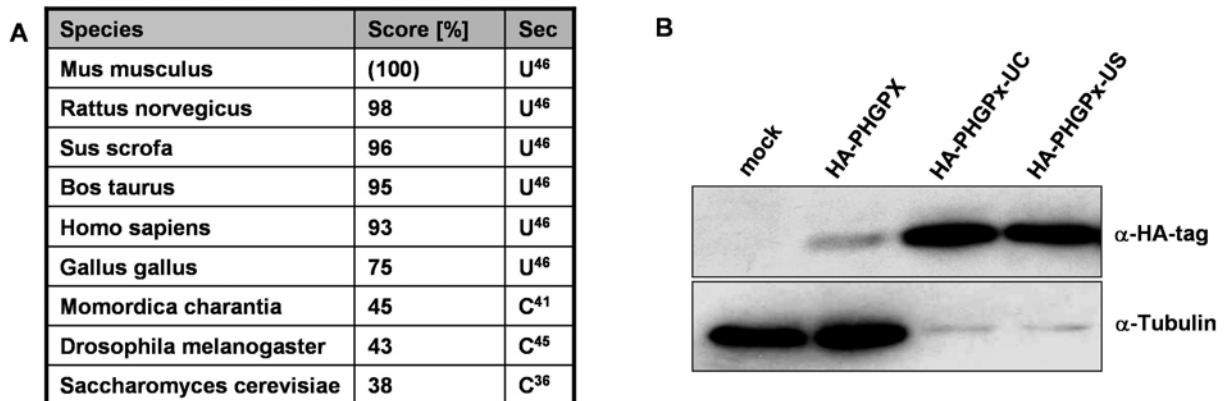


**Figure 30:** (A) PHGPx protein sequence alignment (ClustalW 1.83). The PHGPx amino acid sequence from various species was compared with *mus musculus* PHGPx. (B) Western blot of PFa1<sup>(flox/flox)</sup>-MerCreMer cells, overexpressing wild type and mutant forms of HA-tagged PHGPx. Due to the strong expression of the PHGPx mutants, only 5 % of the respective protein extract was applied.

To determine whether Cys or Ser in the catalytic site of PHGPx are able to maintain PHGPx function, cell viability assays were performed in cells devoid of endogenous PHGPx (figure 31-B). The number of viable cells was recorded until 96 hours after the addition of 4-hydroxytamoxifen. As described in chapter 4.3, HA-PHGPx fully rescued genomic PHGPx depletion. Surprisingly, the Sec to Cys mutant (HA-PHGPx-UC) equally rescued 4-hydroxytamoxifen-treated PFa1<sup>(flox/flox)</sup>-MerCreMer cells from cell death. In contrast, the HA-PHGPx-US mutant was functionally inactive and did not compensate the loss of wild type PHGPx. These cells died at a similar rate like non-infected or mock-infected control cells.

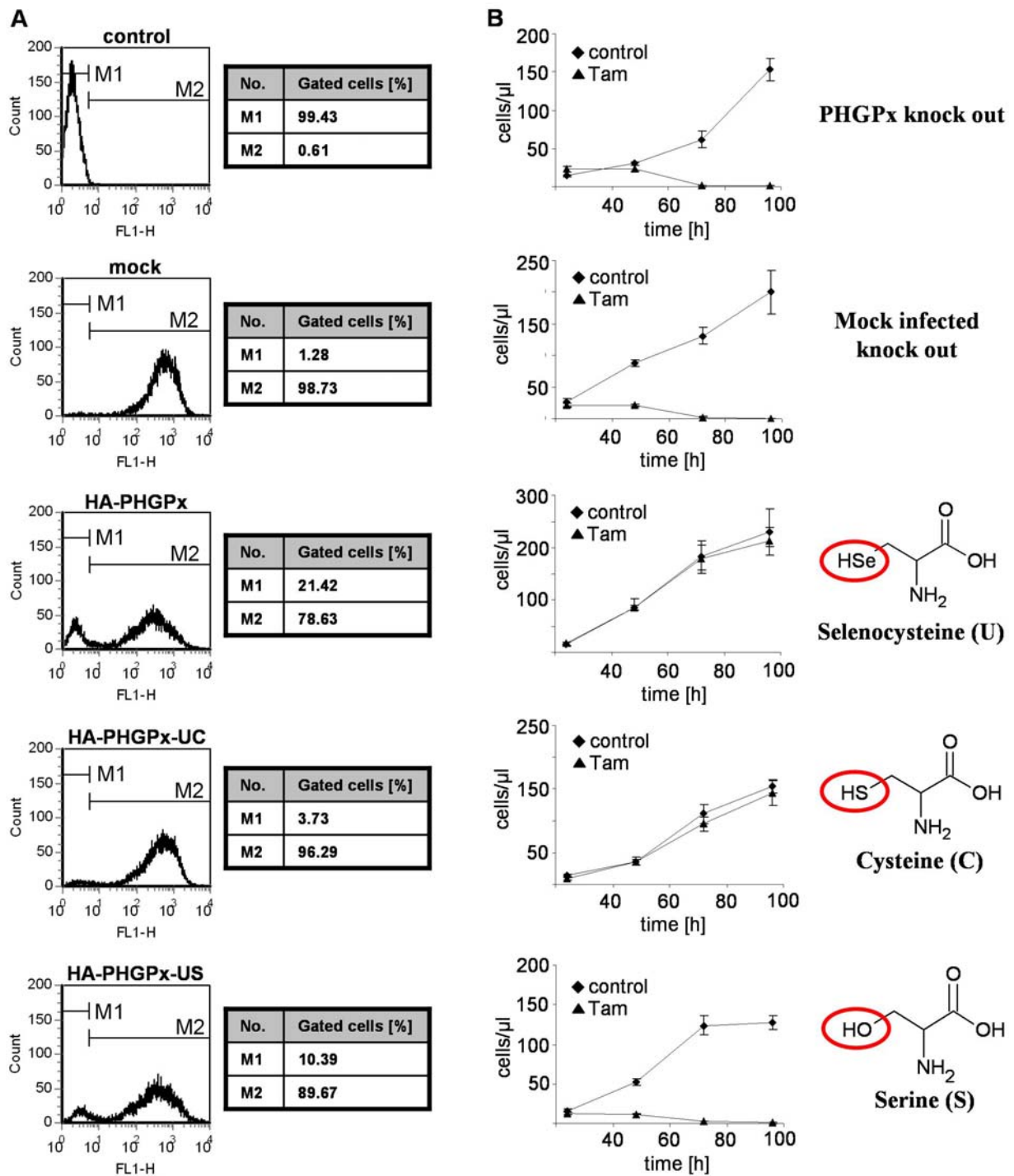


**Figure 31:** Mutational analysis of PHGPx (A) Quantification of lentiviral infection efficiency by flow cytometry. Cells were screened for VENUStnucmem expression on channel FL1 at 530 nm. (M1 = non-infected cells; M2 = infected cells). (B) Growth curves of PHGPx knockout cells, expressing different HA-PHGPx mutants. PHGPx deletion was induced by addition of 4-hydroxytamoxifen (Tam).

The substitution of Sec by Cys has been reported to decrease enzymatic activity in purified recombinant PHGPx protein, at least by three orders of magnitude (Maiorino et al., 1995). To address, whether the Sec to Cys mutant is fully functional, cells lacking endogenous PHGPx but expressing HA-PHGPx-UC, were exposed to pro-oxidants (figure 32). Mock, p442-HA-PHGPx, and p442-HA-PHGPx-UC transfected cells were used in these experiments. The knockout of PHGPx was only induced in cells, expressing HA-PHGPx or HA-PHGPx-UC, since mock cells die within 48 hours. Hence, mock-transfected control cells still express endogenous PHGPx, whereas the two other cell lines express either HA-tagged wild type PHGPx or the HA-tagged Sec/Cys mutant. Cells were treated with increasing concentrations of H<sub>2</sub>O<sub>2</sub> (0.1 – 1.0 mM) and BOOH (10 – 50 μM) and the number of viable cells was assessed after 72 hours. All three cell lines showed a dose dependent increase in cell death after addition of H<sub>2</sub>O<sub>2</sub> or butylhydroperoxide (BOOH). Concentrations above 100 μM H<sub>2</sub>O<sub>2</sub> and 10 μM BOOH caused retarded cell growth and eventually cell death in all cell lines. Of note, no differences was observed between cells, overexpressing HA-tagged wild type PHGPx and the Sec/Cys mutant, suggesting that both cell lines are equally resistant towards oxidative stress, at least in this system.

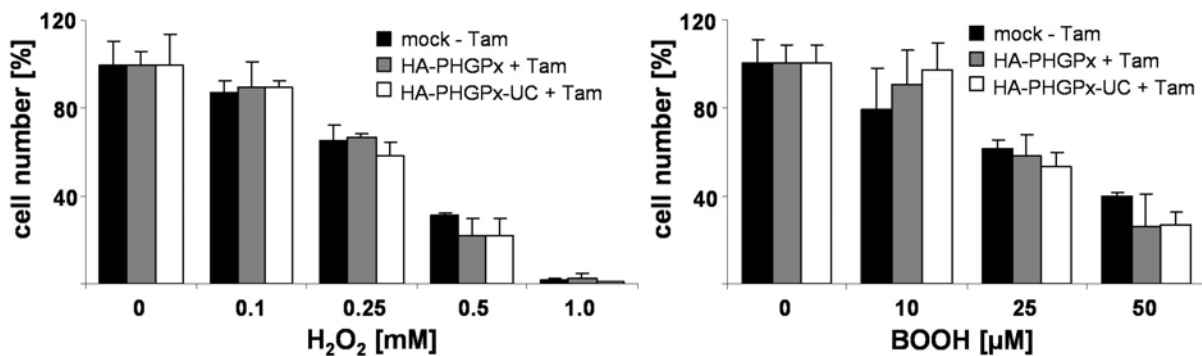


**Figure 32:** PHGPx knockout cells, overexpressing HA-PHGPx or HA-PHGPx-UC, were equally resistant to oxidative stress. Infected PFa1<sup>(flox/flox)</sup>-MerCreMer cells were stressed with different concentrations of H<sub>2</sub>O<sub>2</sub> and BOOH. The number of viable cells is given in per cent, related to non-stressed cells, 72 h after the addition of stressors. PHGPx disruption was induced in indicated cell lines by the addition of 4-hydroxytamoxifen (Tam).

#### **4.9 xCT overexpression rescues $\gamma$ -GCS-deficient cells from GSH depletion**

GSH is the major endogenous scavenger of ROS in the cell by acting as a reducing equivalent for GPxs, but also constitutes a major substrate for other GSH dependent systems, such as glutaredoxins and glutathione-S-transferases. GSH is present in millimolar concentrations in the cell and has long been considered indispensable for cell survival. Shi et al. showed that mice with targeted deletion of the  $\gamma$ -GCS heavy subunit fail to gastrulate and die at embryonic day 7.5. Isolated ES cell like cells from  $\gamma$ -GCS-deficient blastocysts, however, grew indefinitely in GSH-free medium, when supplemented with NAC (Shi et al., 2000).  $\gamma$ -GCS knockout cells were used in this work, to investigate the importance of GSH for cell survival and proliferation, and to address the functional relationship between the  $(\text{Cys})_2/\text{Cys}$  redox cycle and the GSH-dependent system.

$\gamma$ -GCS-deficient ES cell like cells were obtained from Michel W. Lieberman, Houston, Texas (Shi et al., 2000) and were adapted to DMEM standard cell culture medium, supplemented with NAC (chapter 3.1.2). Cells proliferated rapidly but proved to be highly sensitive towards seeding at low cell density and trypsinization. Hence, cells were detached by pipetting up and down and passaging was performed every 48-72 hours at a ratio of only 1:3.

To verify previously described features of  $\gamma$ -GCS knockout cells in our cell culture system, cells were supplemented with various antioxidants. As described by Shi et al., NAC (5 mM) and GSH (2.5 mM) efficiently protected cells from cell death, whereas the lipophilic antioxidant  $\alpha$ -tocopherol did not have any protective effect (figure 33-A). Also glutathione ethyl ester (GSH-EE) (2.5 mM) efficiently rescued  $\gamma$ -GCS-deficient cells from cell death.

Since NAC supplementation efficiently protects  $\gamma$ -GCS-deficient cells from cell death, overexpression of xCT, the substrate specific subunit of  $(\text{Cys})_2/\text{Glu}$  antiporter system  $x_c^-$ , was envisaged a genetic mechanism that may rescue  $\gamma$ -GCS knockout cells from cell death. System  $x_c^-$  was supposed to increase cellular  $(\text{Cys})_2$ -uptake capacity, causing increased cellular Cys levels after reduction of  $(\text{Cys})_2$  within the cell. To test this hypothesis, cells were transfected with pCAG-3SIP, pCAG-3SIP-eGFP, and

pCAG-3SIP-xCT, respectively (figure 33-B). pCAG-3SIP based vectors comprise a strong CMV-chicken  $\beta$ -actin promoter and an IRES-puromycin N-acetyltransferase cassette for coordinated gene expression. This enables a strong and stable expression of the gene of interest by puromycin selection.

Antibiotic selection with 1  $\mu$ M puromycin led to outgrowth of single cell clones, which were individually isolated and expanded gradually. Puromycin selection was highly efficient, as observed in pCAG-3SIP-eGFP transfected cells by fluorescence microscopy (figure 33-C) and FACS analysis (figure 33-D). Less than 1 % of pCAG-3SIP-eGFP transfected cells stained negative on channel FL1 after puromycin selection. For further studies, one mock-transfected clone (mock), one eGFP-transfected (eGFP) clone, and two independently outgrowing xCT-transfected clones (xCT-5 and xCT-7) were used.

Due to the lack of functional antibodies against xCT, transfected cells were assayed for xCT-transcription by Northern blot and quantitative RT-PCR. Northern blot hybridisation signals were obtained in both xCT-transfected clones, corresponding to the bicistronic xCT-IRES-puromycin mRNA sequence of 2.7 kb (figure 33-E). By contrast, no hybridisation signals were detectable in mock- and eGFP-transfected control cells.

Quantitative RT-PCR was performed with primers xCT for1/rev1 and aldolase A/B for the normalisation of xCT expression levels. xCT cDNA was detected in clones xCT-5 and xCT-7 with crossing points at 21.54 and 23.02 cycles, respectively (data not shown). When normalized to aldolase, clone xCT-5 had approximately 8-fold higher xCT cDNA levels than clone xCT-7 (compare Northern blot). No xCT amplification signals were detected until cycle 50 in both control-transfected cell lines, indicating that xCT expression is virtually absent in the parental and the control cell lines.

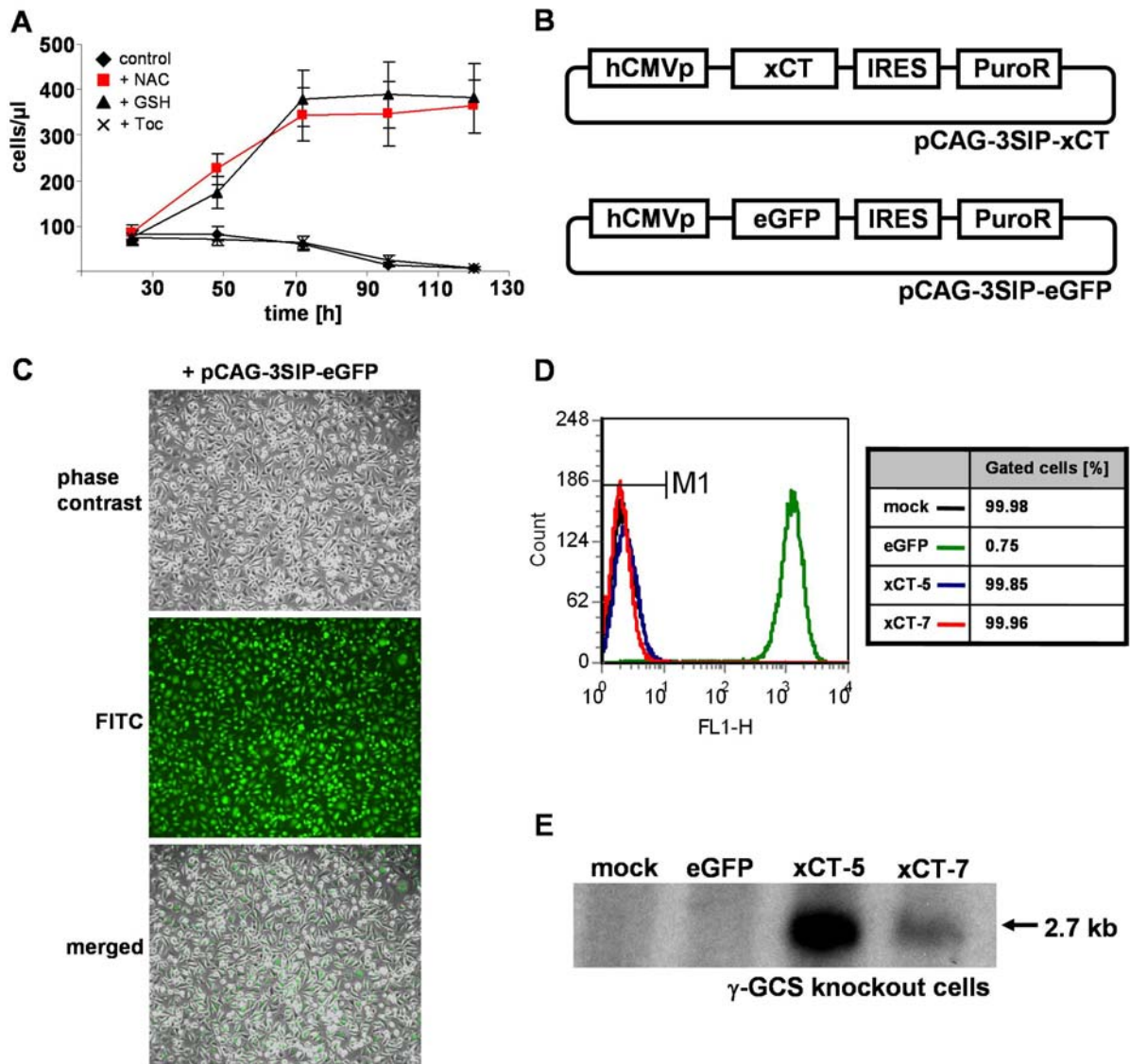


**Figure 33:** xCT overexpression in  $\gamma$ -GCS-deficient cells. **(A)** Growth curves of  $\gamma$ -GCS-deficient cells, supplemented with various antioxidants (5 mM NAC, 2.5 mM GSH, 250  $\mu$ M  $\alpha$ -tocopherol (Toc)). **(B)** Schematic representation of the bicistronic expression vectors, used for stable expression of xCT or eGFP. **(C)** Fluorescence microscopy of pCAG-3SIP-eGFP transfected cells after three weeks of puromycin selection. **(D)** FACS analysis of eGFP-expressing cells after puromycin selection. **(E)** Northern blot with isolated mRNA from transfected  $\gamma$ -GCS knockout cells.

All  $\gamma$ -GCS-deficient cell lines were routinely maintained in medium supplemented with 5 mM NAC. To test xCT-transfected cells for their capability to survive in the absence of antioxidant supplements, cells were seeded in Standard DMEM without antioxidant supplements and cell growth was monitored for 48 hours. Mock and eGFP transfected cells died rapidly in the absence of NAC within 24 to 48 hours after seeding. Of note, a significant amount of control cells did not even adhere to the cell culture dish. xCT-transfected  $\gamma$ -GCS-deficient cells, however, grew until confluence

without showing any impairment in morphology or proliferation. xCT-overexpressing cells could be cultivated indefinitely in cell culture medium, lacking NAC or other antioxidant supplements (figure 34 and 37-A).

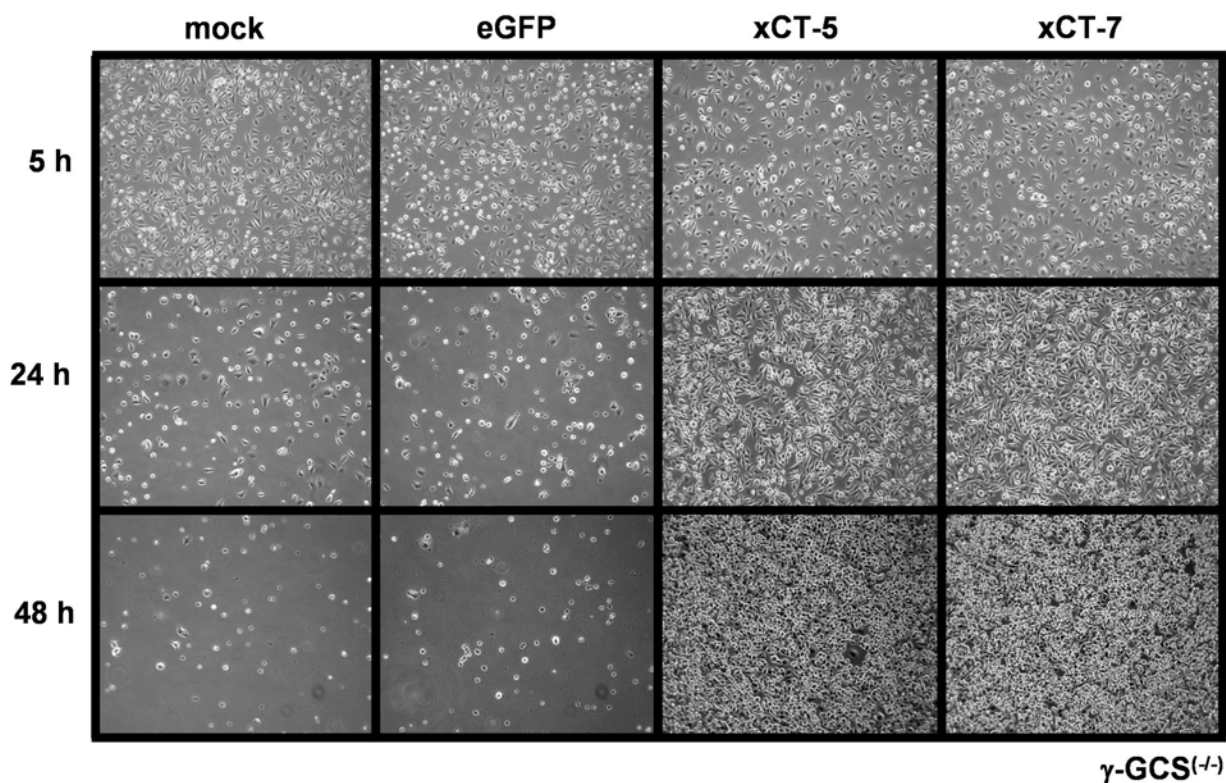


**Figure 34:** Phase contrast microscopy of transfected  $\gamma$ -GCS-deficient cells, in the absence of antioxidants. pCAG-3SIP- and pCAG-3-SIP-eGFP-transfected cells died within 24-48 hours. xCT overexpressing  $\gamma$ -GCS knockout cells survive in the absence of antioxidant supplements.

Cell death was assessed by PI staining and FACS analysis in control- and xCT-transfected  $\gamma$ -GCS knockout cells (figure 35). No increase of PI-positive cells was detected in xCT-overexpressing cells, whereas a vast majority of control cells stained PI-positive, already 24 hours after NAC depletion. Moreover, cell death was accompanied by an increase of intracellular ROS, as demonstrated by DCF staining. Whether increased levels of intracellular ROS trigger or just coincide with cell death could not be determined, due to the extremely fast kinetic of cell death after NAC withdrawal.

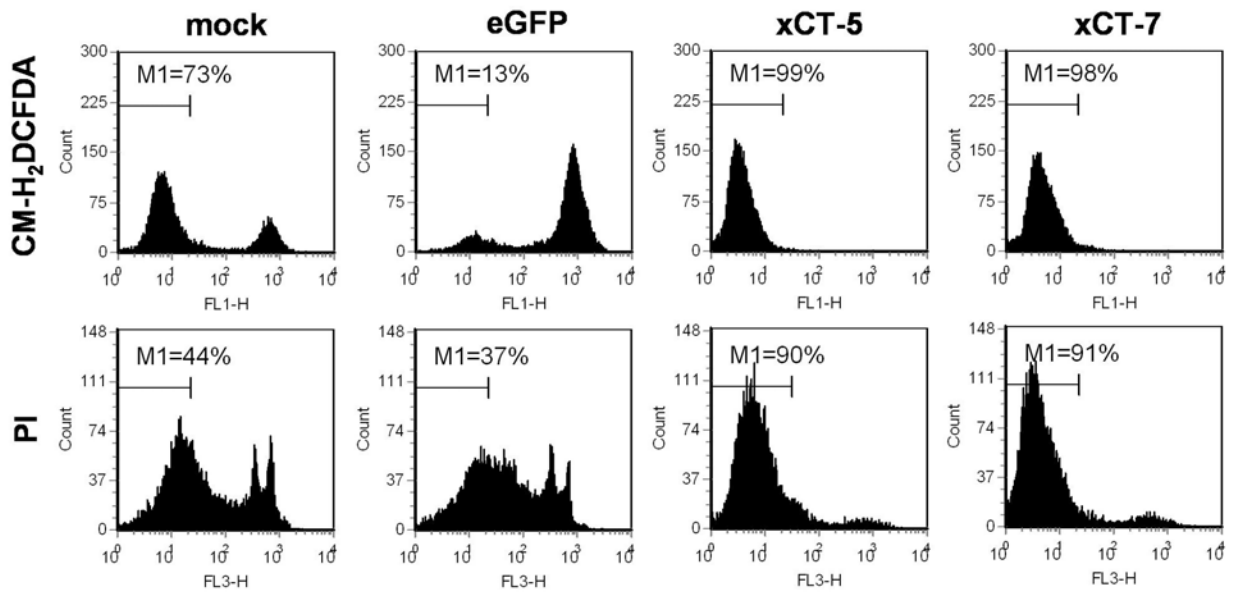


**Figure 35:** CM-H<sub>2</sub>DCFDA and PI staining of transfected  $\gamma$ -GCS-deficient cells, depleted from NAC for 24 hours.

GSH has long been considered as an indispensable player for many cellular processes. It was thus barely conceivable that minute amounts of GSH, synthesized in  $\gamma$ -GCS-deficient cells, may functionally cooperate with xCT overexpression to allow cell survival and proliferation. Since  $\gamma$ -GCS-deficient cells derive from transgenic mice that were designed such that a PGK-*hrpt* cassette of the targeting vector replaced only exon 1 of  $\gamma$ -GCS in AB2.1 embryonic stem cells, it could not be ruled out that a residual  $\gamma$ -GCS activity may cause the synthesis of small amounts of intracellular GSH. To exclude residual  $\gamma$ -GCS activity that may contribute to cell survival,  $\gamma$ -GCS<sup>(-/-)</sup> cells were treated with high concentrations of BSO, a highly specific and potent  $\gamma$ -GCS inhibitor. Cells could be treated with up to 1 mM BSO, which did not impact survival or proliferation (figure 36-A). Of note, cells could be cultivated in the presence of BSO (1 mM) for more than 10 passages, without showing any impairment of proliferation (figure 36-B). Of note, MEFs and other cell lines used in our lab, die at BSO concentrations as low as 10-50  $\mu$ M. These findings provide evidence that  $\gamma$ -GCS knockout cells do not have residual  $\gamma$ -GCS activity, which might have contributed to cell survival under non-permissive conditions.

An alternative source of GSH is the  $\gamma$ -glutamyl transpeptidase (GGT) pathway. GGT cleaves extracellular GSH to  $\gamma$ -Glu-Cys/(Cys)<sub>2</sub>, which may theoretically lead to a  $\gamma$ -GCS-independent recycling of GSH within the cell. To examine whether this GGT-



mediated salvage pathway may contribute to GSH synthesis, xCT-overexpressing  $\gamma$ -GCS knockout cells were treated with increasing concentrations of acivicin (figure 36-C). Acivicin is a general inhibitor of amidotransferases, frequently used to inhibit GGT. xCT-overexpressing cells were used in this experiment, since they could be cultivated in the absence of NAC, GSH, GSH-EE or any other antioxidant. GSH-EE supplemented control cells were used to discriminate between effects possibly arising from acivicin-mediated GSH depletion and unspecific toxic side effects. Cells supplemented with GSH-EE grew significantly faster than non-supplemented cells, but the addition of acivicin affected both cell lines in an equal manner. Acivicin concentrations above 0.5  $\mu$ M reduced cell viability in both cell lines, independently of GSH-EE. Lower acivicin concentrations, however, did not have any effect on  $\gamma$ -GCS-deficient cells, supplemented with or without GSH-EE. Since no increased susceptibility to acivicin was observed, it must be concluded that the GGT salvage pathway does not significantly contribute to cell survival in  $\gamma$ -GCS knockout cells.

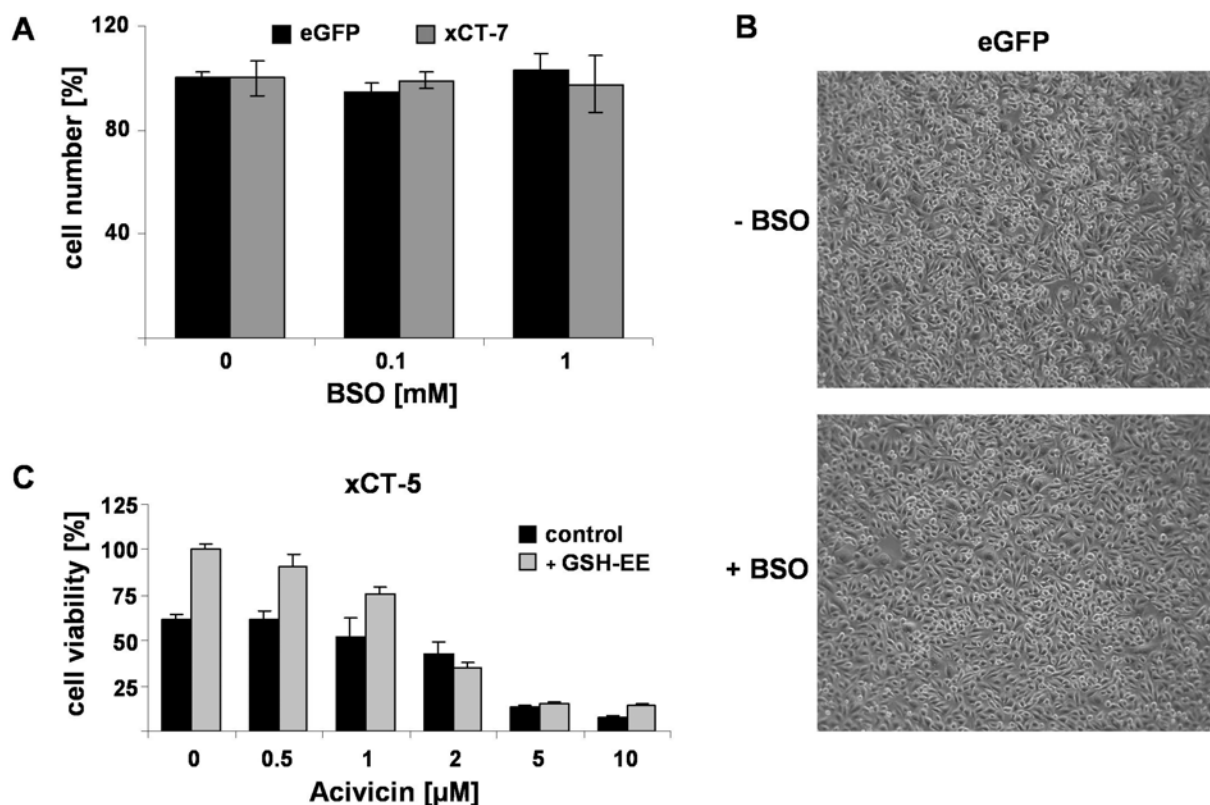


**Figure 36:** Evaluation of a putative residual GSH biosynthesis in  $\gamma$ -GCS knockout cells. **(A)** Cell survival of  $\gamma$ -GCS-deficient cells after BSO treatment. The number of viable cells was determined 72 hours after the addition of BSO. **(B)** Phase contrast microscopy of BSO-treated (1 mM)  $\gamma$ -GCS knockout cells after 10 passages. **(C)** Relative number of viable cells (clone xCT-5), 48 hours after acivicin treatment.

Intracellular GSH levels were measured by HPLC in xCT- and control-transfected cells and in the embryonic stem cell line E14 as a positive control. No significant levels of intracellular GSH were detected in all  $\gamma$ -GCS knockout cell lines. E14 control cells, however, had significantly higher levels of GSH ( $\sim 2$  nmol/mg) (figure 37-B).

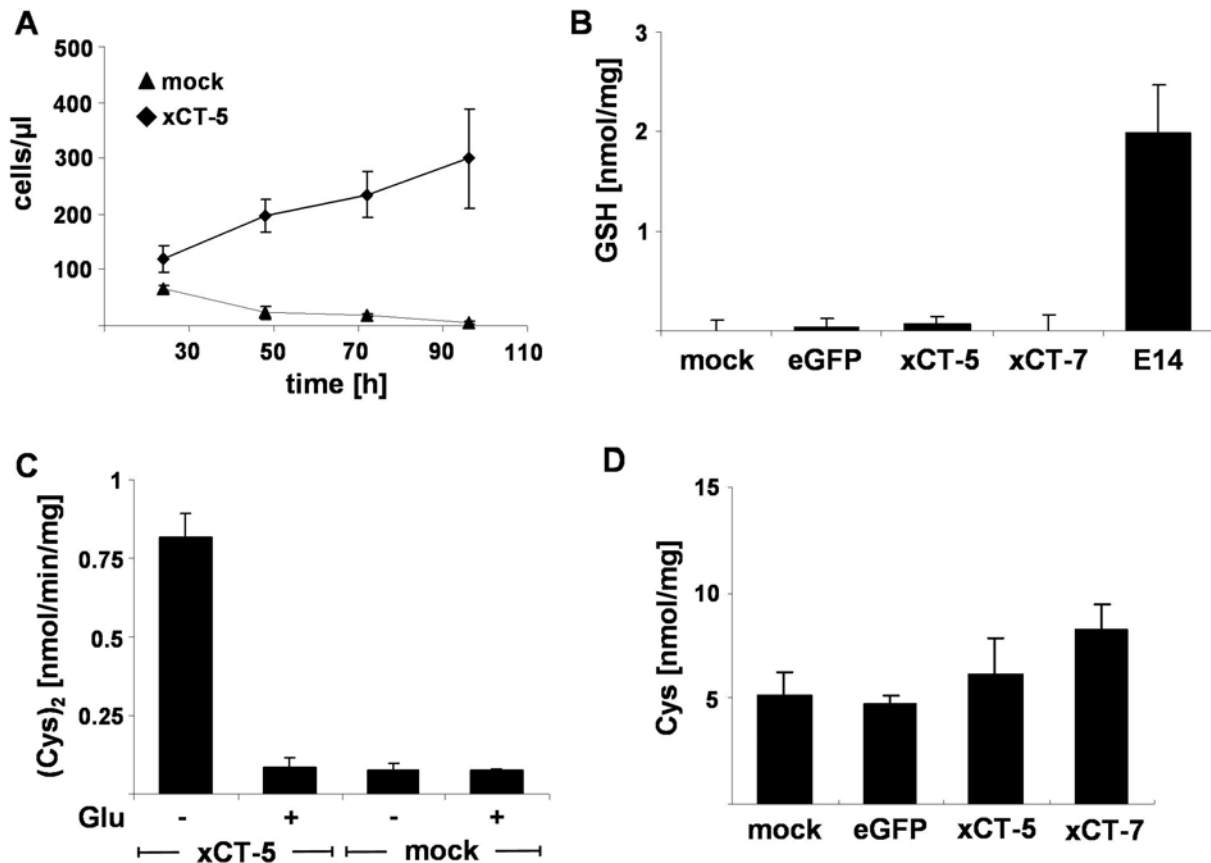


**Figure 37:** (A) Growth curves of mock- and xCT-transfected  $\gamma$ -GCS-deficient cells, in the absence of thiol-containing supplements, such as NAC and GSH. (B) Determination of intracellular GSH levels in transfected  $\gamma$ -GCS knockout and murine wild type ES cells (E14) by HPLC. No significant levels of GSH were detectable in  $\gamma$ -GCS knockout cells. (C)  $(\text{Cys})_2$  uptake activity of mock- and xCT-transfected cells. (D) Measurement of intracellular Cys levels in transfected  $\gamma$ -GCS knockout cells by HPLC.

The  $(\text{Cys})_2$  uptake capacity was measured in mock-transfected cells and clone xCT-5 with radioactively labelled L- $[^{14}\text{C}(\text{U})]$   $(\text{Cys})_2$ . 2.5 mM glutamate was used as specific inhibitor of system  $x_c^-$ -mediated  $(\text{Cys})_2$  uptake. xCT-overexpressing cells had a  $(\text{Cys})_2$  uptake capacity of 0.8 nmol/min/mg, which could be entirely inhibited by the addition of glutamate. Mock-transfected cells had a significantly lower  $(\text{Cys})_2$  uptake capacity of approximately 0.1 nmol/min/mg, which was unaffected by the addition of glutamate (figure 37-C). Hence, the  $(\text{Cys})_2$  uptake capacity increased approximately 8-fold upon overexpression of xCT in  $\gamma$ -GCS knockout cells (clone xCT-5).

Intracellular Cys levels were measured by HPLC in control- and xCT-transfected cells. Yet, despite an 8-fold increase of (Cys)<sub>2</sub>-uptake capacity, only a marginal increase of intracellular Cys was detected in xCT-overexpressing cells (figure 37-D).

This alleged discrepancy was resolved by the determination of extracellular total mercaptans and Cys in particular. Extracellular total mercaptans were quantified in control and xCT-transfected cells by DTNB staining (figure 38). Cells were incubated in DMEM without FCS. Medium was recovered at different time points and subjected to DTNB staining. The levels of extracellular total mercaptans increased dramatically (up to 250  $\mu$ M) in xCT-overexpressing cells. Extracellular total mercaptans in control cells were unaltered after 100 min of incubation, resembling the status of fresh DMEM (figure 38-A). Incubation of cells in (Cys)<sub>2</sub>-free DMEM\* was performed to address if the increase in extracellular mercaptans was indeed caused by augmented (Cys)<sub>2</sub> uptake and subsequent secretion of reduced Cys (figure 38-B). Even after 90 min of incubation, no increase of extracellular total mercaptans could be detected in any cell line incubated in (Cys)<sub>2</sub>-free DMEM\*. These findings highlight (Cys)<sub>2</sub> as the major, if not the only, source of free SH-groups in the cell culture medium of xCT-overexpressing  $\gamma$ -GCS knockout cells.

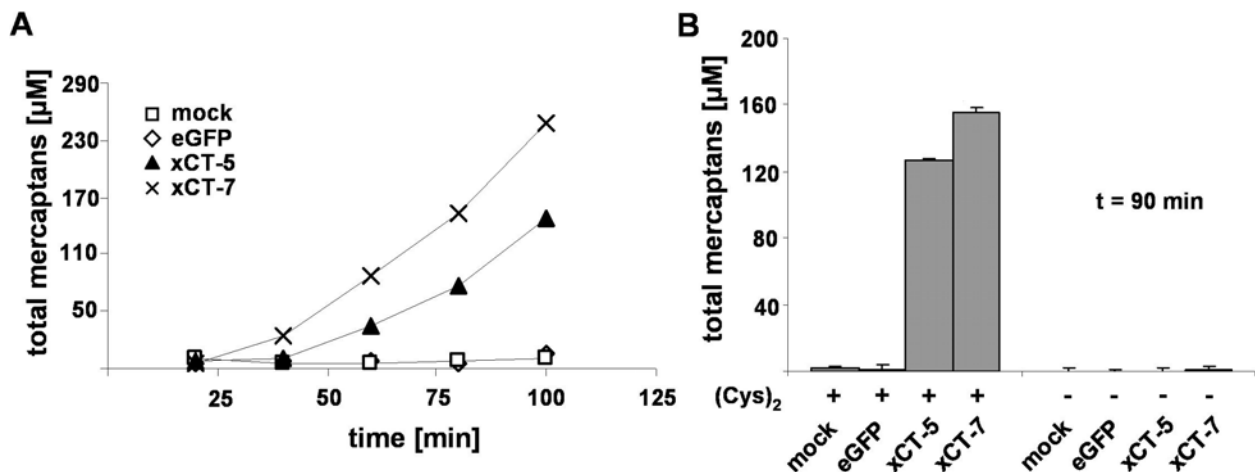


**Figure 38:** Determination of extracellular total mercaptans in xCT-overexpressing cells. (A) Extracellular total mercaptans (free SH-groups) in transfected  $\gamma$ -GCS-deficient cells. (B) Extracellular total mercaptans after 90 min of incubation in DMEM and (Cys)<sub>2</sub>-deficient DMEM\*, respectively.

To prove whether Cys is the major mercaptan secreted into the extracellular space, Cys levels were measured directly by HPLC in control- and xCT-transfected  $\gamma$ -GCS knockout cells after 90 min of incubation in FCS-free DMEM. High extracellular levels of approximately 200  $\mu$ M Cys were detected in both xCT-overexpressing clones,

whereas only marginal amounts were found in control cells (figure 39-A/B). These findings perfectly fit to the results obtained by the quantification of total mercaptan. Of note, intra- and extracellular Cys levels can be directly compared despite different units, since cell extracts contained approximately 1 mg protein per ml. Thus, intracellular Cys levels of xCT-overexpressing cells are stable and remain rather low ( $\sim 5$  nmol/mg) in contrast to the strong increase of extracellular Cys that reaches at least 200 nmol/ml (figure 39-B/C). DMEM contains 200  $\mu\text{M}$   $(\text{Cys})_2$ , which equals 400  $\mu\text{M}$  Cys in a fully reduced state, hence, xCT-overexpressing cells reduce within 90 min at least half of the extracellular  $(\text{Cys})_2$ -pool to Cys.

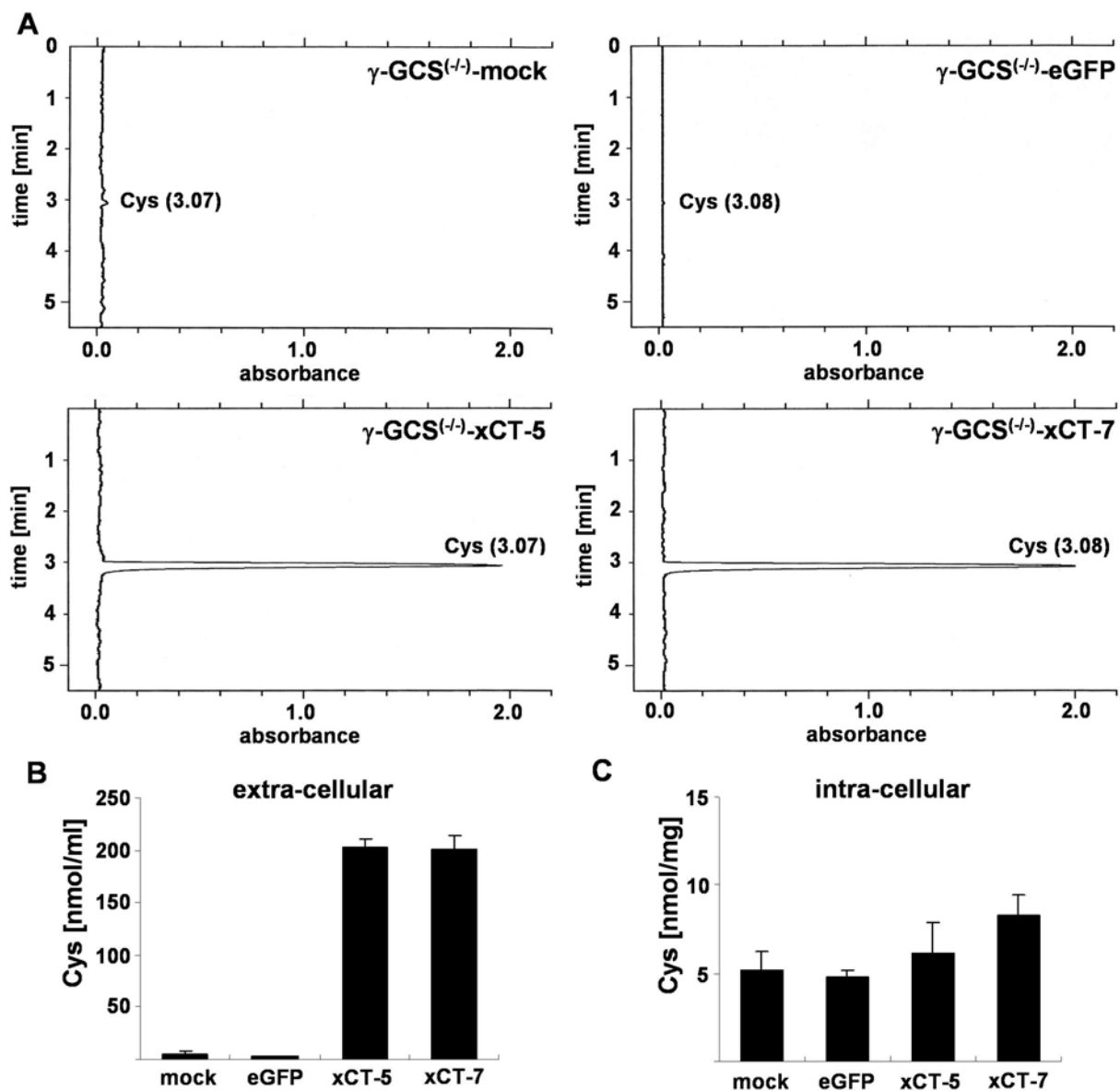


**Figure 39:** Intra- and extracellular Cys levels of control and xCT-transfected  $\gamma\text{-GCS}$  knockout cells. (A/B) HPLC analysis of extracellular Cys levels (C) HPLC analysis of intracellular Cys levels.

Since the overexpression of xCT caused a drastic elevation of extracellular but not intracellular Cys levels, xCT-overexpressing cells were hypothesized to protect control cells from cell death in the absence of any antioxidant supplement, if cultivated in coculture. To this end, clone xCT-7 and eGFP-transfected  $\gamma$ -GCS knockout cells were seeded in equal amounts, supplemented with or without GSH, and the survival rate of eGFP-control cells was monitored by FACS analysis. After 72 hours, the ratio of xCT- and eGFP-overexpressing cells was unaltered even in the absence of GSH. The heterogeneous coculture maintained a stable ratio of 50 % xCT and 50 % eGFP-expressing cells (figure 40), demonstrating that xCT-overexpressing cells act in a feeder-like manner and provide Cys to eGFP-transfected cells. Of note, eGFP-transfected cell cultures died in the absence of GSH, and thus could not be assayed by FACS analysis.

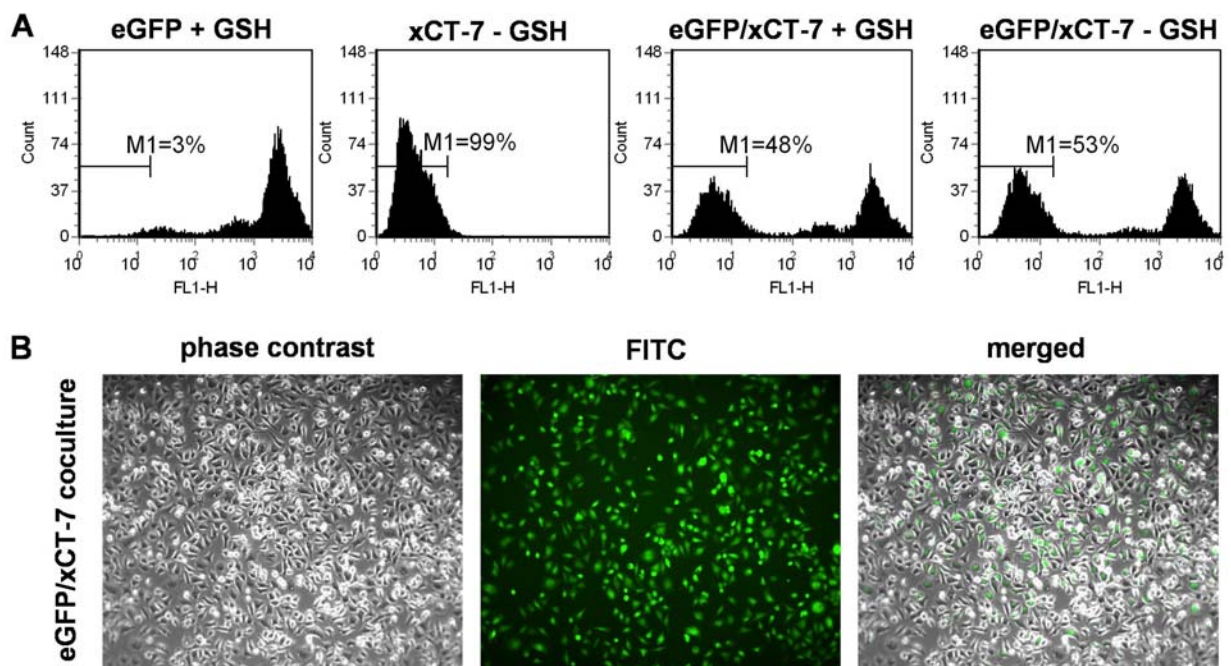


**Figure 40:** Coculture of eGFP- and xCT-overexpressing  $\gamma$ -GCS knockout cells. **(A)** FACS analysis of cells, 72 hours after GSH depletion. **(B)** Fluorescence microscopy of cocultured cells, 72 hours after GSH depletion.

## 5 Discussion

### 5.1 PHGPx regulates cell death via a cascade of events, including 15-LOX activation, lipid peroxidation, and AIF translocation.

The accumulation of detrimental amounts of oxygen derived free radicals in cells and tissues have been frequently linked with acute and chronic degenerative disorders, such as atherosclerosis, myocardial infarction, stroke, and neuronal disorders, such as Alzheimer's and Parkinson's disease. This work describes a comprehensive model of cellular degeneration, triggered by the deregulation of the cellular redox balance. It has been shown that PHGPx abolition triggers a cascade of events, including the deregulation of 15-LOX activity, the lipid peroxidation of biological membranes, and AIF-mediated apoptosis. While individual events of this cascade have been studied in the past, strong evidence for a functional relationship between sensing and transducing oxidative stress in a distinctive cell death inducing pathway can now be provided by the results obtained during these studies.

A variety of enzymatic and non-enzymatic scavenger systems exist in cells that maintain the cellular redox balance. PHGPx is regarded as one of the key redox enzymes within the cell, efficiently protecting biomembranes from lipid peroxidation (Ursini et al., 1982). While its biochemical traits have been analysed to some extent, its physiological role in cells and tissues has remained widely enigmatic. This is largely due to the early embryonic death of PHGPx null embryos, the expression of three distinct forms of PHGPx, and to the lack of suitable *in vivo* as well as *ex vivo* systems.

PHGPx null mice die already at gestational day E7.5 (Imai et al., 2003; Yant et al., 2003). So far, no knockout data are available linking a distinct selenoprotein other than PHGPx to such an early embryonic lethal phenotype. Only mice lacking any of the 24 selenoproteins, achieved by targeted removal of the gene encoding the selenocysteine-specific tRNA, fail to develop beyond E6.5 (Bosl et al., 1997). This strongly argues for PHGPx being indeed one of the most important selenoenzymes, which is also reflected by its high position in the hierarchy of selenoproteins.

To assess the physiological significance of PHGPx in life and death decisions, tissue development and tissue homeostasis, mice with a non-functional PHGPx were generated by Marcus Conrad (Conrad Marcus, PhD thesis, 2001). To bypass the early embryonic lethality of PHGPx deficient mice, the Cre/loxP system was used to create mice with conditional abolition of PHGPx expression.

Since early embryonic lethality impedes further in-depth studies on the molecular and cellular functions of PHGPx, the conditional PHGPx knockout mice were used to create a tamoxifen-inducible *ex vivo* system, including transgenic PHGPx<sup>(flox/flox)</sup> and PHGPx<sup>(wt/flox)</sup> MEF cell lines. In this system, 4-hydroxytamoxifen-mediated activation of MerCreMer (Verrou et al., 1999) caused a rapid decrease of endogenous PHGPx transcripts within 24 hours, followed by efficient depletion of cellular PHGPx protein levels. PHGPx inactivation caused massive cell death, 48 hours after tamoxifen administration. Thus, PHGPx is not only required for early murine development (Imai et al., 2003; Yant et al., 2003) but also for cell survival in *ex vivo* cultured MEFs. The heterozygous cell line PFa37<sup>(wt/flox)</sup> showed a short period of retarded cell growth just after Cre-mediated disruption of the floxed PHGPx allele, but eventually recovered and could be cultivated indefinitely in cell culture. Hence, the loss of one PHGPx allele appears to be compensated by either the upregulation of PHGPx expression from the remaining PHGPx wild type allele or by the upregulation of enzymes with related activity, such as other GPxs, in this cellular system. Yant et al., however, reported that heterozygous knockout cells derived from PHGPx<sup>(wt/-)</sup> mice express reduced PHGPx levels and are more sensitive to oxidative stress (Yant et al., 2003), indicating that the lack of one PHGPx allele can not be fully compensated. This alleged discrepancy may be resolved by applying more provocative stress conditions to the heterozygous cell lines.

To confirm that the specific loss of PHGPx is causally linked to cell death and not due to potential toxic side effects of Cre activity or 4-hydroxytamoxifen itself, a highly efficient lentiviral system for PHGPx reconstitution was established. The add-back of exogenous wild type PHGPx fully rescued the effects caused by the depletion of endogenous PHGPx expression, corroborating that cell death can be unequivocally attributed to PHGPx abolition and not to unspecific toxic side effects.

Previous studies on PHGPx mainly involved heterozygous PHGPx knockout cells (PHGPx<sup>wt/-</sup>) (Yant et al., 2003), overexpression of PHGPx (Imai et al., 1996; Nomura et al., 1999; Shidoji et al., 2006), and indirect inactivation of PHGPx by either Se depletion (Weitzel and Wendel, 1993) or inhibition of GSH biosynthesis (Jakobsson et al., 1992). This cellular system yields for the first time an inducible *ex vivo* knockout model for PHGPx, allowing efficient abolition of PHGPx expression in cell culture. Hence, this unique *in vitro* system proved to be most advantageous for the investigation of the molecular and cellular mechanisms of PHGPx in cell fate decisions.

After PHGPx inactivation, lipid peroxidation was observed as the first event of a cascade, eventually leading to cell death. Lipid peroxidation clearly preceded the accumulation of soluble ROS and the onset of cell death. This finding supports earlier reports in which PHGPx was characterized as an enzyme, efficiently protecting membranous compartments from detrimental peroxidation (Thomas et al., 1990; Ursini et al., 1982). Interestingly, very low concentrations of the lipophilic antioxidant  $\alpha$ -tocopherol fully prevented the increase of intracellular peroxides and cell death in PHGPx knockout MEFs, whereas all other tested antioxidant supplements had only marginal or no effects. This finding underpins the enzymatic function of PHGPx in the protection of biological membranes from lipid peroxidation, yet the fact that  $\alpha$ -tocopherol efficiently substituted PHGPx expression is surprising. Previous studies indicated that the protection against microsomal lipid peroxidation requires a functional cooperation between vitamin E and PHGPx (Maiorino et al., 1989), and that dietary vitamin E impacts PHGPx expression (Bourre et al., 2000; Lei et al., 1997). Our data, however, show that even minor amounts of vitamin E by themselves are sufficient to replace PHGPx activity *in vitro*. This finding may turn out to be of major importance, in particular for *in vivo* experiments using PHGPx knockout mice. Since laboratory animals are generally maintained on a vitamin E fortified diet, some phenotypes of tissue-specific PHGPx knockout mice might be hidden by supra-nutritional amounts of vitamin E.

Vitamin E, the generic term for tocopherol, is an essential antioxidant of which different isomers exist.  $\alpha$ -tocopherol has been shown to be the most reactive isoform in humans. Tocopherols consist of a chromanol ring that provides a hydrogen atom



for the reduction of free radicals. The lipophilic side chain of vitamin E enables the intercalation into biological membranes, enabling an efficient protection from lipid peroxidation in membranes. Vitamin E is discussed to delay the development of coronary heart diseases, cancer, and neurodegenerative disorders, such as Alzheimer's disease (Grundman, 2000) and Parkinson's disease (Bier, 2006), by its antioxidant properties. Nevertheless, results obtained from increased dietary vitamin E intake in humans provided a controversial picture and need further investigation with the focus on long-term clinical trials. Very recently, a meta-analysis on mortality of antioxidant supplements for primary and secondary prevention suggests that vitamin E may even increase mortality (Bjelakovic et al., 2007). Yet, vitamin E has been demonstrated to protect cortical and hippocampal neurons *in vitro* from cerebral ischemia and reperfusion induced detriment (Tagami et al., 1999; Tagami et al., 1998). Moreover, Pratico et al. showed that the oral administration of vitamin E diminished aortic lesions in apolipoprotein E-deficient mice, an *in vivo* model for atherosclerosis, probably by preventing the oxidation of low density lipoprotein (LDL) (Pratico et al., 1998). Of note, 15-LOX is expressed in atherosclerotic lesions and has been implicated in the oxidation of LDL during atherogenesis. Interestingly, apolipoprotein E and 15-LOX compound knockout mice display strongly reduced lipid peroxidation and atherogenesis compared to apolipoprotein E null mice, indicating a functional linkage between the administration of vitamin E and 15-LOX-deficiency (Cyrus et al., 2001; Zhao et al., 2005).

Since lipid peroxidation emerged as the major cell death-inducing event that could be efficiently prevented by  $\alpha$ -tocopherol supplementation, it was hypothesized that lipid peroxidation may be provoked by altered lipoxygenase and/or cyclooxygenase activities. Interestingly, when grown to confluency, PHGPx knockout cells did not require functional PHGPx, suggesting that the lipid peroxidation is caused by endogenous sources that are only active in proliferating cells. Moreover, PHGPx has been previously reported to antagonize LOX and COX activities (Huang et al., 1999). Thus, intermediate hydroperoxyl-metabolites of LOXs and/or COXs, such as PGG<sub>2</sub>, HPETE, and HPODE, were considered as a major source of lipid-associated ROS production in PHGPx-deficient cells.

Incubation of PHGPx knockout cells with arachidonic acid, the common and main substrate of LOXs and COXs, clearly accelerated cell death, indicating a direct link between PHGPx and arachidonic acid metabolism in this system. To investigate the individual contribution of oxygenases to cell death upon PHGPx abolition, knockout cells were treated with a variety of LOX and COX inhibitors. In fact, various LOX inhibitors rescued PHGPx-deficient cells. Yet, it must be taken into account that many LOX inhibitors have been reported to harbour antioxidant properties, such as NDGA (Shappell et al., 1990), ETYA (Takami et al., 2000), baicalein, and caffeic acid (Dailey and Imming, 1999). The antioxidant activity of these inhibitors may protect PHGPx-deficient cells by directly scavenging peroxides rather than by a specific inhibition of LOX activity. PD146176, however, is a specific 15-LOX inhibitor without showing any significant antioxidant activity (Sendobry et al., 1997). Thus, the highly efficient rescue of PHGPx knockout cells by PD146176 implies a major contribution of 15-LOX to this cell death-inducing pathway. Besides PD146176, some 15-LOX inhibitors protected PHGPx-deficient cells from cell death, whereas most other inhibitors were rather ineffective, despite the expression of 5-LOX, 12-LOX, 15-LOX, COX1, and COX2 in this cellular system. These findings strongly argue for a deregulated activity of 15-LOX, rather than of other LOXs or COXs, triggering a lipid peroxidation cascade, which finally leads to cell death in PHGPx-deficient MEFs. This is in line with findings, implicating 15-LOX in the pathophysiology of various degenerative diseases, such as atherosclerosis (Cyrus et al., 2001; Pratico et al., 1998) and many neuronal disorders (Grundman, 2000; Khanna et al., 2003; Tagami et al., 1999). Initially, Li et al. showed that inhibition of the arachidonic acid metabolism by various LOX inhibitors protects cortical neurons from GSH depletion (Li et al., 1997). Neurons isolated from 15-LOX-deficient mice are resistant to Glu-induced cell death, indicating a critical impact of 15-LOX on oxidative stress-induced neuronal death (Khanna et al., 2003). The inhibition of (Cys)<sub>2</sub>-uptake by high concentrations of extracellular Glu is an established model for the investigation of oxidative stress (Murphy et al., 1990; Tan et al., 1998). Besides this non-receptor-mediated Glu toxicity, however, also a receptor-mediated excitotoxicity of Glu is discussed (Choi, 1990). Moreover, the 15-LOX inhibitor baicalein has been shown to protect neurons from ischemia/reperfusion injury, to an extent which is similar to that observed after transient experimental stroke in the brain of 15-LOX knockout mice (van Leyen et al., 2006). Interestingly, a cellular model system for oxidative stress,

including Se-deficient bovine aortic endothelial cells, showed apoptosis via a strong increase of 15-LOX activity and 15-HPETE production (Sordillo et al., 2005), which may be attributed to reduced PHGPx expression.

Still, it can not be concluded from these results that the abolition of PHGPx does not affect the activity of other oxygenases, in particular in other cells and tissues. The severe consequences of an aberrant 15-LOX activity may mask less dramatic effects of PHGPx inactivation towards other LOXs and COXs, at least in this cellular system. This would be in agreement with previous studies, where a rather general role for PHGPx in controlling LOX and COX activities has been documented (Chen et al., 2002, 2003; Imai et al., 1998; Sakamoto et al., 2000).

To underpin the importance of 15-LOX for this cellular system, arachidonic acid metabolites were quantified by HPLC. However, only low levels of HETE/HPETE and no substantial accumulation of these intermediate metabolites in PHGPx null cells could be detected. Likewise, virtually no LTB<sub>4</sub> was released from these cells. The lack of LTB<sub>4</sub> after the activation of the arachidonic acid metabolism in MEFs suggests that despite its expression, only a minor amount of 5-LOX is active in this cell system. This finding also elucidates why 5-LOX inhibitors did not protect PHGPx-deficient cells from cell death, although 5-LOX activity has been frequently linked to the generation of oxidative stress, e.g. during ischemia/reperfusion in the brain of 5-LOX knockout mice (Patel et al., 2004). The detection of only marginal amounts of HPETEs may reflect a short half life of the generated HPETE isoforms, which are rapidly metabolized to leukotrienes, hepoxilins, and lipoxins. However, 15-LOX also accepts linoleic acid as a substrate, catalyzing the production of 13-HODE via a 13-HPODE intermediate. Hence, the biosynthesis of HODE/HPODE from linoleic acid is an alternative peroxide source, which may account for lipid peroxidation. Of note, 13-HODE has been demonstrated to induce apoptosis by decreasing the activation of the transcription factor peroxisome proliferator-activated receptor (PPAR)-delta in colorectal cancer cells (Shureiqi et al., 2003; Zuo et al., 2006), indicating a functional link between the LOX metabolism and programmed cell death.

The increase of lipid peroxidation, which is mediated by the deregulation of 15-LOX in PHGPx deficient MEFs, is generally considered as a potent mediator of apoptosis

via the mitochondrial death pathway (Buttke and Sandstrom, 1994; Kagan et al., 2005; Sarafian and Bredesen, 1994). Moreover, the generation of 15-HPETE has been previously reported to induce apoptosis in bovine aortic endothelial cells (Sordillo et al., 2005). Hence, apoptosis rather than necrosis was considered as the mechanism of cell death in PHGPx-deficient cells. Most apoptotic processes involve the disruption of the mitochondrial inner transmembrane potential ( $\Delta\psi$ ) and an increase of the inner mitochondrial membrane permeability, the so called permeability transition (Bernardi et al., 1999; Loeffler and Kroemer, 2000), causing the release of proteins required for the execution of cell death, such as cytochrome c and AIF (Susin et al., 1999). The classical model of the mitochondrial death pathway involves several pro- and anti-apoptotic Bcl-2 family members, which mediate the mitochondrial permeability transition upon a stress signal. Released cytochrome c forms apoptosomes by aggregating with the apoptotic protease activating factor-1 (APAF-1). The apoptosomes cleave procaspase-9 to release activated caspase-9, triggering a proteolytic cascade that involves caspase-3 activation and further downstream effects. First indications that PHGPx-deficient cells undergo a form of apoptosis were obtained from time-lapse videos, showing stereotypical morphological changes, such as shrinking, deformation, loss of intercellular contacts, and detachment from the cell culture dish.

Oxidative stress induced apoptosis has been previously reported to be prevented in cells overexpressing Bcl-2 (Hockenbery et al., 1993; Kane et al., 1993; Reed, 1998), by blocking cytochrome c release from the mitochondria, possibly through the inhibition of the pro-apoptotic Bcl-2 family members Bax and Bak. In this respect, the anti-apoptotic molecule Bcl-2 was overexpressed in PHGPx knockout cells. In the present system, the overexpression of Bcl-2 or Bcl-2-ActA, including a mitochondrial insertion sequence, did not protect PHGPx-deficient cells from cell death. These findings indicate that Bcl-2 is not involved in the cell death process, triggered by PHGPx depletion, at least in this system. This correlates with previous reports showing that Bcl-2 did not protect Burkitt's lymphoma cells from oxidative stress (Lee and Shacter, 1997) as well as A3.01 human T cells from 15-HPETE and 13-HPODE induced apoptosis (Sandstrom et al., 1995). The discrepancy between studies, reporting that Bcl-2 did or did not protect from oxidative stress, may be due to the fact

that different forms of ROS induce apoptosis via diverse apoptosis inducing pathways, which may also differ between various cell types.

A caspase-independent model of mitochondrial apoptosis involves the flavoprotein AIF. In healthy cells, AIF is located in the mitochondrial intermembranous space or at the inner membrane of mitochondria, where it exerts vital functions as a redox-active enzyme with putative antioxidant activity (Klein and Ackerman, 2003; Lipton and Bossy-Wetzel, 2002). Upon activation, AIF is released from mitochondria and translocates to the nucleus, where it induces chromatin condensation and DNA degradation (Daugas et al., 2000). Thus, AIF comprises a dual role, either as an anti-apoptotic redox-active enzyme or as a pro-apoptotic mediator of DNA fragmentation. Interestingly, AIF-mediated apoptosis has been implicated in ischemia/reperfusion injury (Cao et al., 2003; van Wijk and Hageman, 2005), indicating a direct link between oxidative stress and AIF release. Due to the described pro-apoptotic properties upon oxidative stress, AIF downregulation was considered to prevent cell death in PHGPx-deficient cells. It could be shown that the siRNA-knockdown of AIF efficiently protected MEFs from cell death, induced by PHGPx depletion. This is in line with a previous study, showing that increased lipid peroxidation indeed induces the disruption of  $\Delta\psi$  and permeability transition (Marchetti et al., 1997), causing intrinsic apoptosis via the mitochondrial death pathway. Nevertheless, the findings by Marchetti et al. left open how lipid peroxidation is triggered and what are the upstream components, sensing and transducing oxidative stress in a cellular response.

Inducible PHGPx disruption allowed the dissection of a distinctive pathway, including deregulation of 15-LOX activity, lipid peroxidation, and eventually AIF-mediated apoptosis. In the presented *in vitro* system, the process of lipid peroxidation seems to bypass the Bcl-2-dependent activation of the mitochondrial death pathway by directly releasing AIF. This finding is in agreement with studies by Arnoult et al., demonstrating that the pro-apoptotic Bcl-2 family member Bax triggers the release of cytochrom c, but not of AIF (Arnoult et al., 2002), indicating an independent regulation of the two death pathways. Yet, it is still not understood how apoptosis is mediated via AIF activation. Yu et al. demonstrated that the activation of poly(ADP-ribose) polymerase-1 (PARP-1) is required for AIF translocation in a caspase-

independent manner (Yu et al., 2002). PARP-1 is involved in the DNA repair mechanism of the cell, but also acts as a mediator of cell death after ischemia/reperfusion injury, glutamate toxicity, and various inflammatory processes (van Wijk and Hageman, 2005). Recently, it has been shown that only severe oxidative stress activates the pro-apoptotic function of PARP-1 (Diaz-Hernandez et al., 2007). Thus, PARP-1 mediated AIF translocation may be a common signature of degenerative disorders that are induced by the accumulation of ROS. Interestingly, heat shock protein 70 has been reported to inhibit apoptosis not only by preventing the apoptosome assembly, but also by binding to AIF (Lui and Kong, 2007; Ravagnan et al., 2001). Final proof of an exclusively AIF-mediated apoptosis of PHGPx-deficient cells is still lacking. Further studies are required to address the role of other pro- and anti-apoptotic members in PHGPx knockout cells. In this respect, cytochrome c release, breakdown of  $\Delta\psi$ , and caspase activation are important hallmarks that need further investigation. The impact of various caspases will be addressed by using a set of caspase inhibitors with different specificity for various caspase family members.

Taken together, this work elucidates a cascade of events causing cell death upon PHGPx depletion in primary MEFs (figure 41). PHGPx abolition leads to the activation of 15-LOX, which causes a detrimental increase of lipid-associated hydroperoxides inside the cell. The increase of cellular hydroperoxides causes an autocatalytic chain reaction of lipid peroxidation which severely damages biomembranes, most likely including the mitochondrial membrane. The disruption of the mitochondrial membrane probably initiates the breakdown of the mitochondrial membrane potential  $\Delta\psi$ , followed by permeability transition and AIF release. The process of caspase-independent apoptosis is characterized by the translocation of AIF to the nucleus, where it mediates chromatin condensation and DNA degradation. Whether the release of AIF is supported or even induced by PARP activation due to DNA damage is still unclear. Eventually, the PHGPx knockout in MEFs causes massive cell death.

This cascade of events may be a common signature of various degenerative disorders that include a severe insult by oxidative stress, which inevitably leads to GSH depletion. A detrimental increase of ROS levels is a general characteristic of

acute and chronic inflammation processes, observed in atherosclerosis, arthritis, diabetes, Alzheimer's and Parkinson's disease, but also myocardial infarction and stroke coincides with massive oxidative stress during reperfusion. Therefore, this inducible PHGPx knockout model may prove extremely useful to gain deeper insights into the molecular mechanisms of uncontrolled cell death in the etiology of complex human disorders.

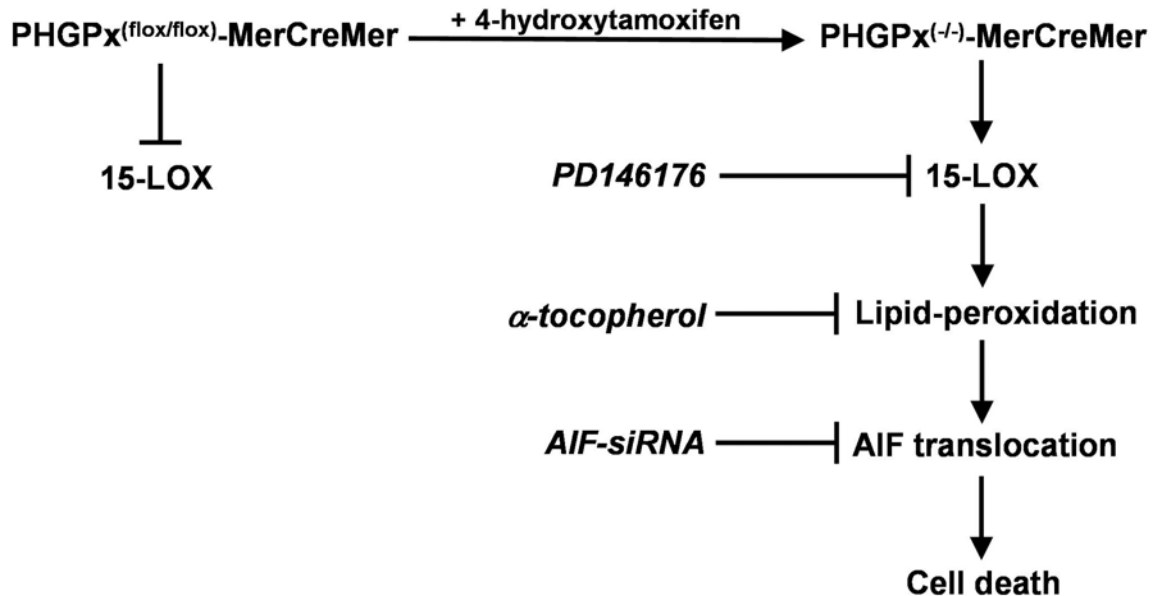


**Figure 41:** Proposed mechanism of cell death, initiated by PHGPx depletion in MEFs. PHGPx controls the 15-LOX activity by regulating the cellular peroxide tone. After the depletion of PHGPx, augmented 15-LOX activity most likely causes an accumulation of cellular HPETE and HPODE levels, which lead to rapid non-specific lipid peroxidation, followed by AIF release and massive cell death. At various steps, this cell death inducing cascade can be disrupted, including inhibitors against 15-LOX, lipophilic antioxidants, or AIF silencing.

## 5.2 Mutational analysis of PHGPx revealed functional interchangeability of Sec with Cys: a model to study a putative redox sensor function of PHGPx

In mammals, the overall homology of PHGPx compared with the other Sec-containing GPxs is less than 40 %, yet they share conserved motifs that include the catalytic triad of Sec, Gln and Trp. This conserved triad forms a catalytic centre in which the selenol group of Sec is stabilized and activated by hydrogen bonds provided by the Gln and Trp residues (Maiorino et al., 1995). An initial mutational and biochemical approach by Maiorino et al. revealed that the conversion of Sec to Cys causes a marked decrease of PHGPx activity by about three orders of magnitude in the recombinant protein (Maiorino et al., 1995). Also mutations of Gln and Trp of the

catalytic triad reduced PHGPx enzyme activity, highlighting the importance of the proposed catalytic centre.

The lentiviral add-back system for wild type and various mutant forms of PHGPx in the PHGPx null background proved to be an ideal tool for mutagenesis studies on a cellular level, with main focus on the active site Sec. MEFs were reconstituted with PHGPx mutants, containing Ser and Cys substitutions for Sec. The Ser-containing mutant of PHGPx did not protect PHGPx-deficient cells from cell death, demonstrating that Sec or Cys at this position is absolutely essential for PHGPx function. Surprisingly, the Cys-containing PHGPx mutant fully rescued MEFs from cell death after Cre-mediated disruption of the endogenous PHGPx alleles and no difference in susceptibility towards peroxides was detected. Of note, the translational insertion of Sec is a complex process with a rather low efficiency, ranging around 4 % compared to the incorporation of other amino acids (Suppmann et al., 1999). Consequently, the expression levels of Sec/Ser and Sec/Cys mutants were significantly higher compared to wild type PHGPx. These findings demonstrate that despite its dramatically reduced enzyme activity (Maiorino et al., 1995), the Sec/Cys PHGPx mutant can fully substitute wild type PHGPx *in vitro*.

This surprising finding raises the question why mammalian cells express selenoproteins at all, when Cys-containing variants are apparently capable to replace Sec-containing wild type counterparts, at least for normal cell function. Certainly, findings obtained from *in vitro* cell culture studies can not be entirely translated to the far more complex system of a whole organism. At present, it can only be speculated that the Sec-containing wild type PHGPx exerts cellular functions beyond its activity as antioxidant enzyme, e.g. during embryonic and tissue development, stress conditions, and sperm development. This hypothesis will be addressed in our laboratory by the production of knockin mice, harbouring the Cys-containing mutant of PHGPx. Moreover, the impact of PHGPx on cellular processes may vary significantly between different cell types. To address this question, ongoing studies in my laboratory will unravel, whether the Cys-containing variant is also able to replace wild type PHGPx in other *in vitro* PHGPx knockout systems, such as ES cells, epithelium precursor cells, and neurons.



Since  $H_2O_2$  and other hydroperoxides are now considered as not mere toxic compounds, but have drawn great attention as important second messengers, it has been speculated that PHGPx regulates various cellular processes by sensing and transducing the redox tone of the cell. Further mutational studies, using the inducible knockout system, may gain novel insights into these enzymatic mechanisms of PHGPx. In this respect, the nine Cys residues in the PHGPx gene are of major interest, since certain Cys residues may form a redox couple or also in cooperation with the Sec.

One putative mechanism involves redox sensor and transducer reactions, as initially described for the yeast PHGPx homologue, GPx3 (Delaunay et al., 2002). Upon increasing  $H_2O_2$  levels, yeast GPx3 senses and transduces the stress signal to the transcription factor Yap1. The peroxidase function of yeast GPx3 was shown to involve the oxidation of Cys<sup>36</sup> and Cys<sup>82</sup> to form a transient intra-molecular Cys<sup>36</sup>-SS-Cys<sup>82</sup> bridge. Subsequently, Yap1 is activated by yeast GPx3, involving a transient disulfide bond between GPx3 Cys<sup>36</sup> (Sec<sup>46</sup> homologue in *mus musculus*) and Cys<sup>598</sup> of Yap1. So far, no equal mechanism has been reported for mammalian PHGPx. But this cellular PHGPx knockout/knockin tool will prove most suitable to investigate this putative  $H_2O_2$  sensing and transducing mechanism of mammalian PHGPx.

In the cell, ROS are not only generated as detrimental side products of the mitochondrial respiration, but are also produced for essential physiological functions.  $H_2O_2$  production is catalysed by NADPH oxidases such as NOXs (NADPH oxidase) and DUOXs (dual oxidase), (Rueckschloss et al., 2003) mainly for the regulation of detoxification processes and inflammatory responses. Upon cellular infection, neutrophils and phagocytic cells produce large amounts of ROS in order to kill invading bacteria. Yet, NOX isoforms were also found in a number of non-phagocytic cells and tissue, indicating that the generation of ROS is a rather general feature of all somatic cells than being restricted to phagocytic cells (Lambeth, 2004). In this regard,  $H_2O_2$  seems to be the major component of receptor mediated ROS production, which can be stimulated by cytokines or growth factors, such as transforming growth factor- $\beta$ 1 (TGF- $\beta$ 1) (Thannickal and Fanburg, 1995), interleukin-1 (Meier et al., 1989), tumor necrosis factor  $\alpha$  (TNF $\alpha$ ) (Lo et al., 1996), platelet-derived growth factor (PDGF) (Krieger-Brauer and Kather, 1995; Sundaresan et al.,

1995), epidermal growth factor (EGF) (Bae et al., 1997) and basic fibroblast growth factor (bFGF) (Krieger-Brauer and Kather, 1995; Lo et al., 1996). ROS have been shown to activate mitogen-activated protein kinases (MAPK) (Sundaresan et al., 1995) and protein kinase C (Konishi et al., 1997), most likely by the specific inactivation of phosphatases (Lee et al., 1998). This has been nicely demonstrated by Kamata et al., showing that JNK-inactivating phosphatases are inhibited by ROS, by converting the catalytically active Cys to sulfenic acid (Kamata et al., 2005). Initially, Meng et al. demonstrated a reversible inactivation of multiple protein tyrosine phosphatases by H<sub>2</sub>O<sub>2</sub> *in vivo* (Meng et al., 2002). Only recently, the established cellular PHGPx knockout system was used in our laboratory, to address a putative impact of PHGPx on PDGF $\beta$  receptor signalling. By using this system, it has been shown that PHGPx antagonizes PDGF $\beta$  receptor signalling in MEFs, most likely by regulating lipid-associated ROS levels. Thereby, lipid-associated ROS transiently oxidize and thus inactivate counteracting protein tyrosine phosphatases (Conrad et al., in preparation).

ROS have also been reported to act as physiological mediators of transcriptional control by activating transcription factors, such as activation protein-1 (AP-1) (Meyer et al., 1993) and NF- $\kappa$ B (Schreck et al., 1991). Interestingly, PHGPx overexpression has been shown to inhibit the expression of NF- $\kappa$ B target genes, such as IL-1 mediated induction of VCAM-1 in smooth muscle cells (Banning et al., 2004) and TNF-induced COX2 expression in L929 cells (Heirman et al., 2006), by dampening intracellular ROS levels.

In conclusion, PHGPx may be involved in various cellular processes which have been masked by the lethal effects, caused by to the complete removal of PHGPx. The presented *in vitro* system, including the efficient reconstitution of PHGPx mutants, provides an ideal tool for further investigations on PHGPx functions. This may provide additional knowledge to the herein identified function of PHGPx, as a regulator of a distinct cell death-inducing pathway by sensing and transducing oxidative stress inside the cell.

### **5.3 The Cys/(Cys)<sub>2</sub>-cycle rescues GSH deficiency in $\gamma$ -GCS knockout cells**

GSH is the major endogenous scavenger of ROS in the cell by acting as a reducing equivalent for GPxs and other detoxifying enzymes. Inside the cell, GSH is present up to millimolar concentrations and has long been considered indispensable for cell survival. This work highlights the significance of the Cys/(Cys)<sub>2</sub>-cycle as an independent redox-cycle, capable to compensate GSH deficiency in  $\gamma$ -GCS knockout cells. The overexpression of the Glu/(Cys)<sub>2</sub> antiporter system  $x_c^-$  boosted the Cys/(Cys)<sub>2</sub>-cycle, rendering GSH dispensable for cell survival and proliferation. The investigation of the Cys/(Cys)<sub>2</sub>-cycle and its implication in cell survival and cell death required a cellular system, free of GSH. Shi et al. generated  $\gamma$ -GCS-deficient ES cell like cells, lacking detectable levels of GSH after the removal of GSH from the cell culture medium (Shi et al., 2000). These  $\gamma$ -GCS-deficient ES cell like cells proved to be an ideal tool to dissect the relevance of the Cys/(Cys)<sub>2</sub>-cycle for cell survival in the absence of endogenous GSH biosynthesis.

Shi et al. showed that no significant levels of intracellular GSH are detectable by HPLC in  $\gamma$ -GCS-deficient cells (Shi et al., 2000). Yet, it is a long-lasting paradigm that GSH is absolutely essential for cell survival, thus the presence of minor amounts of GSH had to be considered in this experimental system. Due to the limited sensitivity of the HPLC method, however, it could not be ruled out that marginal amounts of GSH are still present. In this respect, two possibilities were regarded as a putative source of remaining GSH biosynthesis, a residual  $\gamma$ -GCS enzyme activity and the GGT salvage pathway.  $\gamma$ -GCS-deficient cells derive from transgenic mice that were designed such that a PGK-*hrpt* cassette replaced only exon 1 of gene  $\gamma$ -GCS (Shi et al., 2000). Although no alternative splicing variants of  $\gamma$ -GCS have been reported so far, some remaining enzyme activity could not be entirely excluded. On the other hand, GGT may mediate the salvage of residual GSH, independently from  $\gamma$ -GCS (Anderson and Meister, 1983; Griffith et al., 1981). GGT cleaves secreted GSH to  $\gamma$ -Glu-Cys/(Cys)<sub>2</sub>, which is incorporated into the cell by the  $\gamma$ -Glu-AA transporter. In the cell,  $\gamma$ -Glu-Cys acts as the precursor for GSH, bypassing the rate limiting step of  $\gamma$ -Glu-Cys biosynthesis. GGT is considered to have a significant influence on GSH metabolism and the protection against oxidative stress (Karp et al., 2001; Lieberman

et al., 1995). To address these two possible mechanisms of GSH biosynthesis, proliferation assays were carried out in the presence and absence of specific inhibitors for  $\gamma$ -GCS and GGT, respectively. In case one of these pathways would sustain cell survival, the cells should be particularly susceptible to the inhibition of the respective enzyme.

The proliferation rate of NAC-supplemented  $\gamma$ -GCS-deficient cells was not impaired, even at exceedingly high concentrations of BSO. This remarkable resistance of  $\gamma$ -GCS-deficient cells to BSO strongly suggests the absence of a residual  $\gamma$ -GCS enzyme activity, and against a putative contribution of  $\gamma$ -GCS to cell survival. Of note, BSO proved to be a highly specific  $\gamma$ -GCS inhibitor, since no toxic side effects were observed. In addition, the putative GSH biosynthesis by the GGT-mediated salvage pathway was assessed by treating  $\gamma$ -GCS-deficient cells with the potent GGT inhibitor acivicin. The proliferation assay did not reveal any increased susceptibility to acivicin of  $\gamma$ -GCS-deficient cells as compared to GSH-EE-supplemented cells, indicating that a GGT-mediated GSH biosynthesis does not significantly contribute to cell survival. This finding is conceivable, since the initial presence of GSH is a prerequisite for its recycling by the GGT salvage pathway (Rajpert-De Meyts et al., 1992). Taken together, these findings indicate that no residual GSH biosynthesis is present in  $\gamma$ -GCS-deficient cells, neither by remaining enzymatic  $\gamma$ -GCS activity nor by the GGT salvage pathway. Hence, the  $\gamma$ -GCS knockout cells state an ideal system to investigate the impact of the Cys/(Cys)<sub>2</sub>-cycle, independently from GSH biosynthesis.

Jones et al. reported that the steady-state redox potential of Cys/(Cys)<sub>2</sub> is considerably more oxidized than GSH/GSSG, indicating that both redox couples must be regulated independently (Jones et al., 2004). This finding also supports the notion that the Cys(Cys)<sub>2</sub>-cycle does not act as a mere supplier for GSH biosynthesis. The first indication that GSH may be dispensable for cell survival was obtained by Shi et al., showing that  $\gamma$ -GCS-deficient cells proliferate when supplemented with NAC (Shi et al., 2000). The present work, however, highlights the importance of the physiological Cys/(Cys)<sub>2</sub>-cycle, driven by the Glu/(Cys)<sub>2</sub> antiporter, system x<sub>c</sub><sup>-</sup>. The antiporter system x<sub>c</sub><sup>-</sup> consists of two protein components, xCT light chain and 4F2 heavy chain, whereas xCT mediates substrate specificity for (Cys)<sub>2</sub> (Sato et al., 1999). Since 4F2 heavy chain is constitutively expressed, it was

sufficient to overexpress xCT in order to achieve an increased (Cys)<sub>2</sub> uptake capacity by system x<sub>c</sub><sup>-</sup> (Banjac Ana, PhD thesis, 2005). Two single cell clones were established from  $\gamma$ -GCS-deficient cells, stably overexpressing the xCT subunit. Murine xCT light chain was cloned into a eukaryotic expression vector and used for stable transfection of  $\gamma$ -GCS-deficient ES cell like cells. The xCT-overexpressing cells showed an approximately 8-fold increase in (Cys)<sub>2</sub> uptake capacity, yet intracellular Cys levels were only slightly increased compared to mock-transfected control cells. Determination of secreted mercaptans, however, revealed a dramatic increase of extracellular free thiols in xCT-overexpressing cells. HPLC analysis confirmed that the extracellular mercaptans was virtually exclusively Cys. These findings demonstrate that the overexpression of xCT facilitates the production of a highly reducing environment, by mediating a rapid turnover of (Cys)<sub>2</sub> to Cys inside the cell (figure 42). This is in line with findings by Ana Banjac, demonstrating that xCT overexpression increased extra and intracellular Cys levels in HH514 Burkitt's lymphoma cells (Banjac Ana, PhD thesis, 2005). Obviously, system x<sub>c</sub><sup>-</sup> drives the Cys/(Cys)<sub>2</sub>-cycle, which transports large amounts of oxidized (Cys)<sub>2</sub> into the cell. Intracellular (Cys)<sub>2</sub> is readily reduced to Cys and the surplus is secreted into the medium by the neutral amino acid transport system. The secreted Cys accumulates in the extracellular space, constituting the major part of a highly reducing environment. Eventually Cys is oxidized to (Cys)<sub>2</sub> by oxygen in the medium.

Consequently the question arises, which molecules are responsible for the reduction of (Cys)<sub>2</sub> to Cys inside the cell, especially in the absence of GSH. Under normal conditions, the prime candidate would be glutaredoxin, which usually reduces disulfide bonds in proteins at the expense of 2 molecules GSH. In the absence of GSH, however, GSH reductase with its reducing equivalent NADPH may also accept (Cys)<sub>2</sub> instead of GSSG as an additional substrate. A further possibility is the Trx system, which may take over the function of (Cys)<sub>2</sub> reduction. The Trx system, consisting of Trx, TrxR, and NADPH, represents another major system for cellular protein disulfide reduction (Arner and Holmgren, 2000). Recently it has been shown by our group that wild type but not TrxR2 knockout MEFs survive BSO-mediated GSH depletion (Conrad et al., 2004). This finding indicates that the GSH-dependent system can be at least partially compensated by the Trx system, which may be attributed to the recycling of oxidized (Cys)<sub>2</sub> to Cys inside the cell.

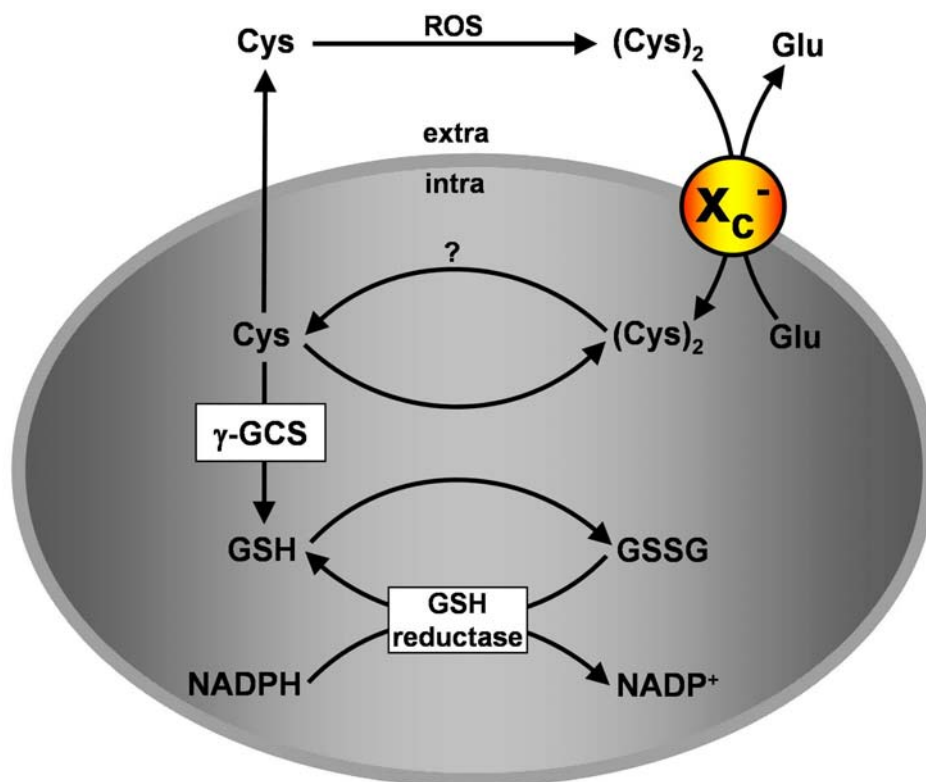


**Figure 42:** The Cys/(Cys)<sub>2</sub>- and the GSH/GSSG-cycle are two individual redox-systems. The Cys/(Cys)<sub>2</sub>-cycle includes the incorporation of (Cys)<sub>2</sub> by system x<sub>c</sub><sup>-</sup>. Intracellular (Cys)<sub>2</sub> is reduced to Cys by a yet unknown mechanism. A large part of Cys is secreted into the extracellular space by neutral amino acid transport systems. Extracellular Cys is readily oxidized to (Cys)<sub>2</sub> by oxygen in the medium. The GSH/GSSG-cycle includes the oxidation of GSH to a GSSG, usually by GSH-dependent enzymes, such as GPxs and glutaredoxins. GSH is reconstituted by GSH reductase at the expense of NADPH. Both redox-cycles are linked via the biosynthesis of GSH, which is catalysed by the rate-limiting enzyme  $\gamma$ -GCS from Cys, Glu, and Gly.

To test whether the increased (Cys)<sub>2</sub> uptake capacity may compensate for GSH deficiency, cells were cultivated in the absence of thiol-containing supplements, such as NAC or GSH. Antiporter system x<sub>c</sub><sup>-</sup> has been reported to protect various cell types from oxidative stress, such as human fibroblasts (Bannai et al., 1989), mouse peritoneal macrophages (Sato et al., 1995), and human peripheral neutrophils (Sakakura et al., 2007), yet this was mainly attributed to increased GSH biosynthesis inside the cell. Since  $\gamma$ -GCS-deficient cells lack the capability to synthesize GSH, the impact of the Cys/(Cys)<sub>2</sub>-cycle on cell fate decisions could be investigated independently from GSH biosynthesis. After withdrawal of glutathione or NAC, mock-transfected  $\gamma$ -GCS knockout cells rapidly died, coinciding with a dramatic increase of soluble ROS. This is in line with findings by Shi et al., showing that  $\gamma$ -GCS knockout cells only grow in medium, supplemented with thiol-containing compounds, such as

NAC or GSH (Shi et al., 2000). In contrast xCT-overexpressing  $\gamma$ -GCS-deficient cells survived and proliferated independently of GSH and NAC, demonstrating that GSH can be replaced at least *in vitro*. This finding adds an important contribution to the work of Ana Banjac, showing that an increased (Cys)<sub>2</sub> uptake capacity by xCT overexpression rendered HH514 Burkitt's lymphoma cells resistant to BSO-induced cell death (Banjac Ana, PhD thesis, 2005). In her work, the GSH levels of BSO-treated HH514 cells were reduced by 80-90 %. Thus, it could not be ruled out that remaining amounts of GSH still played an important role for cell survival, which can now be excluded by the findings presented herein. Reduced availability of Cys has long been regarded to cause the lack of GSH biosynthesis, which eventually becomes limiting for cell survival (Hanigan, 1995). Our work, however, suggests that GSH may not be of exceptional importance for cell survival but can be substituted by other thiol-containing compounds, at least in this cellular system.

Since xCT overexpression caused a dramatic increase of extracellular Cys levels, a putative feeder effect of xCT-overexpressing to mock-transfected cells was explored by coculture experiments. Indeed, xCT-overexpressing cells efficiently protected mock-transfected control cells from cell death. This finding demonstrates that xCT-overexpressing cells secrete sufficient Cys to maintain cell survival of mock-transfected control cells, which can carry Cys via the amino acid transport system ASC. This mechanism resembles a previously described feeder effect of irradiated fibroblasts, which provide reduced Cys to Burkitt's lymphoma cells (Falk et al., 1993). *In vitro* cultivated B cells and Burkitt's lymphoma cells are highly sensitive to suboptimal growth conditions and readily undergo apoptosis when seeded at low cell density. Previous work showed that B cells comprise a very limited (Cys)<sub>2</sub> uptake capacity, causing low levels of intracellular Cys and reduced GSH biosynthesis (Falk et al., 1998; Ishii et al., 1981). Small GSH levels, however, render B cells particularly sensitive to apoptotic stimuli, such as oxidative stress.

How and to what extent intracellular and extracellular Cys contribute to the protection of GSH-deficient cells is still unknown and requires further investigation. Still, it is rather conceivable that high Cys levels directly protect cells from oxidative stress by representing a pool of reduced substrates for the scavenging of ROS. Sato et al. showed that in the brain, system x<sub>c</sub><sup>-</sup> is predominantly expressed in regions facing the

cerebrospinal fluid, implying that relatively high levels of ROS in the brain are counteracted by the supply of reduced Cys (Sato et al., 2002). Yet, beyond its essential role for protein synthesis, Cys comprises a wide range of known functions in the cell, such as mixed disulfide formation, metal binding, hydrolysis, electron donation and redox-catalysis (Giles et al., 2003). Most importantly, the redox state of Cys/(Cys)<sub>2</sub> inside the cell significantly contributes to the maintenance of the cellular redox balance, influencing other redox couples, such as GSSG/GSH, the Trx system, protein disulfide isomerases, and glutaredoxins. Jonas et al. showed that the redox state of Cys/(Cys)<sub>2</sub> strongly affects proliferation rates as well as the response to growth factors in a colon carcinoma cell line (Jonas et al., 2002). In general, changes in the cellular redox state are now believed to be a common regulator of cell signalling pathways, influencing cell survival, proliferation, and death decisions. Since the present cellular system is devoid of GSH, it may prove useful for future studies, aiming at the investigation of Cys-mediated redox regulations as well as the impact of the Cys/(Cys)<sub>2</sub> redox state on diverse cellular processes. In this respect, the maturation of iron-sulfur proteins may turn out to be of major importance. Sipos et al. reported that the maturation of cytosolic iron-sulfur proteins requires GSH (Sipos et al., 2002). They propose a model, in which iron-sulfur clusters are assembled in mitochondria, followed by a GSH-dependent export mechanism into the cytosol (Lill et al., 2006). Recently, the iron-sulfur protein Rli1p was shown to be essential for ribosome biogenesis, whereas the loss of the iron-sulfur cluster in Rli1p caused the loss of cell viability (Kispal et al., 2005). Since at least one cytosolic iron-sulfur protein proved to be indispensable for cell survival, it must be concluded from this work that Cys mediates the maturation of cytosolic iron-sulfur cluster proteins, at least when GSH levels are low or even absent.

As described above, PHGPx was shown to be absolutely necessary for cell survival and proliferation (chapter 4.2). Hence, it must be concluded that PHGPx is still functional in  $\gamma$ -GCS knockout cells, despite the lack of its major substrate GSH. This finding strongly suggests that PHGPx also uses Cys as alternative reducing equivalent, at least under conditions of low GSH availability. That PHGPx accepts other reducing equivalents besides GSH is conceivable, since PHGPx was described as the least substrate specific GPxs for its reducing as well its oxidising substrate. GPx1-3 contain two arginine residues that guide GSH to the catalytic centre, whereas



PHGPx comprises two lysines substitutions, considered to be less specific for GSH (Mauri et al., 2003; Roveri et al., 2001; Ursini et al., 1999; Ursini et al., 1997). PHGPx has been reported to exhibit low specificity towards both the oxidizing and reducing substrate, indeed accepting complex hydroperoxides, such as phospholipid and cholesterol hydroperoxide. Moreover, PHGPx is reduced faster by synthetic dithiols, such as dithiothreitol (DTT) and dithioerythreitol (DTE), than by GSH (Roveri et al., 1994; Thomas et al., 1990). Nevertheless, the finding that  $\alpha$ -tocopherol did not rescue  $\gamma$ -GCS deficient cells but fully protected PHGPx knockout cells, indicates that the effects provoked by GSH depletion are not in total reflected by impaired PHGPx activity. Hence, it must be concluded that further GSH-dependent systems exist that are essential for maintaining cell survival and proliferation.

Interestingly  $\gamma$ -GCS-deficient mice fail to develop beyond embryonic day 7.5 (Shi et al., 2000). This severe phenotype strongly resembles the phenotype of PHGPx deficient mice, both causing early embryonic lethality at E7.5 in mice (Imai et al., 2003; Imai and Nakagawa, 2003; Yant et al., 2003). These findings imply that early embryonic lethality of  $\gamma$ -GCS-deficient mice reflects to a major extent the impairment of PHGPx enzyme activity, lacking its substrate GSH. This hypothesis seems reasonable, since PHGPx is the only reported GSH-dependent enzyme that proved to be essential for this early embryonic stage, unlike other GPx family members (Ho et al., 1997), glutathione-S-transferases (Hayes et al., 2005), or GGT (Lieberman et al., 1996).

Taken together, it has become evident from this work that an increased activity of the Cys/(Cys)<sub>2</sub>-cycle, driven by antiporter system  $x_c^-$ , renders cells independent from GSH biosynthesis. The antiporter system  $x_c^-$  mediates a strong increase of cellular Cys levels, mainly in the extracellular space, efficiently protecting cells from oxidative stress. So far, the Cys/(Cys)<sub>2</sub>-cycle was mainly regarded as a supplier of Cys for the biosynthesis of GSH and proteins. This work provides for the first time genetic proof for the concept that the Cys/(Cys)<sub>2</sub>-cycle involves an additional redox couple of major importance (Jonas et al., 2002; Jones et al., 2004). In conclusion, the maintenance of the cellular redox balance, rather than the GSH level itself, seems to be of major importance for cell survival. The physiological significance of the Cys/(Cys)<sub>2</sub>-cycle

under normal and pathophysiological conditions will be addressed by using mice lacking the xCT gene (Sato et al., 2005).

Oxidative stress and concomitant GSH depletion has been implicated in various degenerative disorders, yet the impact of the Cys/(Cys)<sub>2</sub>-cycle has been so far neglected. Concluding from this work, the Cys/(Cys)<sub>2</sub>-cycle should be viewed as an individual redox-metabolism of major importance, which may be capable to compensate GSH-deficiency under pathophysiological conditions, such as atherosclerosis, Parkinson's disease, myocardial infarction, and stroke. Altogether, the present work depicts a comprehensive picture of the molecular mechanisms occurring under conditions of oxidative stress, mainly caused by GSH depletion and the associated inhibition of essential antioxidant enzymes, such as PHGPx.

## 6 References

- Anderson, M. E., and Meister, A. (1983). Transport and direct utilization of gamma-glutamylcyst(e)ine for glutathione synthesis. *Proc Natl Acad Sci U S A* 80, 707-11.
- Arai, M., Imai, H., Koumura, T., Yoshida, M., Emoto, K., Umeda, M., Chiba, N., and Nakagawa, Y. (1999). Mitochondrial phospholipid hydroperoxide glutathione peroxidase plays a major role in preventing oxidative injury to cells. *J Biol Chem* 274, 4924-33.
- Arner, E. S., and Holmgren, A. (2000). Physiological functions of thioredoxin and thioredoxin reductase. *Eur J Biochem* 267, 6102-9.
- Arnoult, D., Parone, P., Martinou, J. C., Antonsson, B., Estaquier, J., and Ameisen, J. C. (2002). Mitochondrial release of apoptosis-inducing factor occurs downstream of cytochrome c release in response to several proapoptotic stimuli. *J Cell Biol* 159, 923-9.
- Avissar, N., Ornt, D. B., Yagil, Y., Horowitz, S., Watkins, R. H., Kerl, E. A., Takahashi, K., Palmer, I. S., and Cohen, H. J. (1994). Human kidney proximal tubules are the main source of plasma glutathione peroxidase. *Am J Physiol* 266, C367-75.
- Bae, Y. S., Kang, S. W., Seo, M. S., Baines, I. C., Tekle, E., Chock, P. B., and Rhee, S. G. (1997). Epidermal growth factor (EGF)-induced generation of hydrogen peroxide. Role in EGF receptor-mediated tyrosine phosphorylation. *J Biol Chem* 272, 217-21.
- Banjac, A. (2005). Cystine-Import and Regulation of Apoptosis in B-Lymphocytes. PhD thesis, Ludwig-Maximilian-University, Munich, Germany.
- Bannai, S. (1986). Exchange of cystine and glutamate across plasma membrane of human fibroblasts. *J Biol Chem* 261, 2256-63.
- Bannai, S., Sato, H., Ishii, T., and Sugita, Y. (1989). Induction of cystine transport activity in human fibroblasts by oxygen. *J Biol Chem* 264, 18480-4.
- Bannai, S., and Tateishi, N. (1986). Role of membrane transport in metabolism and function of glutathione in mammals. *J Membr Biol* 89, 1-8.
- Banning, A., Schnurr, K., Bol, G. F., Kupper, D., Muller-Schmehl, K., Viita, H., Yla-Herttuala, S., and Brigelius-Flohe, R. (2004). Inhibition of basal and interleukin-1-induced VCAM-1 expression by phospholipid hydroperoxide glutathione peroxidase and 15-lipoxygenase in rabbit aortic smooth muscle cells. *Free Radic Biol Med* 36, 135-44.
- Beck, M. A., Esworthy, R. S., Ho, Y. S., and Chu, F. F. (1998). Glutathione peroxidase protects mice from viral-induced myocarditis. *Faseb J* 12, 1143-9.
- Beck, M. A., Shi, Q., Morris, V. C., and Levander, O. A. (1995). Rapid genomic evolution of a non-virulent coxsackievirus B3 in selenium-deficient mice results in selection of identical virulent isolates. *Nat Med* 1, 433-6.
- Behne, D., Kyriakopoulos, A., Weiss-Nowak, C., Kalckloesch, M., Westphal, C., and Gessner, H. (1996a). Newly found selenium-containing proteins in the tissues of the rat. *Biol Trace Elem Res* 55, 99-110.
- Behne, D., Weiler, H., and Kyriakopoulos, A. (1996b). Effects of selenium deficiency on testicular morphology and function in rats. *J Reprod Fertil* 106, 291-7.
- Bermano, G., Nicol, F., Dyer, J. A., Sunde, R. A., Beckett, G. J., Arthur, J. R., and Hesketh, J. E. (1995). Tissue-specific regulation of selenoenzyme gene expression during selenium deficiency in rats. *Biochem J* 311 ( Pt 2), 425-30.
- Bernardi, P., Scorrano, L., Colonna, R., Petronilli, V., and Di Lisa, F. (1999). Mitochondria and cell death. Mechanistic aspects and methodological issues. *Eur J Biochem* 264, 687-701.

- Bier, E. (2006). Antioxidants put Parkinson flies back in the PINK. *Proc Natl Acad Sci U S A* 103, 13269-70.
- Bjelakovic, G., Nikolova, D., Glud, L. L., Simonetti, R. G., and Glud, C. (2007). Mortality in randomized trials of antioxidant supplements for primary and secondary prevention: systematic review and meta-analysis. *JAMA* 297, 842-57.
- Bjornstedt, M., Xue, J., Huang, W., Akesson, B., and Holmgren, A. (1994). The thioredoxin and glutaredoxin systems are efficient electron donors to human plasma glutathione peroxidase. *J Biol Chem* 269, 29382-4.
- Bosl, M. R., Takaku, K., Oshima, M., Nishimura, S., and Taketo, M. M. (1997). Early embryonic lethality caused by targeted disruption of the mouse selenocysteine tRNA gene (Trsp). *Proc Natl Acad Sci U S A* 94, 5531-4.
- Bourre, J., Dumont, O., Clement, M., Dinh, L., Droy-Lefaix, M., and Christen, Y. (2000). Vitamin E deficiency has different effects on brain and liver phospholipid hydroperoxide glutathione peroxidase activities in the rat. *Neurosci Lett* 286, 87-90.
- Brielmeier, M., Bechet, J. M., Suppmann, S., Conrad, M., Laux, G., and Bornkamm, G. W. (2001). Cloning of phospholipid hydroperoxide glutathione peroxidase (PHGPx) as an anti-apoptotic and growth promoting gene of Burkitt lymphoma cells. *Biofactors* 14, 179-90.
- Brigelius-Flohe, R. (1999). Tissue-specific functions of individual glutathione peroxidases. *Free Radic Biol Med* 27, 951-65.
- Brigelius-Flohe, R., Friedrichs, B., Maurer, S., Schultz, M., and Streicher, R. (1997). Interleukin-1-induced nuclear factor kappa B activation is inhibited by overexpression of phospholipid hydroperoxide glutathione peroxidase in a human endothelial cell line. *Biochem J* 328 ( Pt 1), 199-203.
- Buettner, C., Harney, J. W., and Larsen, P. R. (1998). The 3'-untranslated region of human type 2 iodothyronine deiodinase mRNA contains a functional selenocysteine insertion sequence element. *J Biol Chem* 273, 33374-8.
- Butenko, I. G., Gladchenko, S. V., and Galushko, S. V. (1993). Anti-inflammatory properties and inhibition of leukotriene C4 biosynthesis in vitro by flavonoid baicalein from *Scutellaria baicalensis* Georgy roots. *Agents Actions* 39 Spec No, C49-51.
- Buttke, T. M., and Sandstrom, P. A. (1994). Oxidative stress as a mediator of apoptosis. *Immunol Today* 15, 7-10.
- Cao, G., Clark, R. S., Pei, W., Yin, W., Zhang, F., Sun, F. Y., Graham, S. H., and Chen, J. (2003). Translocation of apoptosis-inducing factor in vulnerable neurons after transient cerebral ischemia and in neuronal cultures after oxygen-glucose deprivation. *J Cereb Blood Flow Metab* 23, 1137-50.
- Chambers, I., Frampton, J., Goldfarb, P., Affara, N., McBain, W., and Harrison, P. R. (1986). The structure of the mouse glutathione peroxidase gene: the selenocysteine in the active site is encoded by the 'termination' codon, TGA. *Embo J* 5, 1221-7.
- Chavatte, L., Brown, B. A., and Driscoll, D. M. (2005). Ribosomal protein L30 is a component of the UGA-selenocysteine recoding machinery in eukaryotes. *Nat Struct Mol Biol* 12, 408-16.
- Chen, C. J., Huang, H. S., and Chang, W. C. (2002). Inhibition of arachidonate metabolism in human epidermoid carcinoma a431 cells overexpressing phospholipid hydroperoxide glutathione peroxidase. *J Biomed Sci* 9, 453-9.
- Chen, C. J., Huang, H. S., and Chang, W. C. (2003). Depletion of phospholipid hydroperoxide glutathione peroxidase up-regulates arachidonate metabolism by

- 12S-lipoxygenase and cyclooxygenase 1 in human epidermoid carcinoma A431 cells. *Faseb J* 17, 1694-6.
- Cheng, W. H., Ho, Y. S., Ross, D. A., Valentine, B. A., Combs, G. F., and Lei, X. G. (1997). Cellular glutathione peroxidase knockout mice express normal levels of selenium-dependent plasma and phospholipid hydroperoxide glutathione peroxidases in various tissues. *J Nutr* 127, 1445-50.
- Cheng, W. H., Ho, Y. S., Valentine, B. A., Ross, D. A., Combs, G. F., Jr., and Lei, X. G. (1998). Cellular glutathione peroxidase is the mediator of body selenium to protect against paraquat lethality in transgenic mice. *J Nutr* 128, 1070-6.
- Chiarugi, P., and Buricchi, F. (2007). Protein tyrosine phosphorylation and reversible oxidation: two cross-talking posttranslation modifications. *Antioxid Redox Signal* 9, 1-24.
- Choi, D. W. (1990). Methods for antagonizing glutamate neurotoxicity. *Cerebrovasc Brain Metab Rev* 2, 105-47.
- Chu, F. F., Esworthy, R. S., Ho, Y. S., Bermeister, M., Swiderek, K., and Elliott, R. W. (1997). Expression and chromosomal mapping of mouse Gpx2 gene encoding the gastrointestinal form of glutathione peroxidase, GPX-GI. *Biomed Environ Sci* 10, 156-62.
- Conrad, M. (2001). Etablierung von Mausstämmen defizient für die Selenoproteine mitochondriale Thioredoxin-Reduktase und Phospholipid-Hydroperoxid-Glutathion-Peroxidase (PHGPx) und Charakterisierung einer Spermienkern-spezifischen Form der PHGPx. PhD thesis, Ludwig-Maximilian-University, Munich, Germany.
- Conrad, M., Jakupoglu, C., Moreno, S. G., Lippl, S., Banjac, A., Schneider, M., Beck, H., Hatzopoulos, A. K., Just, U., Sinowatz, F., Schmahl, W., Chien, K. R., Wurst, W., Bornkamm, G. W., and Brielmeier, M. (2004). Essential role for mitochondrial thioredoxin reductase in hematopoiesis, heart development, and heart function. *Mol Cell Biol* 24, 9414-23.
- Conrad, M., Moreno, S. G., Sinowatz, F., Ursini, F., Kollé, S., Roveri, A., Brielmeier, M., Wurst, W., Maiorino, M., and Bornkamm, G. W. (2005). The nuclear form of phospholipid hydroperoxide glutathione peroxidase is a protein thiol peroxidase contributing to sperm chromatin stability. *Mol Cell Biol* 25, 7637-44.
- Copeland, P. R., Fletcher, J. E., Carlson, B. A., Hatfield, D. L., and Driscoll, D. M. (2000). A novel RNA binding protein, SBP2, is required for the translation of mammalian selenoprotein mRNAs. *Embo J* 19, 306-14.
- Crack, P. J., Taylor, J. M., Flentjar, N. J., de Haan, J., Hertzog, P., Iannello, R. C., and Kola, I. (2001). Increased infarct size and exacerbated apoptosis in the glutathione peroxidase-1 (Gpx-1) knockout mouse brain in response to ischemia/reperfusion injury. *J Neurochem* 78, 1389-99.
- Cyrus, T., Pratico, D., Zhao, L., Witztum, J. L., Rader, D. J., Rokach, J., FitzGerald, G. A., and Funk, C. D. (2001). Absence of 12/15-lipoxygenase expression decreases lipid peroxidation and atherogenesis in apolipoprotein e-deficient mice. *Circulation* 103, 2277-82.
- Dailey, L. A., and Imming, P. (1999). 12-Lipoxygenase: classification, possible therapeutic benefits from inhibition, and inhibitors. *Curr Med Chem* 6, 389-98.
- Daugas, E., Susin, S. A., Zamzami, N., Ferri, K. F., Irinopoulou, T., Larochette, N., Prevost, M. C., Leber, B., Andrews, D., Penninger, J., and Kroemer, G. (2000). Mitochondrio-nuclear translocation of AIF in apoptosis and necrosis. *FASEB J* 14, 729-39.

- Delaunay, A., Pflieger, D., Barrault, M. B., Vinh, J., and Toledano, M. B. (2002). A thiol peroxidase is an H<sub>2</sub>O<sub>2</sub> receptor and redox-transducer in gene activation. *Cell* 111, 471-81.
- Deschamps, J. D., Kenyon, V. A., and Holman, T. R. (2006). Baicalein is a potent in vitro inhibitor against both reticulocyte 15-human and platelet 12-human lipoxygenases. *Bioorg Med Chem* 14, 4295-301.
- Diamond, A. M., Hu, Y. J., and Mansur, D. B. (2001). Glutathione peroxidase and viral replication: implications for viral evolution and chemoprevention. *Biofactors* 14, 205-10.
- Diaz-Hernandez, J. I., Moncada, S., Bolanos, J. P., and Almeida, A. (2007). Poly(ADP-ribose) polymerase-1 protects neurons against apoptosis induced by oxidative stress. *Cell Death Differ* 14, 1211-21.
- Dypbukt, J. M., Ankarcona, M., Burkitt, M., Sjöholm, A., Strom, K., Orrenius, S., and Nicotera, P. (1994). Different prooxidant levels stimulate growth, trigger apoptosis, or produce necrosis of insulin-secreting RINm5F cells. The role of intracellular polyamines. *J Biol Chem* 269, 30553-60.
- Esworthy, R. S., Mann, J. R., Sam, M., and Chu, F. F. (2000). Low glutathione peroxidase activity in Gpx1 knockout mice protects jejunum crypts from gamma-irradiation damage. *Am J Physiol Gastrointest Liver Physiol* 279, G426-36.
- Fagegaltier, D., Hubert, N., Yamada, K., Mizutani, T., Carbon, P., and Krol, A. (2000). Characterization of mSelB, a novel mammalian elongation factor for selenoprotein translation. *Embo J* 19, 4796-805.
- Falk, M. H., Hultner, L., Milner, A., Gregory, C. D., and Bornkamm, G. W. (1993). Irradiated fibroblasts protect Burkitt lymphoma cells from apoptosis by a mechanism independent of bcl-2. *Int J Cancer* 55, 485-91.
- Falk, M. H., Meier, T., Issels, R. D., Brielmeier, M., Scheffer, B., and Bornkamm, G. W. (1998). Apoptosis in Burkitt lymphoma cells is prevented by promotion of cysteine uptake. *Int J Cancer* 75, 620-5.
- Fanidi, A., Harrington, E. A., and Evan, G. I. (1992). Cooperative interaction between c-myc and bcl-2 proto-oncogenes. *Nature* 359, 554-6.
- Fernandes, A. P., and Holmgren, A. (2004). Glutaredoxins: glutathione-dependent redox enzymes with functions far beyond a simple thioredoxin backup system. *Antioxid Redox Signal* 6, 63-74.
- Finkel, T., and Holbrook, N. J. (2000). Oxidants, oxidative stress and the biology of ageing. *Nature* 408, 239-47.
- Fletcher, J. E., Copeland, P. R., Driscoll, D. M., and Krol, A. (2001). The selenocysteine incorporation machinery: interactions between the SECIS RNA and the SECIS-binding protein SBP2. *Rna* 7, 1442-53.
- Flohe, L., Gunzler, W. A., and Schock, H. H. (1973). Glutathione peroxidase: a selenoenzyme. *FEBS Lett* 32, 132-4.
- Forchhammer, K., Leinfelder, W., and Bock, A. (1989). Identification of a novel translation factor necessary for the incorporation of selenocysteine into protein. *Nature* 342, 453-6.
- Fu, Y., Cheng, W. H., Porres, J. M., Ross, D. A., and Lei, X. G. (1999). Knockout of cellular glutathione peroxidase gene renders mice susceptible to diquat-induced oxidative stress. *Free Radic Biol Med* 27, 605-11.
- Fujieda, M., Naruse, K., Hamazu, T., Miyazaki, E., Hayashi, Y., Enomoto, R., Lee, E., Ohta, K., Yamaguchi, Y., Wakiguchi, H., and Enza, H. (2007). Effect of selenium-deficient diet on tubular epithelium in normal rats. *Pediatr Nephrol* 22, 192-201.
- Funk, C. D. (2001). Prostaglandins and leukotrienes: advances in eicosanoid biology. *Science* 294, 1871-5.

- Funk, C. D., and Cyrus, T. (2001). 12/15-lipoxygenase, oxidative modification of LDL and atherogenesis. *Trends Cardiovasc Med* 11, 116-24.
- Giles, N. M., Giles, G. I., and Jacob, C. (2003). Multiple roles of cysteine in biocatalysis. *Biochem Biophys Res Commun* 300, 1-4.
- Gillmor, S. A., Villasenor, A., Fletterick, R., Sigal, E., and Browner, M. F. (1997). The structure of mammalian 15-lipoxygenase reveals similarity to the lipases and the determinants of substrate specificity. *Nat Struct Biol* 4, 1003-9.
- Glass, R. S., Singh, W. P., Jung, W., Veres, Z., Scholz, T. D., and Stadtman, T. C. (1993). Monoselenophosphate: synthesis, characterization, and identity with the prokaryotic biological selenium donor, compound SePX. *Biochemistry* 32, 12555-9.
- Griffith, O. W., Bridges, R. J., and Meister, A. (1981). Formation of gamma-glutamylcyst(e)ine in vivo is catalyzed by gamma-glutamyl transpeptidase. *Proc Natl Acad Sci U S A* 78, 2777-81.
- Grundman, M. (2000). Vitamin E and Alzheimer disease: the basis for additional clinical trials. *Am J Clin Nutr* 71, 630S-636S.
- Guimaraes, M. J., Peterson, D., Vicari, A., Cocks, B. G., Copeland, N. G., Gilbert, D. J., Jenkins, N. A., Ferrick, D. A., Kastelein, R. A., Bazan, J. F., and Zlotnik, A. (1996). Identification of a novel selD homolog from eukaryotes, bacteria, and archaea: is there an autoregulatory mechanism in selenocysteine metabolism? *Proc Natl Acad Sci U S A* 93, 15086-91.
- Hampton, M. B., and Orrenius, S. (1998). Redox regulation of apoptotic cell death. *Biofactors* 8, 1-5.
- Hanigan, M. H. (1995). Expression of gamma-glutamyl transpeptidase provides tumor cells with a selective growth advantage at physiologic concentrations of cyst(e)ine. *Carcinogenesis* 16, 181-5.
- Hayes, J. D., Flanagan, J. U., and Jowsey, I. R. (2005). Glutathione transferases. *Annu Rev Pharmacol Toxicol* 45, 51-88.
- Hayes, J. D., and Pulford, D. J. (1995). The glutathione S-transferase supergene family: regulation of GST and the contribution of the isoenzymes to cancer chemoprotection and drug resistance. *Crit Rev Biochem Mol Biol* 30, 445-600.
- Heirman, I., Ginneberge, D., Brigelius-Flohe, R., Hendrickx, N., Agostinis, P., Brouckaert, P., Rottiers, P., and Grooten, J. (2006). Blocking tumor cell eicosanoid synthesis by GP x 4 impedes tumor growth and malignancy. *Free Radic Biol Med* 40, 285-94.
- Hill, K. E., Lloyd, R. S., Yang, J. G., Read, R., and Burk, R. F. (1991). The cDNA for rat selenoprotein P contains 10 TGA codons in the open reading frame. *J Biol Chem* 266, 10050-3.
- Hill, K. E., Zhou, J., McMahan, W. J., Motley, A. K., Atkins, J. F., Gesteland, R. F., and Burk, R. F. (2003). Deletion of selenoprotein P alters distribution of selenium in the mouse. *J Biol Chem* 278, 13640-6.
- Ho, Y. S., Magnenat, J. L., Bronson, R. T., Cao, J., Gargano, M., Sugawara, M., and Funk, C. D. (1997). Mice deficient in cellular glutathione peroxidase develop normally and show no increased sensitivity to hyperoxia. *J Biol Chem* 272, 16644-51.
- Hockenbery, D. M., Oltvai, Z. N., Yin, X. M., Millman, C. L., and Korsmeyer, S. J. (1993). Bcl-2 functions in an antioxidant pathway to prevent apoptosis. *Cell* 75, 241-51.
- Holmgren, A. (1979a). Glutathione-dependent synthesis of deoxyribonucleotides. Characterization of the enzymatic mechanism of Escherichia coli glutaredoxin. *J Biol Chem* 254, 3672-8.

- Holmgren, A. (1979b). Glutathione-dependent synthesis of deoxyribonucleotides. Purification and characterization of glutaredoxin from *Escherichia coli*. *J Biol Chem* 254, 3664-71.
- Huang, H. S., Chen, C. J., Suzuki, H., Yamamoto, S., and Chang, W. C. (1999). Inhibitory effect of phospholipid hydroperoxide glutathione peroxidase on the activity of lipoxygenases and cyclooxygenases. *Prostaglandins Other Lipid Mediat* 58, 65-75.
- Imai, H., Hirao, F., Sakamoto, T., Sekine, K., Mizukura, Y., Saito, M., Kitamoto, T., Hayasaka, M., Hanaoka, K., and Nakagawa, Y. (2003). Early embryonic lethality caused by targeted disruption of the mouse PHGPx gene. *Biochem Biophys Res Commun* 305, 278-86.
- Imai, H., and Nakagawa, Y. (2003). Biological significance of phospholipid hydroperoxide glutathione peroxidase (PHGPx, GPx4) in mammalian cells. *Free Radic Biol Med* 34, 145-69.
- Imai, H., Narashima, K., Arai, M., Sakamoto, H., Chiba, N., and Nakagawa, Y. (1998). Suppression of leukotriene formation in RBL-2H3 cells that overexpressed phospholipid hydroperoxide glutathione peroxidase. *J Biol Chem* 273, 1990-7.
- Imai, H., Sumi, D., Sakamoto, H., Hanamoto, A., Arai, M., Chiba, N., and Nakagawa, Y. (1996). Overexpression of phospholipid hydroperoxide glutathione peroxidase suppressed cell death due to oxidative damage in rat basophile leukemia cells (RBL-2H3). *Biochem Biophys Res Commun* 222, 432-8.
- Ishii, T., Hishinuma, I., Bannai, S., and Sugita, Y. (1981). Mechanism of growth promotion of mouse lymphoma L1210 cells in vitro by feeder layer or 2-mercaptoethanol. *J Cell Physiol* 107, 283-93.
- Ivanov, I., Saam, J., Kuhn, H., and Holzhutter, H. G. (2005). Dual role of oxygen during lipoxygenase reactions. *Febs J* 272, 2523-35.
- Jakobsson, P. J., Steinhilber, D., Odlander, B., Radmark, O., Claesson, H. E., and Samuelsson, B. (1992). On the expression and regulation of 5-lipoxygenase in human lymphocytes. *Proc Natl Acad Sci U S A* 89, 3521-5.
- Jakupoglu, C., Przemeczek, G. K., Schneider, M., Moreno, S. G., Mayr, N., Hatzopoulos, A. K., de Angelis, M. H., Wurst, W., Bornkamm, G. W., Brielmeier, M., and Conrad, M. (2005). Cytoplasmic thioredoxin reductase is essential for embryogenesis but dispensable for cardiac development. *Mol Cell Biol* 25, 1980-8.
- Jonas, C. R., Ziegler, T. R., Gu, L. H., and Jones, D. P. (2002). Extracellular thiol/disulfide redox state affects proliferation rate in a human colon carcinoma (Caco2) cell line. *Free Radic Biol Med* 33, 1499-506.
- Jones, D. P., Go, Y. M., Anderson, C. L., Ziegler, T. R., Kinkade, J. M., Jr., and Kirilin, W. G. (2004). Cysteine/cystine couple is a newly recognized node in the circuitry for biologic redox signaling and control. *FASEB J* 18, 1246-8.
- Kagan, V. E., Tyurin, V. A., Jiang, J., Tyurina, Y. Y., Ritov, V. B., Amoscato, A. A., Osipov, A. N., Belikova, N. A., Kapralov, A. A., Kini, V., Vlasova, II, Zhao, Q., Zou, M., Di, P., Svistunenko, D. A., Kurnikov, I. V., and Borisenko, G. G. (2005). Cytochrome c acts as a cardiolipin oxygenase required for release of proapoptotic factors. *Nat Chem Biol* 1, 223-32.
- Kamata, H., Honda, S., Maeda, S., Chang, L., Hirata, H., and Karin, M. (2005). Reactive oxygen species promote TNFalpha-induced death and sustained JNK activation by inhibiting MAP kinase phosphatases. *Cell* 120, 649-61.
- Kane, D. J., Sarafian, T. A., Anton, R., Hahn, H., Gralla, E. B., Valentine, J. S., Ord, T., and Bredesen, D. E. (1993). Bcl-2 inhibition of neural death: decreased generation of reactive oxygen species. *Science* 262, 1274-7.



- Karp, D. R., Shimooku, K., and Lipsky, P. E. (2001). Expression of gamma-glutamyl transpeptidase protects Ramos B cells from oxidation-induced cell death. *J Biol Chem* 276, 3798-804.
- Khanna, S., Roy, S., Ryu, H., Bahadduri, P., Swaan, P. W., Ratan, R. R., and Sen, C. K. (2003). Molecular basis of vitamin E action: tocotrienol modulates 12-lipoxygenase, a key mediator of glutamate-induced neurodegeneration. *J Biol Chem* 278, 43508-15.
- Kispal, G., Sipos, K., Lange, H., Fekete, Z., Bedekovics, T., Janaky, T., Bassler, J., Aguilar Netz, D. J., Balk, J., Rotte, C., and Lill, R. (2005). Biogenesis of cytosolic ribosomes requires the essential iron-sulphur protein Rli1p and mitochondria. *EMBO J* 24, 589-98.
- Klein, J. A., and Ackerman, S. L. (2003). Oxidative stress, cell cycle, and neurodegeneration. *J Clin Invest* 111, 785-93.
- Kohrle, J. (2000). The deiodinase family: selenoenzymes regulating thyroid hormone availability and action. *Cell Mol Life Sci* 57, 1853-63.
- Konishi, H., Tanaka, M., Takemura, Y., Matsuzaki, H., Ono, Y., Kikkawa, U., and Nishizuka, Y. (1997). Activation of protein kinase C by tyrosine phosphorylation in response to H<sub>2</sub>O<sub>2</sub>. *Proc Natl Acad Sci U S A* 94, 11233-7.
- Kretz-Remy, C., Mehlen, P., Mirault, M. E., and Arrigo, A. P. (1996). Inhibition of I kappa B-alpha phosphorylation and degradation and subsequent NF-kappa B activation by glutathione peroxidase overexpression. *J Cell Biol* 133, 1083-93.
- Krieger-Brauer, H. I., and Kather, H. (1995). Antagonistic effects of different members of the fibroblast and platelet-derived growth factor families on adipose conversion and NADPH-dependent H<sub>2</sub>O<sub>2</sub> generation in 3T3 L1-cells. *Biochem J* 307 ( Pt 2), 549-56.
- Kryukov, G. V., Castellano, S., Novoselov, S. V., Lobanov, A. V., Zehtab, O., Guigo, R., and Gladyshev, V. N. (2003). Characterization of mammalian selenoproteomes. *Science* 300, 1439-43.
- Kryukov, G. V., Kumar, R. A., Koc, A., Sun, Z., and Gladyshev, V. N. (2002). Selenoprotein R is a zinc-containing stereo-specific methionine sulfoxide reductase. *Proc Natl Acad Sci U S A* 99, 4245-50.
- Lambeth, J. D. (2004). NOX enzymes and the biology of reactive oxygen. *Nat Rev Immunol* 4, 181-9.
- Lee, S. R., Bar-Noy, S., Kwon, J., Levine, R. L., Stadtman, T. C., and Rhee, S. G. (2000). Mammalian thioredoxin reductase: oxidation of the C-terminal cysteine/selenocysteine active site forms a thioselenide, and replacement of selenium with sulfur markedly reduces catalytic activity. *Proc Natl Acad Sci U S A* 97, 2521-6.
- Lee, S. R., Kwon, K. S., Kim, S. R., and Rhee, S. G. (1998). Reversible inactivation of protein-tyrosine phosphatase 1B in A431 cells stimulated with epidermal growth factor. *J Biol Chem* 273, 15366-72.
- Lee, Y., and Shacter, E. (1997). Bcl-2 does not protect Burkitt's lymphoma cells from oxidant-induced cell death. *Blood* 89, 4480-92.
- Lei, X. G., Evenson, J. K., Thompson, K. M., and Sunde, R. A. (1995). Glutathione peroxidase and phospholipid hydroperoxide glutathione peroxidase are differentially regulated in rats by dietary selenium. *J Nutr* 125, 1438-46.
- Lei, X. G., Ross, D. A., Parks, J. E., and Combs, G. F., Jr. (1997). Effects of dietary selenium and vitamin E concentrations on phospholipid hydroperoxide glutathione peroxidase expression in reproductive tissues of pubertal maturing male rats. *Biol Trace Elem Res* 59, 195-206.

- Li, Y., Maher, P., and Schubert, D. (1997). A role for 12-lipoxygenase in nerve cell death caused by glutathione depletion. *Neuron* 19, 453-63.
- Lieberman, M. W., Barrios, R., Carter, B. Z., Habib, G. M., Lebovitz, R. M., Rajagopalan, S., Sepulveda, A. R., Shi, Z. Z., and Wan, D. F. (1995). gamma-Glutamyl transpeptidase. What does the organization and expression of a multipromoter gene tell us about its functions? *Am J Pathol* 147, 1175-85.
- Lieberman, M. W., Wiseman, A. L., Shi, Z. Z., Carter, B. Z., Barrios, R., Ou, C. N., Chevez-Barrios, P., Wang, Y., Habib, G. M., Goodman, J. C., Huang, S. L., Lebovitz, R. M., and Matzuk, M. M. (1996). Growth retardation and cysteine deficiency in gamma-glutamyl transpeptidase-deficient mice. *Proc Natl Acad Sci U S A* 93, 7923-6.
- Lill, R., Dutkiewicz, R., Elsasser, H. P., Hausmann, A., Netz, D. J., Pierik, A. J., Stehling, O., Urzica, E., and Muhlenhoff, U. (2006). Mechanisms of iron-sulfur protein maturation in mitochondria, cytosol and nucleus of eukaryotes. *Biochim Biophys Acta* 1763, 652-67.
- Lipton, S. A., and Bossy-Wetzel, E. (2002). Dueling activities of AIF in cell death versus survival: DNA binding and redox activity. *Cell* 111, 147-50.
- Lo, Y. Y., Wong, J. M., and Cruz, T. F. (1996). Reactive oxygen species mediate cytokine activation of c-Jun NH2-terminal kinases. *J Biol Chem* 271, 15703-7.
- Loeffler, M., and Kroemer, G. (2000). The mitochondrion in cell death control: certainties and incognita. *Exp Cell Res* 256, 19-26.
- Low, S. C., Grundner-Culemann, E., Harney, J. W., and Berry, M. J. (2000). SECIS-SBP2 interactions dictate selenocysteine incorporation efficiency and selenoprotein hierarchy. *Embo J* 19, 6882-90.
- Lui, J. C., and Kong, S. K. (2007). Heat shock protein 70 inhibits the nuclear import of apoptosis-inducing factor to avoid DNA fragmentation in TF-1 cells during erythropoiesis. *FEBS Lett* 581, 109-17.
- Maiorino, M., Aumann, K. D., Brigelius-Flohe, R., Doria, D., van den Heuvel, J., McCarthy, J., Roveri, A., Ursini, F., and Flohe, L. (1995). Probing the presumed catalytic triad of selenium-containing peroxidases by mutational analysis of phospholipid hydroperoxide glutathione peroxidase (PHGPx). *Biol Chem Hoppe Seyler* 376, 651-60.
- Maiorino, M., Coassin, M., Roveri, A., and Ursini, F. (1989). Microsomal lipid peroxidation: effect of vitamin E and its functional interaction with phospholipid hydroperoxide glutathione peroxidase. *Lipids* 24, 721-6.
- Maiorino, M., Roveri, A., Benazzi, L., Bosello, V., Mauri, P., Toppo, S., Tosatto, S. C., and Ursini, F. (2005). Functional interaction of phospholipid hydroperoxide glutathione peroxidase with sperm mitochondrion-associated cysteine-rich protein discloses the adjacent cysteine motif as a new substrate of the selenoperoxidase. *J Biol Chem* 280, 38395-402.
- Mannervik, B., and Danielson, U. H. (1988). Glutathione transferases--structure and catalytic activity. *CRC Crit Rev Biochem* 23, 283-337.
- Marchetti, P., Decaudin, D., Macho, A., Zamzami, N., Hirsch, T., Susin, S. A., and Kroemer, G. (1997). Redox regulation of apoptosis: impact of thiol oxidation status on mitochondrial function. *Eur J Immunol* 27, 289-96.
- Mauri, P., Benazzi, L., Flohe, L., Maiorino, M., Pietta, P. G., Pilawa, S., Roveri, A., and Ursini, F. (2003). Versatility of selenium catalysis in PHGPx unraveled by LC/ESI-MS/MS. *Biol Chem* 384, 575-88.
- Meier, B., Radeke, H. H., Selle, S., Younes, M., Sies, H., Resch, K., and Habermehl, G. G. (1989). Human fibroblasts release reactive oxygen species in response to interleukin-1 or tumour necrosis factor-alpha. *Biochem J* 263, 539-45.

- Meng, T. C., Fukada, T., and Tonks, N. K. (2002). Reversible oxidation and inactivation of protein tyrosine phosphatases in vivo. *Mol Cell* 9, 387-99.
- Menon, S. G., and Goswami, P. C. (2007). A redox cycle within the cell cycle: ring in the old with the new. *Oncogene* 26, 1101-9.
- Meyer, M., Schreck, R., and Baeuerle, P. A. (1993). H<sub>2</sub>O<sub>2</sub> and antioxidants have opposite effects on activation of NF-kappa B and AP-1 in intact cells: AP-1 as secondary antioxidant-responsive factor. *Embo J* 12, 2005-15.
- Mills, G. C. (1957). Hemoglobin catabolism. I. Glutathione peroxidase, an erythrocyte enzyme which protects hemoglobin from oxidative breakdown. *J Biol Chem* 229, 189-97.
- Modjtahedi, N., Giordanetto, F., Madeo, F., and Kroemer, G. (2006). Apoptosis-inducing factor: vital and lethal. *Trends Cell Biol* 16, 264-72.
- Murphy, T. H., Schnaar, R. L., and Coyle, J. T. (1990). Immature cortical neurons are uniquely sensitive to glutamate toxicity by inhibition of cystine uptake. *FASEB J* 4, 1624-33.
- Nakadate, T., Yamamoto, S., Aizu, E., and Kato, R. (1985). Inhibition of mouse epidermal 12-lipoxygenase by 2,3,4-trimethyl-6-(12-hydroxy-5,10-dodecadiynyl)-1,4-benzoquinone (AA861). *J Pharm Pharmacol* 37, 71-3.
- Nomura, K., Imai, H., Koumura, T., Arai, M., and Nakagawa, Y. (1999). Mitochondrial phospholipid hydroperoxide glutathione peroxidase suppresses apoptosis mediated by a mitochondrial death pathway. *J Biol Chem* 274, 29294-302.
- Park, S. I., Park, J. M., Chittum, H. S., Yang, E. S., Carlson, B. A., Lee, B. J., and Hatfield, D. L. (1997). Selenocysteine tRNAs as central components of selenoprotein biosynthesis in eukaryotes. *Biomed Environ Sci* 10, 116-24.
- Patel, N. S., Cuzzocrea, S., Chatterjee, P. K., Di Paola, R., Sauterin, L., Britti, D., and Thiemermann, C. (2004). Reduction of renal ischemia-reperfusion injury in 5-lipoxygenase knockout mice and by the 5-lipoxygenase inhibitor zileuton. *Mol Pharmacol* 66, 220-7.
- Pfeifer, H., Conrad, M., Roethlein, D., Kyriakopoulos, A., Brielmeier, M., Bornkamm, G. W., and Behne, D. (2001). Identification of a specific sperm nuclei selenoenzyme necessary for protamine thiol cross-linking during sperm maturation. *Faseb J* 15, 1236-8.
- Pratico, D., Tangirala, R. K., Rader, D. J., Rokach, J., and FitzGerald, G. A. (1998). Vitamin E suppresses isoprostane generation in vivo and reduces atherosclerosis in ApoE-deficient mice. *Nat Med* 4, 1189-92.
- Pushpa-Rekha, T. R., Burdsall, A. L., Oleksa, L. M., Chisolm, G. M., and Driscoll, D. M. (1995). Rat phospholipid-hydroperoxide glutathione peroxidase. cDNA cloning and identification of multiple transcription and translation start sites. *J Biol Chem* 270, 26993-9.
- Rajpert-De Meyts, E., Shi, M., Chang, M., Robison, T. W., Groffen, J., Heisterkamp, N., and Forman, H. J. (1992). Transfection with gamma-glutamyl transpeptidase enhances recovery from glutathione depletion using extracellular glutathione. *Toxicol Appl Pharmacol* 114, 56-62.
- Ravagnan, L., Gurbuxani, S., Susin, S. A., Maise, C., Daugas, E., Zamzami, N., Mak, T., Jaattela, M., Penninger, J. M., Garrido, C., and Kroemer, G. (2001). Heat-shock protein 70 antagonizes apoptosis-inducing factor. *Nat Cell Biol* 3, 839-43.
- Reed, J. C. (1998). Bcl-2 family proteins. *Oncogene* 17, 3225-36.
- Rocher, C., Lalanne, J. L., and Chaudiere, J. (1992). Purification and properties of a recombinant sulfur analog of murine selenium-glutathione peroxidase. *Eur J Biochem* 205, 955-60.

- Rotruck, J. T., Pope, A. L., Ganther, H. E., Swanson, A. B., Hafeman, D. G., and Hoekstra, W. G. (1973). Selenium: biochemical role as a component of glutathione peroxidase. *Science* 179, 588-90.
- Roveri, A., Maiorino, M., Nisii, C., and Ursini, F. (1994). Purification and characterization of phospholipid hydroperoxide glutathione peroxidase from rat testis mitochondrial membranes. *Biochim Biophys Acta* 1208, 211-21.
- Roveri, A., Ursini, F., Flohe, L., and Maiorino, M. (2001). PHGPx and spermatogenesis. *Biofactors* 14, 213-22.
- Rozen, S., and Skaletsky, H. (2000). Primer3 on the WWW for general users and for biologist programmers. *Methods Mol Biol* 132, 365-86.
- Rueckschloss, U., Duerrschmidt, N., and Morawietz, H. (2003). NADPH oxidase in endothelial cells: impact on atherosclerosis. *Antioxid Redox Signal* 5, 171-80.
- Sakakura, Y., Sato, H., Shiiya, A., Tamba, M., Sagara, J., Matsuda, M., Okamura, N., Makino, N., and Bannai, S. (2007). Expression and function of cystine/glutamate transporter in neutrophils. *J Leukoc Biol* 81, 974-82.
- Sakamoto, H., Imai, H., and Nakagawa, Y. (2000). Involvement of phospholipid hydroperoxide glutathione peroxidase in the modulation of prostaglandin D2 synthesis. *J Biol Chem* 275, 40028-35.
- Sandstrom, P. A., Pardi, D., Tebbey, P. W., Dudek, R. W., Terrian, D. M., Folks, T. M., and Buttke, T. M. (1995). Lipid hydroperoxide-induced apoptosis: lack of inhibition by Bcl-2 over-expression. *FEBS Lett* 365, 66-70.
- Sandstrom, P. A., Tebbey, P. W., Van Cleave, S., and Buttke, T. M. (1994). Lipid hydroperoxides induce apoptosis in T cells displaying a HIV-associated glutathione peroxidase deficiency. *J Biol Chem* 269, 798-801.
- Sarafian, T. A., and Bredesen, D. E. (1994). Is apoptosis mediated by reactive oxygen species? *Free Radic Res* 21, 1-8.
- Sato, H., Shiiya, A., Kimata, M., Maebara, K., Tamba, M., Sakakura, Y., Makino, N., Sugiyama, F., Yagami, K., Moriguchi, T., Takahashi, S., and Bannai, S. (2005). Redox imbalance in cystine/glutamate transporter-deficient mice. *J Biol Chem* 280, 37423-9.
- Sato, H., Takenaka, Y., Fujiwara, K., Yamaguchi, M., Abe, K., and Bannai, S. (1995). Increase in cystine transport activity and glutathione level in mouse peritoneal macrophages exposed to oxidized low-density lipoprotein. *Biochem Biophys Res Commun* 215, 154-9.
- Sato, H., Tamba, M., Ishii, T., and Bannai, S. (1999). Cloning and expression of a plasma membrane cystine/glutamate exchange transporter composed of two distinct proteins. *J Biol Chem* 274, 11455-8.
- Sato, H., Tamba, M., Okuno, S., Sato, K., Keino-Masu, K., Masu, M., and Bannai, S. (2002). Distribution of cystine/glutamate exchange transporter, system x(c)-, in the mouse brain. *J Neurosci* 22, 8028-33.
- Schneider, M., Vogt Weisenhorn, D. M., Seiler, A., Bornkamm, G. W., Brielmeier, M., and Conrad, M. (2006). Embryonic expression profile of phospholipid hydroperoxide glutathione peroxidase. *Gene Expr Patterns*.
- Schomburg, L., Schweizer, U., Holtmann, B., Flohe, L., Sendtner, M., and Kohrle, J. (2003). Gene disruption discloses role of selenoprotein P in selenium delivery to target tissues. *Biochem J* 370, 397-402.
- Schreck, R., Rieber, P., and Baeuerle, P. A. (1991). Reactive oxygen intermediates as apparently widely used messengers in the activation of the NF-kappa B transcription factor and HIV-1. *Embo J* 10, 2247-58.
- Schwaab, V., Lareyre, J. J., Vernet, P., Pons, E., Faure, J., Dufaure, J. P., and Drevet, J. R. (1998). Characterization, regulation of the expression and putative roles of two

- glutathione peroxidase proteins found in the mouse epididymis. *J Reprod Fertil Suppl* 53, 157-62.
- Schweizer, U., Brauer, A. U., Kohrle, J., Nitsch, R., and Savaskan, N. E. (2004a). Selenium and brain function: a poorly recognized liaison. *Brain Res Brain Res Rev* 45, 164-78.
- Schweizer, U., Michaelis, M., Kohrle, J., and Schomburg, L. (2004b). Efficient selenium transfer from mother to offspring in selenoprotein-P-deficient mice enables dose-dependent rescue of phenotypes associated with selenium deficiency. *Biochem J* 378, 21-6.
- Sekiya, K., and Okuda, H. (1982). Selective inhibition of platelet lipoxygenase by baicalein. *Biochem Biophys Res Commun* 105, 1090-5.
- Sendobry, S. M., Cornicelli, J. A., Welch, K., Bocan, T., Tait, B., Trivedi, B. K., Colbry, N., Dyer, R. D., Feinmark, S. J., and Daugherty, A. (1997). Attenuation of diet-induced atherosclerosis in rabbits with a highly selective 15-lipoxygenase inhibitor lacking significant antioxidant properties. *Br J Pharmacol* 120, 1199-206.
- Shappell, S. B., Taylor, A. A., Hughes, H., Mitchell, J. R., Anderson, D. C., and Smith, C. W. (1990). Comparison of antioxidant and nonantioxidant lipoxygenase inhibitors on neutrophil function. Implications for pathogenesis of myocardial reperfusion injury. *J Pharmacol Exp Ther* 252, 531-8.
- Sharma, R., Yang, Y., Sharma, A., Awasthi, S., and Awasthi, Y. C. (2004). Antioxidant role of glutathione S-transferases: protection against oxidant toxicity and regulation of stress-mediated apoptosis. *Antioxid Redox Signal* 6, 289-300.
- Shi, Z. Z., Osei-Frimpong, J., Kala, G., Kala, S. V., Barrios, R. J., Habib, G. M., Lukin, D. J., Danney, C. M., Matzuk, M. M., and Lieberman, M. W. (2000). Glutathione synthesis is essential for mouse development but not for cell growth in culture. *Proc Natl Acad Sci U S A* 97, 5101-6.
- Shidoji, Y., Okamoto, K., Muto, Y., Komura, S., Ohishi, N., and Yagi, K. (2006). Prevention of geranylgeranoic acid-induced apoptosis by phospholipid hydroperoxide glutathione peroxidase gene. *J Cell Biochem* 97, 178-87.
- Shureiqi, I., Jiang, W., Zuo, X., Wu, Y., Stimmel, J. B., Leesnitzer, L. M., Morris, J. S., Fan, H. Z., Fischer, S. M., and Lippman, S. M. (2003). The 15-lipoxygenase-1 product 13-S-hydroxyoctadecadienoic acid down-regulates PPAR-delta to induce apoptosis in colorectal cancer cells. *Proc Natl Acad Sci U S A* 100, 9968-73.
- Sipos, K., Lange, H., Fekete, Z., Ullmann, P., Lill, R., and Kispal, G. (2002). Maturation of cytosolic iron-sulfur proteins requires glutathione. *J Biol Chem* 277, 26944-9.
- Sordillo, L. M., Weaver, J. A., Cao, Y. Z., Corl, C., Sylte, M. J., and Mullarky, I. K. (2005). Enhanced 15-HPETE production during oxidant stress induces apoptosis of endothelial cells. *Prostaglandins Other Lipid Mediat* 76, 19-34.
- Steinbeck, M. J., Kim, J. K., Trudeau, M. J., Hauschka, P. V., and Karnovsky, M. J. (1998). Involvement of hydrogen peroxide in the differentiation of clonal HD-11EM cells into osteoclast-like cells. *J Cell Physiol* 176, 574-87.
- Sundaresan, M., Yu, Z. X., Ferrans, V. J., Irani, K., and Finkel, T. (1995). Requirement for generation of H<sub>2</sub>O<sub>2</sub> for platelet-derived growth factor signal transduction. *Science* 270, 296-9.
- Suppmann, S., Persson, B. C., and Bock, A. (1999). Dynamics and efficiency in vivo of UGA-directed selenocysteine insertion at the ribosome. *Embo J* 18, 2284-93.
- Susin, S. A., Lorenzo, H. K., Zamzami, N., Marzo, I., Snow, B. E., Brothers, G. M., Mangion, J., Jacotot, E., Costantini, P., Loeffler, M., Larochette, N., Goodlett, D. R., Aebersold, R., Siderovski, D. P., Penninger, J. M., and Kroemer, G. (1999).

- Molecular characterization of mitochondrial apoptosis-inducing factor. *Nature* 397, 441-6.
- Sutherland, M., Shankaranarayanan, P., Schewe, T., and Nigam, S. (2001). Evidence for the presence of phospholipid hydroperoxide glutathione peroxidase in human platelets: implications for its involvement in the regulatory network of the 12-lipoxygenase pathway of arachidonic acid metabolism. *Biochem J* 353, 91-100.
- Tagami, M., Ikeda, K., Yamagata, K., Nara, Y., Fujino, H., Kubota, A., Numano, F., and Yamori, Y. (1999). Vitamin E prevents apoptosis in hippocampal neurons caused by cerebral ischemia and reperfusion in stroke-prone spontaneously hypertensive rats. *Lab Invest* 79, 609-15.
- Tagami, M., Yamagata, K., Ikeda, K., Nara, Y., Fujino, H., Kubota, A., Numano, F., and Yamori, Y. (1998). Vitamin E prevents apoptosis in cortical neurons during hypoxia and oxygen reperfusion. *Lab Invest* 78, 1415-29.
- Takami, M., Preston, S. L., and Behrman, H. R. (2000). Eicosatetraenoic and eicosatrienoic acids, lipoxygenase inhibitors, block meiosis via antioxidant action. *Am J Physiol Cell Physiol* 278, C646-50.
- Tan, S., Sagara, Y., Liu, Y., Maher, P., and Schubert, D. (1998). The regulation of reactive oxygen species production during programmed cell death. *J Cell Biol* 141, 1423-32.
- Thannickal, V. J., and Fanburg, B. L. (1995). Activation of an H<sub>2</sub>O<sub>2</sub>-generating NADH oxidase in human lung fibroblasts by transforming growth factor beta 1. *J Biol Chem* 270, 30334-8.
- Thomas, J. P., Geiger, P. G., Maiorino, M., Ursini, F., and Girotti, A. W. (1990a). Enzymatic reduction of phospholipid and cholesterol hydroperoxides in artificial bilayers and lipoproteins. *Biochim Biophys Acta* 1045, 252-60.
- Thomas, J. P., Maiorino, M., Ursini, F., and Girotti, A. W. (1990b). Protective action of phospholipid hydroperoxide glutathione peroxidase against membrane-damaging lipid peroxidation. In situ reduction of phospholipid and cholesterol hydroperoxides. *J Biol Chem* 265, 454-61.
- Tujebajeva, R. M., Copeland, P. R., Xu, X. M., Carlson, B. A., Harney, J. W., Driscoll, D. M., Hatfield, D. L., and Berry, M. J. (2000). Decoding apparatus for eukaryotic selenocysteine insertion. *EMBO Rep* 1, 158-63.
- Ursini, F., Heim, S., Kiess, M., Maiorino, M., Roveri, A., Wissing, J., and Flohe, L. (1999). Dual function of the selenoprotein PHGPx during sperm maturation. *Science* 285, 1393-6.
- Ursini, F., Maiorino, M., and Gregolin, C. (1985). The selenoenzyme phospholipid hydroperoxide glutathione peroxidase. *Biochim Biophys Acta* 839, 62-70.
- Ursini, F., Maiorino, M., and Roveri, A. (1997). Phospholipid hydroperoxide glutathione peroxidase (PHGPx): more than an antioxidant enzyme? *Biomed Environ Sci* 10, 327-32.
- Ursini, F., Maiorino, M., Valente, M., Ferri, L., and Gregolin, C. (1982). Purification from pig liver of a protein which protects liposomes and biomembranes from peroxidative degradation and exhibits glutathione peroxidase activity on phosphatidylcholine hydroperoxides. *Biochim Biophys Acta* 710, 197-211.
- Utomo, A., Jiang, X., Furuta, S., Yun, J., Levin, D. S., Wang, Y. C., Desai, K. V., Green, J. E., Chen, P. L., and Lee, W. H. (2004). Identification of a novel putative non-selenocysteine containing phospholipid hydroperoxide glutathione peroxidase (NPGPx) essential for alleviating oxidative stress generated from polyunsaturated fatty acids in breast cancer cells. *J Biol Chem* 279, 43522-9.
- van Leyen, K., Kim, H. Y., Lee, S. R., Jin, G., Arai, K., and Lo, E. H. (2006). Baicalein and 12/15-lipoxygenase in the ischemic brain. *Stroke* 37, 3014-8.

- van Wijk, S. J., and Hageman, G. J. (2005). Poly(ADP-ribose) polymerase-1 mediated caspase-independent cell death after ischemia/reperfusion. *Free Radic Biol Med* 39, 81-90.
- Vernet, P., Rigaudiere, N., Ghyselinck, N., Dufaure, J. P., and Drevet, J. R. (1996). In vitro expression of a mouse tissue specific glutathione-peroxidase-like protein lacking the selenocysteine can protect stably transfected mammalian cells against oxidative damage. *Biochem Cell Biol* 74, 125-31.
- Verrou, C., Zhang, Y., Zurn, C., Schamel, W. W., and Reth, M. (1999). Comparison of the tamoxifen regulated chimeric Cre recombinases MerCreMer and CreMer. *Biol Chem* 380, 1435-8.
- Watanabe, T., and Endo, A. (1991). Effects of selenium deficiency on sperm morphology and spermatocyte chromosomes in mice. *Mutat Res* 262, 93-9.
- Weitzel, F., and Wendel, A. (1993). Selenoenzymes regulate the activity of leukocyte 5-lipoxygenase via the peroxide tone. *J Biol Chem* 268, 6288-92.
- Wingler, K., Bocher, M., Flohe, L., Kollmus, H., and Brigelius-Flohe, R. (1999). mRNA stability and selenocysteine insertion sequence efficiency rank gastrointestinal glutathione peroxidase high in the hierarchy of selenoproteins. *Eur J Biochem* 259, 149-57.
- Xu, X. M., Mix, H., Carlson, B. A., Grabowski, P. J., Gladyshev, V. N., Berry, M. J., and Hatfield, D. L. (2005). Evidence for direct roles of two additional factors, SECp43 and soluble liver antigen, in the selenoprotein synthesis machinery. *J Biol Chem* 280, 41568-75.
- Yagi, K., Komura, S., Kojima, H., Sun, Q., Nagata, N., Ohishi, N., and Nishikimi, M. (1996). Expression of human phospholipid hydroperoxide glutathione peroxidase gene for protection of host cells from lipid hydroperoxide-mediated injury. *Biochem Biophys Res Commun* 219, 486-91.
- Yamamoto, Y., Nagata, Y., Niki, E., Watanabe, K., and Yoshimura, S. (1993). Plasma glutathione peroxidase reduces phosphatidylcholine hydroperoxide. *Biochem Biophys Res Commun* 193, 133-8.
- Yamazaki, T., Higuchi, K., Kominami, S., and Takemori, S. (1996). 15-lipoxygenase metabolite(s) of arachidonic acid mediates adrenocorticotropin action in bovine adrenal steroidogenesis. *Endocrinology* 137, 2670-5.
- Yant, L. J., Ran, Q., Rao, L., Van Remmen, H., Shibata, T., Belter, J. G., Motta, L., Richardson, A., and Prolla, T. A. (2003). The selenoprotein GPX4 is essential for mouse development and protects from radiation and oxidative damage insults. *Free Radic Biol Med* 34, 496-502.
- Yoshida, T., Maulik, N., Engelman, R. M., Ho, Y. S., Magnenat, J. L., Rousou, J. A., Flack, J. E., 3rd, Deaton, D., and Das, D. K. (1997). Glutathione peroxidase knockout mice are susceptible to myocardial ischemia reperfusion injury. *Circulation* 96, II-216-20.
- Yu, S. W., Wang, H., Poitras, M. F., Coombs, C., Bowers, W. J., Federoff, H. J., Poirier, G. G., Dawson, T. M., and Dawson, V. L. (2002). Mediation of poly(ADP-ribose) polymerase-1-dependent cell death by apoptosis-inducing factor. *Science* 297, 259-63.
- Yuste, V. J., Sanchez-Lopez, I., Sole, C., Moubarak, R. S., Bayascas, J. R., Dolcet, X., Encinas, M., Susin, S. A., and Comella, J. X. (2005). The contribution of apoptosis-inducing factor, caspase-activated DNase, and inhibitor of caspase-activated DNase to the nuclear phenotype and DNA degradation during apoptosis. *J Biol Chem* 280, 35670-83.
- Zhang, Y., Fomenko, D. E., and Gladyshev, V. N. (2005). The microbial selenoproteome of the Sargasso Sea. *Genome Biol* 6, R37.

- Zhang, Y. Y., Hamberg, M., Radmark, O., and Samuelsson, B. (1994). Stabilization of purified human 5-lipoxygenase with glutathione peroxidase and superoxide dismutase. *Anal Biochem* 220, 28-35.
- Zhao, L., Pratico, D., Rader, D. J., and Funk, C. D. (2005). 12/15-Lipoxygenase gene disruption and vitamin E administration diminish atherosclerosis and oxidative stress in apolipoprotein E deficient mice through a final common pathway. *Prostaglandins Other Lipid Mediat* 78, 185-93.
- Zhong, L., Arner, E. S., and Holmgren, A. (2000). Structure and mechanism of mammalian thioredoxin reductase: the active site is a redox-active selenolthiol/selenenylsulfide formed from the conserved cysteine-selenocysteine sequence. *Proc Natl Acad Sci U S A* 97, 5854-9.
- Zhu, W., Cowie, A., Wasfy, G. W., Penn, L. Z., Leber, B., and Andrews, D. W. (1996). Bcl-2 mutants with restricted subcellular location reveal spatially distinct pathways for apoptosis in different cell types. *Embo J* 15, 4130-41.
- Zinoni, F., Birkmann, A., Stadtman, T. C., and Bock, A. (1986). Nucleotide sequence and expression of the selenocysteine-containing polypeptide of formate dehydrogenase (formate-hydrogen-lyase-linked) from *Escherichia coli*. *Proc Natl Acad Sci U S A* 83, 4650-4.
- Zuo, X., Wu, Y., Morris, J. S., Stimmel, J. B., Leesnitzer, L. M., Fischer, S. M., Lippman, S. M., and Shureiqi, I. (2006). Oxidative metabolism of linoleic acid modulates PPAR-beta/delta suppression of PPAR-gamma activity. *Oncogene* 25, 1225-41.



## 7 Summary

Acute or chronic oxidative stress, accompanied by GSH depletion, has been frequently linked with many degenerative human diseases, such as atherosclerosis, myocardial infarction, stroke, and Parkinson's disease. While the accumulation of reactive oxygen species is known being detrimental to cells and tissues, it has remained enigmatic if this is just a pleiotropic effect or whether a distinct signalling pathway is involved in oxidative stress-mediated cell death. Phospholipid hydroperoxide glutathione peroxidase (PHGPx) has emerged as an essential antioxidant enzyme in cells, efficiently detoxifying phospholipid hydroperoxides within biological membranes at the expense of GSH. To study PHGPx functions on life and death decisions in a cellular context, an inducible knockout model for PHGPx was established in mouse embryonic fibroblasts (MEFs), by using the 4-hydroxytamoxifen-inducible MerCreMer/loxP system. Targeted PHGPx abolition enabled to pinpoint a specific cell death inducing pathway, including activation of 15-lipoxygenase (15-LOX), lipid peroxidation, translocation of apoptosis inducing factor (AIF), and eventually cell death. The onset and execution of cell death could be efficiently prevented at each single step, either by the administration of the antioxidant  $\alpha$ -tocopherol, by the highly specific 15-LOX inhibitor PD146176, or by siRNA-mediated knockdown of AIF. Since PHGPx is considered as the major GSH-dependent enzyme, this cell death-inducing pathway may be a common signature in the etiology of many degenerative disorders, involving a detrimental accumulation of reactive oxygen species (ROS). To gain further insights into the role of GSH for cellular life and death decisions, a GSH-deficient *in vitro* model of  $\gamma$ -glutamylcysteine synthetase ( $\gamma$ -GCS) knockout cells was used. The glutamate/cystine (Cys)<sub>2</sub> antiporter, system x<sub>c</sub><sup>-</sup>, consists of two protein components, xCT light chain and 4F2 heavy chain, whereas xCT mediates transport specificity. The overexpression of xCT in  $\gamma$ -GCS knockout cells increased intra- and extracellular cysteine (Cys)-levels, rendering cell survival and proliferation independent from GSH. The elevated Cys levels are generated by the increased uptake of (Cys)<sub>2</sub>, intracellular reduction to Cys, and subsequent secretion to the extracellular space. These findings also imply that in the absence of GSH PHGPx accepts cysteine (Cys) as an alternative reducing equivalent when present in sufficient amounts. Since the maintenance of the cellular redox balance rather than GSH itself appeared to be essential for the maintenance of

cell integrity, the Cys/(Cys)<sub>2</sub>-cycle has to be regarded as a distinct redox cycle of major importance. In conclusion, we propose that acute or chronic oxidative stress in cells and tissues triggers the herein described cell death pathway, including GSH depletion, impaired PHGPx enzyme activity, 15-LOX activation, lipid peroxidation, and AIF release. Whether up-regulation of xCT expression may represent a back-up system for low GSH levels, as observed under various pathophysiological conditions, certainly deserves further investigations.

**Curriculum Vitae, Alexander Seiler**

July, 2007

**1. Personal details**

Surname:	Seiler
Forename:	Alexander
Title:	Dipl.-Ing. Biotechnology
Nationality:	German
Date and place of birth:	21. October 1976, Freising, Germany
Private Address:	Pantaleonstr. 4, 85402 Kranzberg, Germany
Telephone:	0049-173-6204928
Work Address:	Marchioninstr. 25, 81377 Munich, Germany
Telephone:	0049-89-7099-526
Fax and e-mail:	0049-89-7099-500, <a href="mailto:alexander.seiler@gsf.de">alexander.seiler@gsf.de</a>

**2. Education**

**2.1 University entrance qualification**

Abitur (high school diploma) 1996, Josef-Hofmiller Gymnasium, Freising, Germany

**2.2 University studies**

October 1996 – August 1999

Basic study period at the Faculty of Biotechnology of the Technical University, Berlin, Germany

September 1999 – July 2003

Main study period with emphasis on Medical Biotechnology at the Technical University, Berlin, Germany

October 2003 – present

PhD student at the Department of Clinical Molecular Biology and Tumor Genetics, GSF-National Research Center for Environment and Health, Munich, Germany

**2.3 Final examination**

Diplom-Ingenieur Biotechnology, July 2003, Technical University, Berlin, Germany

**2.4 Diploma thesis**

Title: "Characterization of a Fungal Phosphopantetheinyl Transferase"

Institute: Department of Molecular Biology and Biotechnology, University of Sheffield, UK

### **3. Work experience**

June 2000 – March 2002

Student assistant with teaching assignment, Department of Microbiology and Genetics, Faculty of Biotechnology, Technical University, Berlin, Germany

February 2001 – July 2001

Student research project, Department of Biochemistry, Max-Planck-Institute, Munich, Germany

October 2003 – present

PhD student at the Department of Clinical Molecular Biology and Tumor Genetics, GSF-National Research Center for Environment and Health, Munich, Germany

### **4. Work experience abroad**

November 2002 – April 2003

Diploma thesis at the Department of Molecular Biology and Biotechnology, University of Sheffield, UK

June 2006 – July 2006

Collaboration with the Department of Medical Biochemistry and Biophysics, Karolinska Institute, Stockholm, Sweden, funded by a personal scholarship from Boehringer Ingelheim Fonds.

### **5. Publications**

Kappert K, Sparwel J, Sandin A, Seiler A, Siebolts U, Leppänen O, Rosenkranz S, Ostman A. (2006). Antioxidants relieve phosphatase inhibition and reduce PDGF signaling in cultured VSMCs and in restenosis. *Arterioscler Thromb Vasc Biol* 26(12):2644-51.

Schneider M, Vogt Weisenhorn DM, Seiler A, Bornkamm GW, Brielmeier M, Conrad M. (2006). Embryonic expression profile of phospholipid hydroperoxide glutathione peroxidase. *Gene Expr Patterns* 6(5):489-94.

Conrad M, Schneider M, Seiler A, Bornkamm GW. (2007). The physiological role of phospholipid hydroperoxide glutathione peroxidase in mammals. *Biological Chemistry* 388(10):1019-25.

Banjac A, Perisic T, Sato H, Seiler A, Bannai S, Weiss N, Kölle P, Tschöep K, Issels RD, Daniel PT, Conrad M, Bornkamm GW. (2007). The cystine/cysteine cycle: a redox cycle regulating susceptibility versus resistance to cell death. *Oncogene*. Sep 10; [Epub ahead of print].

Seiler A, Schneider M, Förster H, Roth S, Wirth EK, Culmsee C, Plesnila N, Rådmark O, Wurst W, Bornkamm GW, Schweizer U, Conrad M. (2007). Oxidative stress is transduced into AIF-mediated cell death via the glutathione peroxidase 4 - 12/15 lipoxygenase pathway (submitted).

Schneider M, Förster H, Seiler A, Wehnes H, Boersma A, Sinowatz F, Neumüller C, Kremmer E, Walch A, Wurst W, Ursini F, Bornkamm GW, Maiorino M, Conrad M. (2007). Targeted disruption of mitochondrial PHGPx expression allows normal embryonic development but abolishes male fertility (submitted).

Seiler A, Weiss N, Koelle P, Lieberman MW, Bornkamm GW, Conrad M (2007). The cysteine/cystine cycle, driven by antiporter system  $x_c^-$ , rescues glutathione deficiency in  $\gamma$ -GCS knockout cells (in preparation).

## **6. Presentations**

Seiler A, Weiss N, Koelle P, Lieberman MW, Bornkamm GW, Conrad M (2006). xCT, the substrate specific subunit of the amino acid transporter system  $x_c^-$ , rescues  $\gamma$ -glutamylcysteine synthetase deficiency in embryonic stem cell-like cells. Poster presentation at the 57<sup>th</sup> Mosbach Colloquium "Redoxsignaling".

## **Acknowledgement**

This dissertation has been of extensive and demanding work, but first of all exciting, instructive, and also fun. Without help, support, and encouragement from many people, I would not have been able to complete this work.

First of all, I would like to thank my supervisor Dr. Marcus Conrad for his encouraging way to guide me to a deeper understanding of science, and his invaluable support during this work and beyond.

I would like to express my gratitude to all those who gave me the possibility to do my PhD thesis at the GSF National Research Center for Environment and Health.

I am very grateful to my official supervisor, Prof. Georg W. Bornkamm, Head of the Department at the Institute of Clinical Molecular Biology and Tumor Genetics, for his detailed and constructive comments, and for his important support throughout this work.

I would like to thank my PhD supervisor Prof. Dirk Eick, who monitored my work and took effort in reading and providing me with valuable comments. I also want to thank the other members of my PhD committee who took effort in reading this thesis and monitored my work.

I am very grateful to all the people in my lab for physical and mental support, Tamara Perisic, Ana Banjac, Heidi Förster, Pankaj Mandal, Manuela Schneider, Stephanie Moréno, and Alexander Mannes, and to some further people from my institute, Thomas Harasim, Rob Chapman, and Florian Rückerl.

I want to thank Hideo Sato from the Yamagata University, Japan, for important suggestions, fruitful discussions, and not least for discovering xCT.

I owe gratitude to Markus Moosmüller for the post-production of the time-lapse videos.

I owe a great deal of gratitude to Dr. Norbert Weiss and Pirkko Kölle from the “Medizinische Poliklinik Innenstadt” of the “Klinikum der LMU” for great help with the HPLC analysis and Louisa Papatheodorou for excellent supervision.

Due to the support and hospitality of many people, I was able to work in other laboratories during my thesis. A major contribution came from Boehringer Ingelheim, who funded my two months stay at the Karolinska Institute in Sweden. Therefore I would like to thank Boehringer Ingelheim and especially Dr. Sabine Achten who made this trip possible.

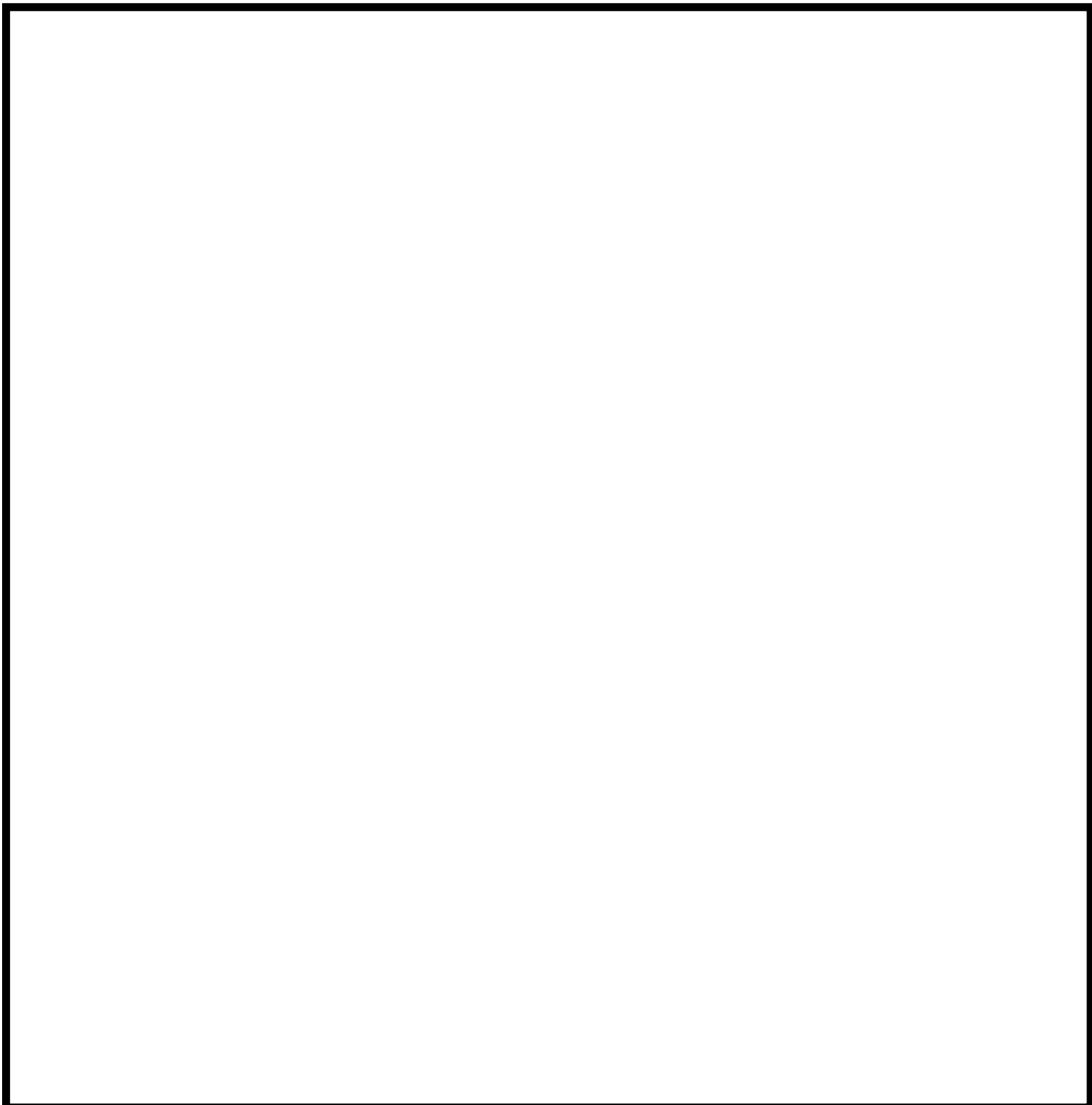
I am very grateful to all the people in Stockholm, who supported me during my work at the Department of Medical Biochemistry and Biophysics (MBB) at the Karolinska Institute. Especially I want to thank Dr. Olof Rådmark and Prof. Jesper Haeggström for their kind invitation, for great support and valuable discussions. Special thanks to Anders Wetterholm for the patient introduction into the HPLC techniques. Moreover, I owe gratitude to Daniel Hägerstrand for his hospitality and guidance in and around Stockholm and for a great collection.

Thanks to Prof. Roland Lill and Dr. Oliver Stehling from the Philipps-University in Marburg for their great hospitality during my stay in their lab. Unfortunately, the generated data did not make into this thesis, but I am very confident that this collaboration will pay off in the near future.

I want to thank my parents, who made all this possible by supporting me ever since I can remember.

## Supplementary data on CD

- PhD thesis, Seiler Alexander (2007).pdf
- Supplementary data (time-lapse videos).pps
- PFa1-MerCreMer.avi
- PFa1-MerCreMer + Tam.avi





## **Erklärung:**

Hiermit versichere ich, Alexander Seiler, dass ich die vorliegende Doktorarbeit zum Thema „Dissecting the molecular mechanism of glutathione-dependent regulation of cell proliferation and cell death“ eigenständig verfasst und keine anderen als die angegebenen Quellen und Hilfsmittel verwendet habe.

München, August 2007

---

Alexander Seiler